

RSC Advances



This is an *Accepted Manuscript*, which has been through the Royal Society of Chemistry peer review process and has been accepted for publication.

Accepted Manuscripts are published online shortly after acceptance, before technical editing, formatting and proof reading. Using this free service, authors can make their results available to the community, in citable form, before we publish the edited article. This *Accepted Manuscript* will be replaced by the edited, formatted and paginated article as soon as this is available.

You can find more information about *Accepted Manuscripts* in the [Information for Authors](#).

Please note that technical editing may introduce minor changes to the text and/or graphics, which may alter content. The journal's standard [Terms & Conditions](#) and the [Ethical guidelines](#) still apply. In no event shall the Royal Society of Chemistry be held responsible for any errors or omissions in this *Accepted Manuscript* or any consequences arising from the use of any information it contains.

An overview of the recent developments on Hg^{2+} recognition

Prasenjit Mahato,^a Sukdeb Saha,^b Priyadip Das,^c Hridayesh Agarwal,^d Amitava Das.^{d*}

^aDept. of Chemistry and Biochemistry, Graduate School of Engineering, Kyushu University, Fukuoka-819-0385, Japan; ^bBen-Gurion University, Israel; ^cInstitute of Chemistry, Center for Nanoscience and Nanotechnology, Hebrew University, Jerusalem-91904, Israel; ^dOrganic Chemistry Division, CSIR-National Chemical Laboratory, Pune, Maharashtra 411008, India

Abstract:

Adverse influences of mercury on living organisms are well known. Despite efforts from various regulatory agencies, the buildup of Hg^{2+} concentration in the environment is of serious concern. This necessitates the search for new and efficient reagent for recognition and detection of Hg^{2+} in environmental samples as well as for application in diagnostic. Among various detection processes adopted for designing such reagents, generally methodologies that allow associated changes in spectra properties are preferred for the obvious ease in the detection process. Significant changes in the electronic spectral pattern in the visible region of the spectrum also induces detectable changes in solution colour for naked eye detection and is useful for developing reagent for in-field sample analysis with *yes-no* type binary responses. However, reagents those allow detection of Hg^{2+} with associated fluorescence on response are useful for detection of Hg^{2+} in environmental samples as well as for use as an imaging reagent for detection of cellular uptake. High spin orbit coupling constant for Hg^{2+} along with its high solvation energy in aqueous medium pose a challenge in developing efficient reagent with fluorescence on response that works in aqueous medium/physiological condition. To get around this problem, several methodologies like conversion of rhodamine derivative spirolactam to strongly fluorescent xanthenes form on binding to Hg^{2+} , chemodosimetric reaction for generation of a new luminescent derivative, etc. have been adopted. Apart from these, modified charge transfer processes on binding to Hg^{2+} has also been utilized for designing reagents for optical detection of Hg^{2+} . Immobilization of such reagents on solid surfaces also led to the development of self indicating Hg^{2+} ion scavengers. All such examples are discussed in the present review.

Introduction

Mercury in its various forms are known to be the most potent neurotoxin for human physiology and its detrimental influences on human life, other living organisms and the surrounding environment are amply described in various contemporary literatures. Despite efforts of different regulatory agencies as well as governmental policies in various countries for curbing the mercury emission in the environment, the global mercury contamination from natural and industrial processes have posed a serious threat to the human race in the last few decades.¹ The concern over its deleterious effects on various living organisms and the surrounding environment has actually led chemist and more broadly the sensing community to develop new mercury detection methods that are cost-effective, rapid, facile and applicable to the environmental and biological milieus.² All these have triggered an exponential surge in interest for developing an efficient receptor for recognition and detection of Hg^{2+} in aqueous medium and in physiological conditions. This has consequently resulted in an innumerable publication from various research groups globally in last one decade. There are review articles on the general theme of metal ion recognition and sensing and a few among these have also discussed about possible application potential of such receptors for treating environmental and biological samples as well as use as an imaging reagents.³ A closer scrutiny of all these review articles reveals that there has been only one review article by Lippard et. al. that has discussed specifically about the various approaches for optical detection of Hg^{2+} in environmental and biological samples.¹ Apart from this, there has been no specific review article that has covered recent advances achieved in developing reagents that are efficient for specific recognition of Hg^{2+} under physiological condition as well as in using such reagents as a biomarkers or imaging reagents for in-vivo studies. Present review article aims to discuss such articles with specific emphasis on receptors that exhibit 'yes-no' type binary response on specific binding or reaction of Hg^{2+} ion and use of such reagents for analysis of environmental samples as well as use as biomarker/imaging reagent. Design of such receptors depends primarily on the nature of the binding site for achieving the desired specificity for the Hg^{2+} ion as well as on the nature of the optical response(s) that is/are preferred for probing the receptor-analyte binding process. Among various

photophysical pathways like Charge Transfer (CT),⁴ Electron Transfer (ET),⁵ Energy Transfer (eT),⁶ Förster Resonance Energy Transfer (FRET),⁷ Through bond energy Transfer (TBET),⁸ are generally utilized for reporting the binding induced phenomena; while photoactive moieties like 1,8-naphthalimide, coumarin, pyrene, anthracene, BODIPY, squaraine, xanthenes, cyanine, rhodamine, fluorescein etc. are commonly being used as the reporter moiety.⁹ Apart from these, optical responses, more specifically the luminescence responses associated with receptor-Hg²⁺ binding on account of change(s) in conformational flexibility, heavy atom effect and dye displacement methodologies are also discussed in this present article.¹⁰

Bio-activity of Hg²⁺ ions

For centuries, mercury was used as an important component for various medicines, such as diuretics, antibacterial agents, antiseptics, and laxatives. However, adverse role of mercury on human physiology on prolong exposure was realized over the years and now mercury is being considered as one of the most potent neurotoxins for humans and mammals. Perhaps the most deadly form of mercury is organic mercury compounds compared to two other forms of mercury, namely, elemental mercury and inorganic salts that are generally available in the environment. Organic mercury compounds, more specifically methylmercury, is accumulated in the food chain. Industrial effluents often contain mercury in the inorganic form. However, anaerobic methylation of inorganic mercury by microorganisms and abiotic chemical processes in sediments generates methyl mercury. Reports also suggest that vegetation in water-bodies also convert inorganic mercury to methylmercury. In waterbodies, methylmercury bioaccumulates in living aquatic organisms and biomagnifies up the food chain. Methylmercury is better absorbed and shows a higher mobility in the human body. It easily passes through biological membranes, such as skin, respiratory, and gastrointestinal tissues, which eventually damages the central nervous and endocrine system.¹¹

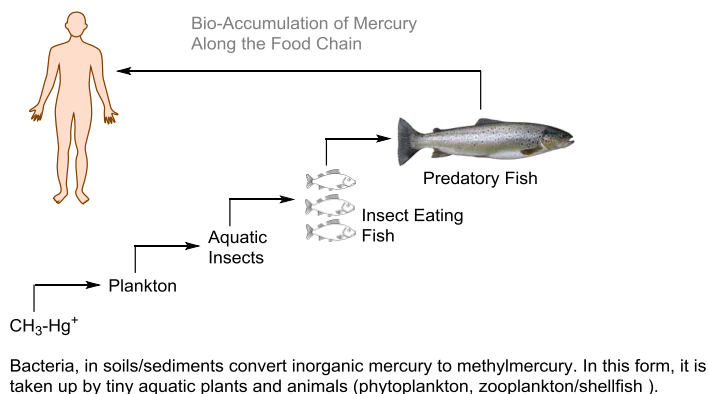


Figure 1. Scheme showing the bio-accumulation and magnification of $\text{CH}_3\text{-Hg}^{2+}$ along the food chain.

Considering its acute toxicity, international regulatory agency like, Environmental Protection Agency (EPA) in US has set an upper limit of 2 ppb (10 nM) for Hg(II) for safe drinking water.¹ The well known toxicity of the Hg^{2+} towards living organisms and the very stringent norms set more recently by the various regulatory agencies, it has become almost imperative to develop suitable colorimetric or fluorescence based sensors for water quality determination in terms of the Hg^{2+} ion concentration and this has actually led to a surge of interests among researchers for designing Hg^{2+} ion specific sensor that works in aqueous medium as well as under the physiological condition that allows the detection of Hg^{2+} ion uptake in lower organisms.

Colorimetric Sensors for Hg^{2+} Ion

Design of the colorimetric chemosensor for Hg(II) ion has gained interest as this allows simple ‘in-field’ visual detection and semi-quantitative analysis. This simplicity in the detection process is the primary reason for the present emphasis on the development of the colorimetric sensors for Hg^{2+} ion.

Li et al. reported a heptamethine cyanine dye containing dithia-dioxa-monoaza crown ether moiety (**1**) for the detection of Hg^{2+} .¹² Spectral change for this reagent on specific binding to Hg^{2+} in methanol medium appeared in the NIR region of the spectrum (Figure 2). Spectral changes in the NIR region has a special significance; as biological background is supposed to induce less interference when detecting in the red to NIR (700 – 1000 nm) region compared with detection in the UV and visible region. A large (~ 122 nm) red shift in the absorption spectrum (λ_{max} shifted from 695 nm for **1** to 817 nm for Hg^{2+} .**1**) with a visually detectable change in colour from blue to colourless. A moderate

binding constant ($K_a = 4.335 \times 10^4 \text{ M}^{-1}$) was evaluated for 1:1 binding stoichiometry based on the electronic spectral titrations.

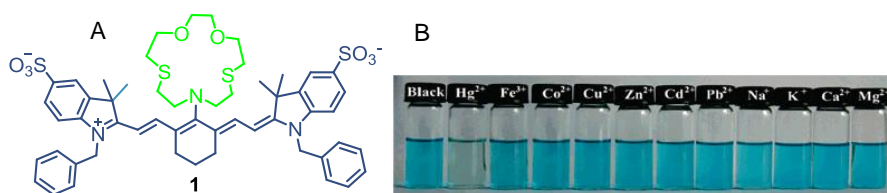


Figure 2. (A) Molecular structure of the chemosensor **1** and (B) naked eye colour change of the solution of **1** in presence of different metal ions. Reprinted with permission from ref 12. Copyright 2008 American Chemical Society.

Lee and co-workers reported two Azo-coupled macrocyclic ionophores having benzene (**2**) or pyridine (**3**) subunits (Figure 3).¹³ Both receptors showed selectivity towards Hg^{2+} and Job plot analysis confirmed a 1:1 (**2/3**: Hg^{2+}) stoichiometry for complexation. However, more significant cation-induced hypsochromic shift was observed for **2**, suggesting that the presence of the pyridine unit in **3** could have inhibited the $\text{Hg}^{2+} \cdots \text{N}$ -azo interaction.

A hemicyanine dye **4**, (Figure 3), consists of an aniline donor and benzothiazolium acceptor, was reported by Palomares and co-workers for colorimetric detection of $\text{Hg}(\text{II})$ in mixed EtOH/ H_2O (1:10, v/v) at neutral pH.¹⁴ On selective binding to Hg^{2+} , **4** produced a colour change from pink to green (Figure 3) on formation of a 1:1 complex with Hg^{2+} with an associated blue-shift in absorption maxima from ~ 550 to ~ 450 nm, (isosbestic point at ~ 480 nm). Interestingly, the evaluated binding constant was $\sim 10^7 \text{ M}^{-1}$ even in mixed aqueous medium.



Figure 3. Molecular structure of chemosensors (A) **2**, **3** & (B) **4**; (C) change in solution colour of **4** on binding to $\text{Hg}(\text{II})$ in 1:10 EtOH/ H_2O (pH 7, HEPES buffer). Reprinted with permission from ref 14. Copyright 2006 American Chemical Society.

Upadhyay and co-workers reported a ninhydrin-based colorimetric molecular switch (**5**) (Figure 4) which gets 'ON' (blue) in the simultaneous presence of Hg^{2+} and $\text{CH}_3\text{COO}^-/\text{F}^-$ while the absence of any one of these leads the system 'OFF' (purple) in ethanol-water (1:1, v/v) medium.¹⁵ The corresponding spectral responses (shift from 535 to 590 nm in the CT band of receptor **5**) could be correlated for demonstrating the AND logic function.

Tew et al. reported a series of terpyridine derivatives (**6-9**) (Figure 4) which selectively detect Hg^{2+} in DMSO-water (1:3.5, v/v) medium.¹⁶ These compounds turned into pink colour with Hg^{2+} , whereas pale blue colour with Cu^{2+} . For reagent **6**, the lowest detection limit for Hg^{2+} was 2 ppm for naked eye, while it was 2 ppb (USEPA limit for Hg^{2+} in drinking water) through spectrophotometrically. Crystallographic and isothermal titration calorimetry (ITC) studies proved that the 2:1 binding stoichiometry for $[\text{6}]\cdot\text{Hg}^{2+}$ formation. Further the paper strip developed using **9** could detect Hg^{2+} over a wide pH range (2.5 to 9) demonstrated its practical applicability.

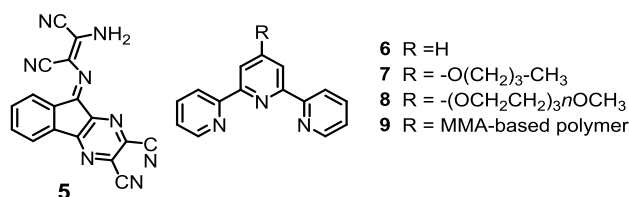


Figure 4. Structures of the chemosensors **5-9**.

Sun et al. synthesized a series of platinum(II) terpyridine complexes featuring an aminostilbene donor-acceptor framework (**10-14**) (Figure 5) for the selective colorimetric recognition of Hg^{2+} .¹⁷ The complex with a dithiaazacrown moiety (**12** and **13**) exhibits a highly sensitive and selective colorimetric response to Hg^{2+} in DMF medium through modulation of the relative strength of ICT and MLCT transitions. Spectrophotometric titration of **14** with $\text{Hg}(\text{ClO}_4)_2$ gave similar response which excluded any interfering effect of counter ions.

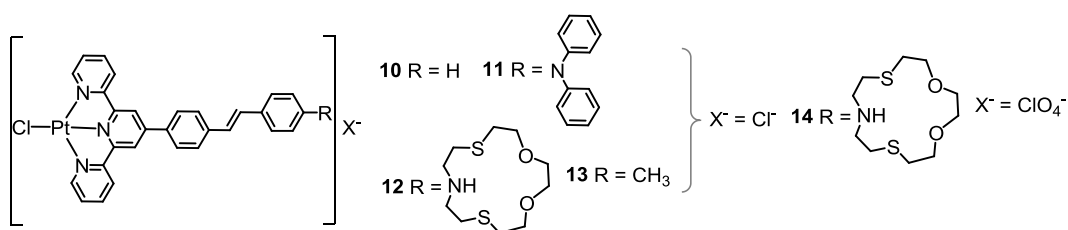


Figure 5. Structure of the chemosensor **10-14**.

Initially Hg^{2+} was bound to the Pt(II)-centre through an usual Hg(II)-Pt(II) bond formation ($K_1 = 1.33 \times 10^4 \text{ M}^{-1}$), which further favored the ICT process. With excess $[\text{Hg}^{2+}]$, the second Hg^{2+} was bound to the dithiaazacrown moiety ($K_2 = 1.64 \times 10^3 \text{ M}^{-1}$) and suppress the ICT process, however turned on the MLCT based colorimetric response. The weak $\text{Pt}^{\text{II}} \dots \text{Hg}^{\text{II}}$ metallophilic interaction at lower $[\text{Hg}^{2+}]$ was proved by ^1H NMR titration. These reagents allowed detection of Hg^{2+} in the micromolar level.

Citrate coated silver nanoparticles (**15**) (Figure 6) were synthesized by Wang and co-workers in order to selectively recognize Hg^{2+} in aqueous medium.¹⁸ In presence of $10 \mu\text{M}$ Hg^{2+} the solution colour of Cit-AgNPs changed (from light yellow to deep yellow) accompanying with a corresponding intensity decrease and a slight blue shift in the absorption maxima from 400 to 397 nm. This phenomenon may be ascribed to the reduction of Hg^{2+} by AgNPs and subsequent deposition of elementary Hg on the surface of AgNPs, yielding amalgam particles. However in presence of H_2O_2 the system was able to detect nM level of Hg^{2+} present in aqueous solution. In presence of H_2O_2 , reduction from Hg^{2+} to $\text{Hg}(0)$ was more efficient and $\text{Hg}(0)$ was deposited on the nanoparticle surface with decrease in the surface charge density and this lead to the aggregation and a red shift in absorption spectra.

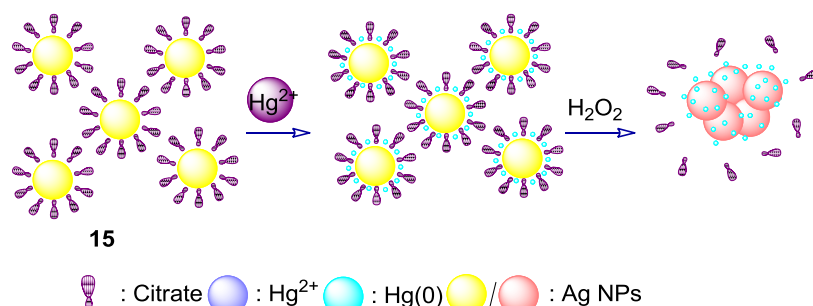


Figure 6. Proposed mechanism for the Hg^{2+} -induced colorimetric response of AgNPs (**15**) in the presence of H_2O_2 .¹⁸

Das and co-workers developed a diametrically disubstituted 1,4,8,11-tetraazacyclotetradecane (cyclam) derivative, functionalized with 4-(4-dimethylamino)phenyl azobenzene as the signalling moiety, has shown remarkable specificity towards Hg^{2+} (Figure 7) in CH_3CN -aq. HEPES buffer (2:3, v/v; pH 7.2) medium.¹⁹ However, solubility of the reagent **16** could be further improved simply by allowing this to form an inclusion complex ([3]pseudo rotaxane; **16.2 β -CD**) with β -cyclodextrine (β -CD). This inclusion complex (L.2 β -CD) could be used for developing a more intense color on binding

to Hg^{2+} in CH_3CN -HEPES buffer medium. Non-toxic nature of **L** and **L.2 β -CD** was checked with the living cells of a *Gram negative* bacterium (*Pseudomonas putida*). Experiments revealed that these two reagents could be used as a staining agent for detection of Hg^{2+} present in this microorganism, while the intensity of the stained bacterium cells was more intense for **L.2 β -CD**.

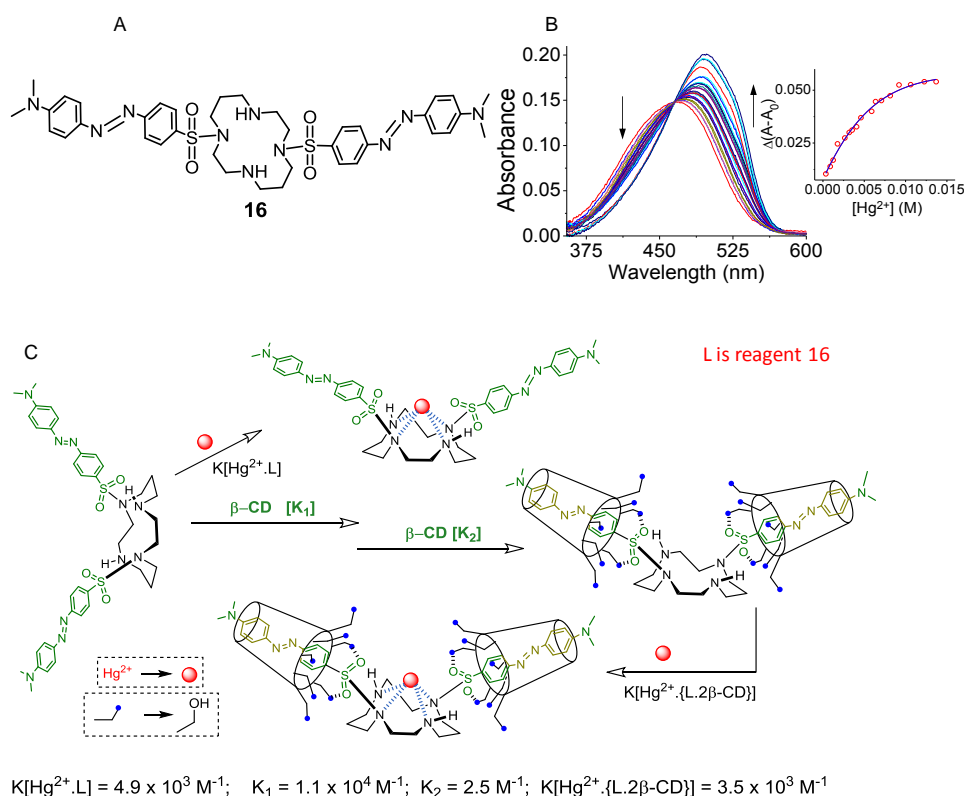


Figure 7. (A) Diametrically disubstituted cyclam unit with azo-chromophore (**16**) for the recognition of Hg^{2+} (B) change in absorption spectra of azamacrocyclic derivative (**16**) as a function of $[\text{Hg}^{2+}]$; (C) schematic presentation for the formation of **L**, $\text{Hg}^{2+} \cdot \text{L}$, **L.2 β -CD**, $\text{Hg}^{2+} \cdot [\text{L.2 β -CD}]$. Reprinted with permission from ref 19. Copyright 2010 American Chemical Society.

The same group later developed a colorimetric sensor **17** (Figure 8), which could act as a colorimetric sensor for Hg^{2+} ($K_a = 6.54 \pm 10^4 \text{ M}^{-1}$) and Cr^{3+} ($K_a = 4.31 \pm 10^4 \text{ M}^{-1}$) among various Group 1A, IIA and all other common transition metal ions in acetonitrile medium.²⁰

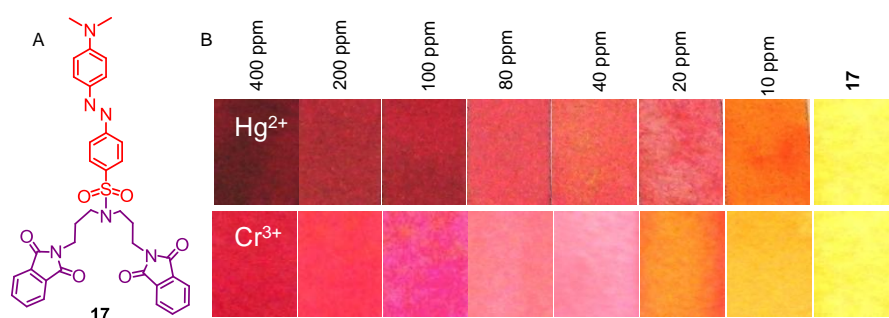


Figure 8. (A) Structure of the chemosensor **17**. (B) The variation in the colour of the test strip for **17** after dipping in aqueous solutions with varying concentrations of Hg^{2+} and Cr^{3+} . A solution of **17** with a concentration of 0.002 M was used to develop the strip. Reprinted with permission from ref 20. Copyright 2012 Royal Society of Chemistry.

On binding of **17** to the Hg^{2+} or Cr^{3+} ions, the absorption band at 440 nm for **17** was found to decrease with a simultaneous growth of an absorption band with a maxima at 509 nm along with an isosbestic point at 464 nm, which was attributed to a charge transfer transition. A visually detectable change in the solution colour from yellow to red was observed. A test paper kit for the detection of Hg^{2+} or Cr^{3+} in neutral aqueous media was also developed (Figure 8).

Rhodamine based reversible receptors for the recognition of Hg^{2+} ions

Xanthenes based fluorophores including rhodamine and fluoresceine are being used extensively for molecular recognition, because of their rich spectral properties. These dyes show high extinction coefficients for electronic spectral band at ≥ 475 nm, strong emission band at ≥ 550 nm with high quantum yield value and appreciably high photo-stability towards radiation of visible wavelength.²¹ More recently, rhodamine derivatives have received certain importance as a staining agent or as an imaging reagent as these derivatives in their spirolactone or spirolactam form either show any absorption nor any emission spectral band beyond 380 nm; while in acyclic xanthene form have a strong absorption (~ 525 nm) and emission (~ 560 nm) bands. These attribute to the visually detectable strong pink solution colour and red solution fluorescence for these derivatives, which offer the option for the 'turn on' response for probing processes that involve reversible conversion between the corresponding spirolactam to acyclic xanthene forms. In general, the carbonyl group in rhodamine spirolactam form gets activated in presence of appropriate metal ions under certain solvent system and pH according to the Figure 9.

Utilizing these optical spectral responses and reversible equilibrium that exists between spirolactam/spirolactone and the corresponding xanthene form, several probes have been designed for the recognition of certain metal ions. Possibility of using such probes as biomarkers has been explored in certain instances.

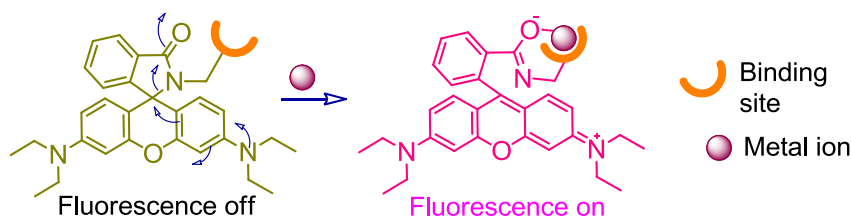


Figure 9. Schematic presentation of the change from cyclic lactam form to an acyclic xanthenes form of the rhodamine derivatives on binding to a metal ion.

Chang and his co-workers had shown that colourless solution of rhodamine B hydrazine (**18**), in methanol-aq. acetate buffer (1:9, v/v; pH = 5) turned red with associated emission band maximum at 578 nm on binding to Hg^{2+} within 10 min (Figure 10) of the addition of Hg^{2+} to the reagent solution.²² Studies revealed that **18** underwent a decomposition reaction with Hg^{2+} to regenerate the acyclic xanthene form with turn on absorption and emission responses at about 530 and 560 nm, respectively. Minimum detection limit for Hg^{2+} was found to be $2\ \mu\text{M}$, while no rate constant was reported.

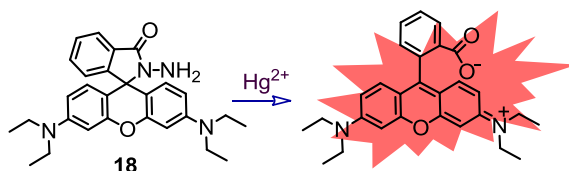


Figure 10. Schematic representation of rhodamine B hydrazine hydrolysis with switch on absorption and emission responses at 530 nm and 560 nm, respectively.

Huang et al. recently reported a multi-signaling sensor **19** for the recognition of Hg^{2+} using a rhodamine derivative functionalized with a redox active ferrocenyl (Fc) and a 8-hydroxyquinoline moieties for probing the binding phenomena either through change(s) in optical spectra or in electrochemical redox potentials (Figure 11).²³ On selective binding to Hg^{2+} in ethanol-HEPES (4-(2-hydroxyethyl)-1-piperazineethanesulfonic acid) buffer (1:1, v/v, pH 7.2), sensor **19** displayed a visually detectable *fluorescence on response*, along with a change in colour from colourless to pink. Presence of the Fc moiety also helped in monitoring the Hg^{2+} .**19** formation through changes in the redox potential of Fc/Fc^+ couple from 0.40 to 0.15 V on binding to Hg^{2+} ion. A moderate formation constant ($3.7 \times 10^3\ \text{M}^{-1}$) for Hg^{2+} .**19** was observed. Confocal laser scanning microscopic studies further revealed the possibility of using this as an imaging reagent for *in vivo* detection of Hg^{2+} in living cells.²³

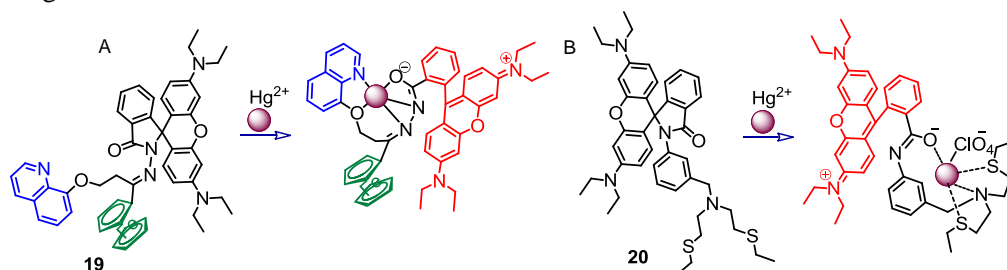


Figure 11. (A) Schematic presentation for the receptors **19** and **20** with possible binding modes to Hg^{2+} .

Qian et al. developed a rhodamine-based sensor (**20**) bearing ionophore NS_2 (Figure 11B), which showed high affinity towards Hg^{2+} .²⁴ In CH_3CN -HEPES buffer (3:17, v/v; pH 6.98) solution **20** was found to bind selectively to Hg^{2+} (1:1 binding stoichiometry) with change in colour from colourless to purple with associated *fluorescence on* response at ~ 570 nm. A binding constant of $1.18 \times 10^6 \text{ M}^{-1}$ was evaluated for Hg^{2+} .**20** formation.

Zheng, Xu, and their co-workers utilized a rhodamine B thiohydrazone derivative **21**²⁵ (Figure 12), as a fluorescent chemosensor for Hg^{2+} , which could reversibly bind Hg^{2+} in aqueous solution at pH 3.4 in a highly selective manner. Coordination of Hg^{2+} to the N and S binding sites in **21** with 1:2 (Hg^{2+} :**21**) stoichiometry and opening of the spirolactam ring was proposed. Zhang and co-workers reported another fluorescent probe, **22** (Figure 12) in which rhodamine unit was functionalized with coumarin moiety and used that for the detection of Hg^{2+} .²⁵ Moderately high binding constant ($1.18 \times 10^6 \text{ M}^{-1}$) in ethanol-Tris-HCl buffer (1:1, v/v; pH 7.24) was reported. Binding stoichiometry of 1:1 and specificity in binding towards Hg^{2+} in presence of all other competing metal ions was established by detailed spectral studies. Reversibility in the Hg^{2+} .**22** formation was established using little excess of EDTA as the competing ligand. Reported lower detection limit of 8 ppb was much closer to the concentration permitted by United States environment protection agency (US EPA) for safe drinking water and could be used for the detection of Hg^{2+} in both tap and river water samples.

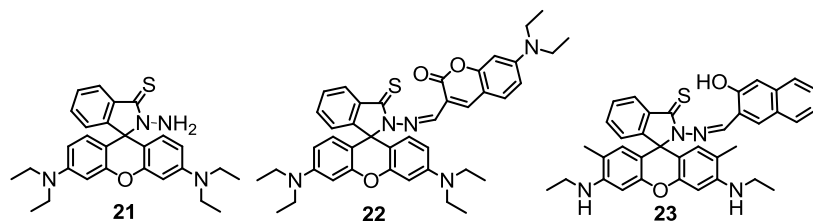


Figure 12. Molecular structures of the receptors **21**, **22** and **23**.

Li and co-workers reported a rhodamine derivative functionalized with a β -naphthol moiety and this receptor (**23**, Figure 12) showed selective binding to Hg^{2+} over other metal ions in aqueous solution, except Cu^{2+} .²⁶ Job plot analysis suggested a 1:1 binding stoichiometry. Binding process ($K_a^{\text{Hg}^{2+}} = 8.42 \times 10^4 \text{ M}^{-1}$) was probed by monitoring fluorescence enhancements at ~ 555 nm. However, fluorescence

responses of **23** at 555 nm for a definite sequence of ionic inputs in the form of Hg^{2+} and/or Cu^{2+} ion could be correlated for demonstrating a molecular level keypad lock.

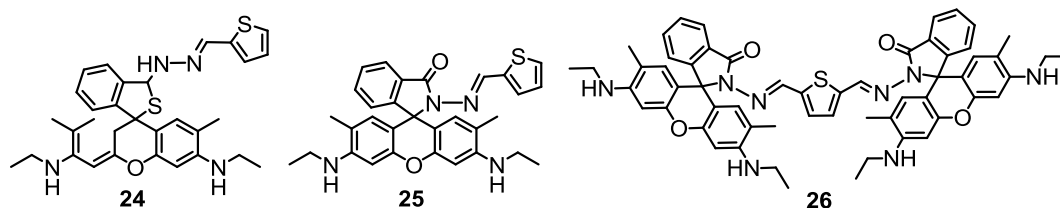


Figure 13. Structure of the chemosensors **24-26**.

Selective detection of Hg^{2+} in aqueous media was also reported by He and Duan et al. using a set of rhodamine based sensors, **24**, **25** and **26** (Figure 13), having thiophene moiety as one of the coordination mode.²⁷ In case of **24** and **26**, interference from Cu^{2+} and $\text{Pb}^{2+}/\text{Ag}^{+}$, respectively in the detection of Hg^{2+} ; whereas in case of **25** no such interference was observed. For **25**, a 1:2 ($\text{Hg}^{2+}:\mathbf{25}$) binding stoichiometry and relatively high binding constant ($K_a = 8.18 \times 10^7 \text{ M}^{-2}$) were observed. Reagent **24** also showed similar binding mode with high association constant ($K_a = 1.58 \times 10^{13} \text{ M}^{-2}$); while **26** showed 1:1 binding stoichiometry with moderate affinity constant ($4.8 \times 10^6 \text{ M}^{-1}$). Lowest detectable concentration for Hg^{2+} reported as low as ~ 1 ppb for **26**, which was lower than the limit set by various regulatory agencies (EPA or WHO) for safe drinking water.

Colorimetric and fluorescent *off-on* responses for a thiospirolactam-rhodamine derivative (**27**) (Figure 14) were reported for the detection of Hg^{2+} by Xu and his coworkers.²⁸ Moderate association constant for $\text{Hg}^{2+} \cdot \{\mathbf{27}\}_2$ ($K_a = 5.20 \times 10^5 \text{ M}^{-2}$) formation was estimated. This reagent could be used for *in vivo* imaging of Hg^{2+} present in Rat Schwann cells.

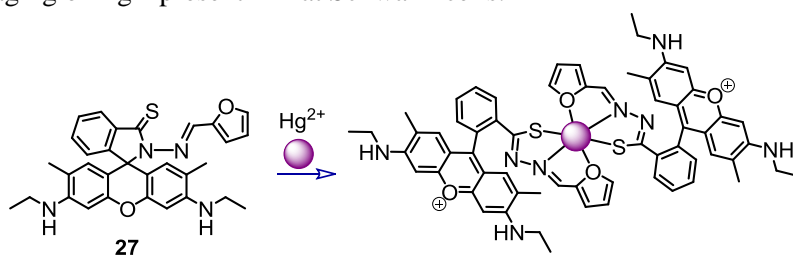


Figure 14. Structure of **27** and the possible binding mode for Hg^{2+} .

Recently, Das and his research group have reported a rhodamine 6G derivative (**28**), which showed changes in the absorption and emission spectral pattern with associated changes in visually detectable

solution colour and fluorescence, respectively, on specific binding to Hg^{2+} in $\text{CH}_3\text{OH}:\text{H}_2\text{O}$ medium (1:1, v/v; pH 7.0) (Figure 15).²⁹

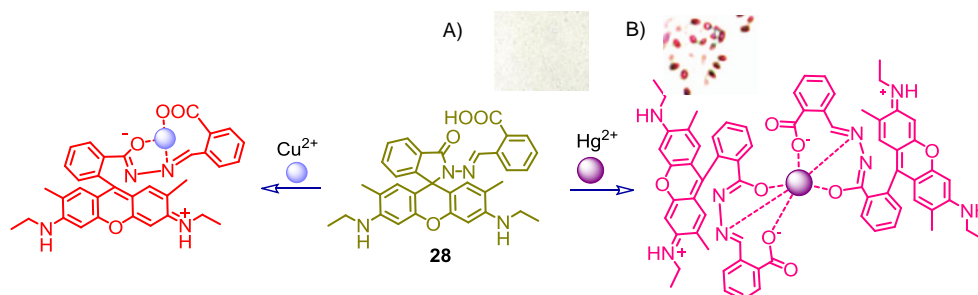


Figure 15. Binding mode of Hg^{2+} and Cu^{2+} with **28** in MeOH/Water (1:1, v/v, pH 7.0) [Inset: a) bacteria cells exposed to Hg^{2+} solution (10 μM); (b) cells exposed to aqueous solution of Hg^{2+} (10 μM) and then to a water-ethanol (7/3, v/v) solution of **28** (20 μM). Reprinted with permission from ref 29. Copyright 2008 American Chemical Society.

For Cu^{2+} , analogous changes in absorption spectra and solution colour were also observed. However, no new emission band beyond was observed on binding to Cu^{2+} following excitation at ~ 530 nm and this could be attributed to the paramagnetic effect of the unpaired $\text{Cu}^{\text{II}}\text{-d}^9$ electron. Observed binding stoichiometry for Cu^{2+} was 1:1, while that for Hg^{2+} was 1:2. The receptor **28** was found to be reversible with KI as the solution of 28.Hg^{2+} turned colourless due to formation of HgI_4^{2-} . The receptor **28** was further utilised as a staining as well as an imaging reagent for the detection of Hg^{2+} uptake in a bacteria for viewing through optical and fluorescence microscope, respectively.

Duan, Li and their associates have developed a water soluble rhodamine derivative (Figure 16) by tagging the hydrophilic glucose unit and this modified receptor could bind specifically to Hg^{2+} in aqueous medium following a 1:1 binding stoichiometry.³⁰

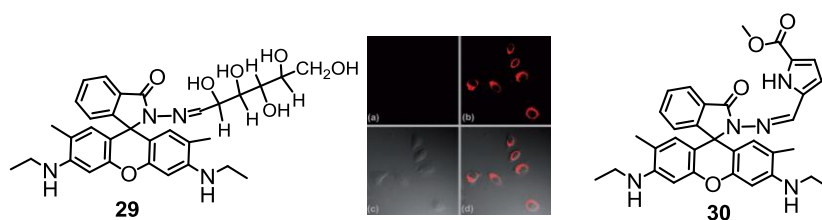


Figure 16. Molecular structure of the receptors **29** and **30** [Inset: a) Cells stained with 100 μM **29** for 10 min at 25°C, b) supplemented cells loaded with 10 μM $\text{Hg}(\text{NO}_3)_2$, c) bright field image and d) overlay image. Reprinted with permission from ref 30. Copyright 2009 Royal Society of Chemistry.

The lowest detection limit evaluated for Hg^{2+} detection was 1 ppb. The receptor **29** exhibited a very weak fluorescence at 550 nm, while on binding to Hg^{2+} , the corresponding xanthene a significant

enhancement in the emission band intensity was observed. The association constant determined from the emission titration was $(5.4 \pm 0.1) \times 10^5 \text{ M}^{-1}$. Reversibility of the binding process was established following treatment with Na_2S or NaI . Confocal laser microscopic studies revealed that this imaging reagent could detect Hg^{2+} uptake in HeLa cells from a solution having $[\text{Hg}^{2+}]$ as low as $10 \mu\text{M}$. The red fluorescence along the periphery of the cells indicated accumulation of Hg^{2+} at the cytosol.

Receptor **30** was reported by Tang, Nandhakumar and their co-workers (Figure 16).³¹ This reagent showed Cu^{2+} -specific enhancement in the intensity of the electronic spectra with maxima at $\sim 530 \text{ nm}$. Due to paramagnetic coupling, no change in emission was observed on binding to Cu^{2+} . In contrast, a significant enhancement in emission intensity at $\sim 550 \text{ nm}$ was observed for Hg^{2+} .

Ferrocene containing rhodamine 6G based multi responsive chemosensors, **31** and **32** were also developed by Duan's group for the recognition of Hg^{2+} in pure water medium (Figure 17).³² As anticipated, absorption and emission spectral data recorded for both receptors showed 'turn on' response on binding to Hg^{2+} for the generation of the corresponding acyclic xanthene forms. The emission quantum yield value for reagent **31** was evaluated as 0.38 at 550 nm when bound to Hg^{2+} .

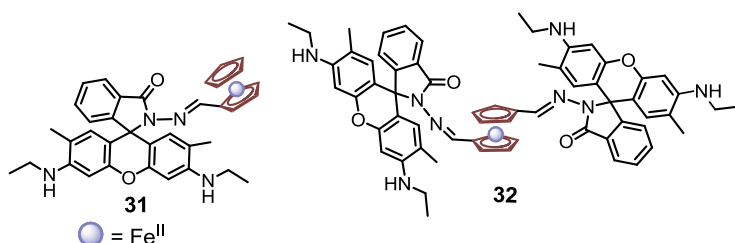


Figure 17. Multichannel receptors for the recognition of Hg^{2+} in natural water medium.

The Benesi-Hildebrand plot based on the ΔI (I is changes in emission intensity at 550 nm for **31**) from the systematic titration data confirmed the 1:1 binding stoichiometry with an association constant of $1.16 (\pm 0.04) \times 10^6 \text{ M}^{-1}$. Presence of Ferrocene unit allowed probing the binding process by monitoring the Fc/Fc^+ potential changes on binding to Hg^{2+} . An anodic shift of 50 mV for Fc/Fc^+ redox couple was observed on binding of **31** to Hg^{2+} . For the reagent **32** (Figure 17), changes were comparatively less, which signified a slight weaker binding of this reagent to Hg^{2+} . B-H plot revealed an association constant of $2.8 \pm 0.2 \times 10^5 \text{ M}^{-1}$ and a binding stoichiometry of 1:2. Cyclen (1,4,7,10-tetraazacyclododecane) could also be used as an additional binding site in a rhodamine derivative for the co-ordination

to a metal ion and accordingly, a new receptor **33** was used for studies for binding to Hg^{2+} (Figure 18).³³ B-H plot revealed a 1:2 binding stoichiometry and was also confirmed from the ESI-MS data. It showed a 1700 fold enhancement in the emission intensity at maxima of 580 nm upon addition of 10 equivalent of Hg^{2+} . Association constant was evaluated from the B-H plot and found to be $2.3 \times 10^8 \text{ M}^{-2}$. Ghosh and co-workers developed a bis-sulfonamide derivative of rhodamine B (**34**) for the selective recognition of Hg^{2+} and Cu^{2+} in $\text{CH}_3\text{CN}:\text{H}_2\text{O} = 4:1$, v/v (10 mM tris HCl buffer, pH 6.8) medium (Figure 18).³⁴ The colourless solution of **34** turned pinkish along with the increase in absorption at 555 nm in presence of both Hg^{2+} and Cu^{2+} ions due to the opening of the spirocyclic rings of rhodamine moieties. Again, on excitation at 510 nm, Cu^{2+} induced strong emission at 524 and 580 nm, however in case of Hg^{2+} there was ratiometric response, decrease in emission at 524 nm and moderate enhancement of emission at 580 nm. It was stated that **34** showed different emission response towards Hg^{2+} and Cu^{2+} due to the different binding behaviour of the receptor.



Figure 18. Molecular structures for receptors **33** [Inset: change in solution luminescence of **33** on binding to Hg^{2+} under Uv-light]; Structure of the chemosensor **34**. Reprinted with permission from ref 33. Copyright 2008 American Chemical Society.

Binding stoichiometry of 1:1 was evaluated for both Cu^{2+} and Hg^{2+} ions towards **34**. Binding constant for respective metal ion was evaluated from emission titration results ($(9.05 \pm 0.63) \times 10^4 \text{ M}^{-1}$ for Cu^{2+} and $(7.87 \pm 0.55) \times 10^4 \text{ M}^{-1}$ for Hg^{2+}). The reagent was also used as an imaging reagent for the detection of these ions in human cervical cancer (HeLa) cells.

Boronic acid based receptors **35** and **36** were reported by Yoon and his coworkers (Figure 19).³⁵ Both reagents showed 'on-off' type response on binding to Hg^{2+} in acetonitrile/aq.-HEPES buffer medium (9:1, v/v) following a 1:1 stoichiometry. Respective association constants of $3.3 \times 10^3 \text{ M}^{-1}$ and $2.1 \times 10^4 \text{ M}^{-1}$ were reported for reagents **35** and **36**. Presence of additional boronic acid moiety at the binding site could have contributed to the higher association constant of Receptor **36**.

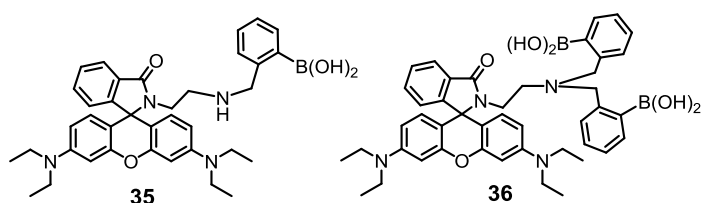


Figure 19. Bonoic acid containing rhodamine B derivatives for the recognition of Hg^{2+} in aqueous environment.

Das and co-workers developed a new rhodamine-based receptor (**37**; Figure 20) that was functionalized with an additional fluorophore (quinoline), which could selectively recognize Hg^{2+} with an interference of Cr^{3+} in an acetonitrile/HEPES buffer medium of pH 7.3.³⁶ **37** could be used as a dual probe and allowed detection of these two ions by probing changes in absorption and the fluorescence spectral pattern. In both instances, the extent of the changes was significant enough to allow visual detection. Interestingly, quinoline based emission was not observed either in **37** or in **37**. Hg^{2+} owing to C=N isomerization and intersystem crossing during the recognition of Hg^{2+} ions, respectively.

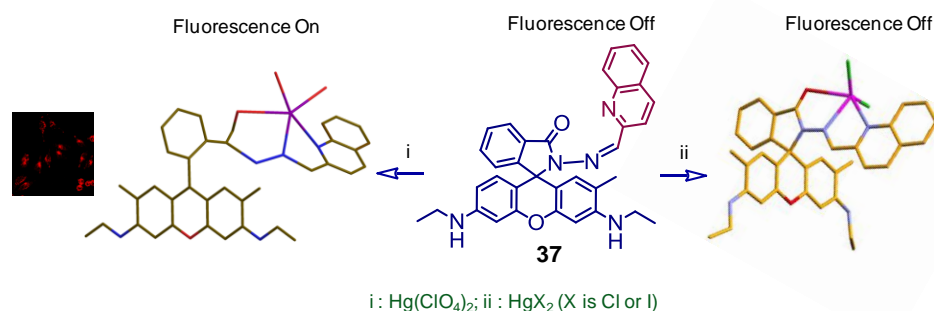


Figure 20. Receptor **37** showed spirolactam ring opening phenomenon with ionic $\text{Hg}(\text{II})$ salts but could not show similar property with covalent $\text{Hg}(\text{II})$ salts [Inset: Dark field image of MCF7 cells with **37** (4.0 μM) and ionic Hg^{2+} (2.0 μM)]. Reprinted with permission from ref 36. Copyright 2012 American Chemical Society.

More importantly, the receptor molecule could be used as an imaging reagent for detection of Hg^{2+} uptake in live human cancer cells (MCF7) using laser confocal microscopic studies. Unlike $\text{Hg}(\text{ClO}_4)_2$ or $\text{Hg}(\text{NO}_3)_2$ salts, HgCl_2 or HgI_2 failed to induce any visually detectable change in colour or fluorescence upon interaction with **37** under identical experimental conditions. Presumably, the higher covalent nature of $\text{Hg}(\text{II})$ in HgCl_2 or HgI_2 accounts for its lower acidity and its inability to open up the spirolactam ring of the reagent **37**. The issue had been addressed on the basis of the single-crystal X-ray structures of $\text{37} \cdot \text{HgX}_2$ ($\text{X}^- = \text{Cl}^-$ or I^-) and results from other spectral studies. Thus, this article

also revealed the role of the metal ion acidity in effectively opening the spirolactam ring of the rhodamine derivatives.

A new tripodal receptor **38** (Figure 21) was reported by Ghosh and co-workers, which could selectively recognize Hg^{2+} ions in CH_3CN -water (4 : 1, v/v; 10 μM tris HCl buffer, pH 7.0) medium.³⁷ Upon gradual addition of Hg^{2+} emission at 536 nm was quenched and a new emission was observed at 580 nm. Author proposed that the ratiometric response of **38** towards the Hg^{2+} ion was attributed to the involvement of the binding centre in different ways (Figure 21). A binding stoichiometry of 1:1 was proposed with binding constant of $6.31 \pm 0.74) \times 10^5 \text{ M}^{-1}$ between **38** and Hg^{2+} . Further the receptor showed *in vitro* detection of Hg^{2+} ions in human cervical cancer (HeLa) cells. However, one major limitation of this reagent was the non-specific binding to most transition metal ions with a binding constant lower by an order of magnitude as compared to that for Hg^{2+} .

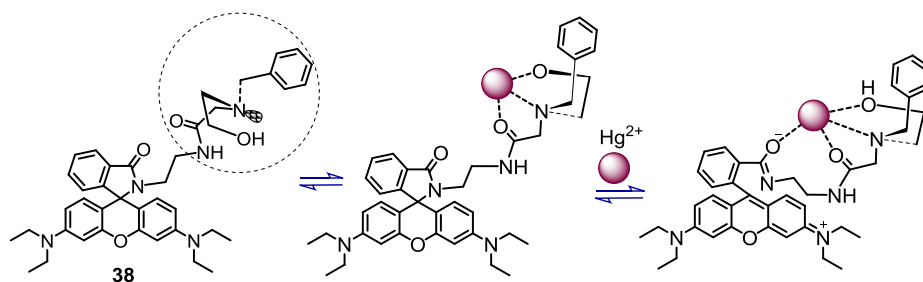


Figure 21. Structure of **38** and the possible binding modes for Hg^{2+} .

Li et. al. introduced hydrazinobenzothiazole unit in rhodamine systems **39** (Figure 22A) for the development of first six-membered spirocycle ring for the recognition of Hg^{2+} in ethanol/ PBS buffer (4:6, pH 7.4).³⁸ A change in emission enhancement of 1000 fold with the quantum yield of 0.87 was observed for Hg^{2+} while the reported lower detection limit was 30 nM. The observed association constant was $1.02 \times 10^6 \text{ M}^{-1}$ with binding stoichiometry 1:1. However, receptor **39** showed some affinity towards Ag^+ ions under the experiment condition. Probe **39** was further used to map the sorption of Hg^{2+} to bacteria-EPS-mineral aggregates under anoxic condition and absorption of Hg^{2+} on the cell surface was confirmed from the overlay of fluorescence and reflection image.

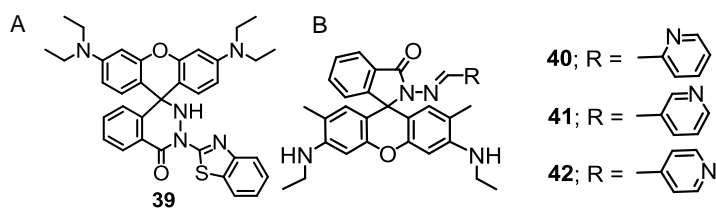


Figure 22. (A) Structure of six-membered spirocycle containing rhodamine **39** for Hg^{2+} recognition. (B) Structure of the rhodamine derivatives **40**, **41** and **42**.

Bhattacharya and coworkers developed rhodamine based positional isomers (**40**, **41** and **42**; Figure 22B) for the detection of metal ions in aqueous medium.³⁹ The chemosensor **40**, with pyridine nitrogen at *o*-position, showed a selective response towards Cu(II), whereas **41** and **42** with pyridine nitrogen at *m*- and *p*- position, respectively, could show specificity towards Hg^{2+} among various cations tested. The colourless solution of **41** and **42** became pink in presence of Hg^{2+} typically with the appearance of new absorbance maxima at 530 nm due to the opening of the spirocyclic ring of these rhodamine derivatives, while the associated emission maxima appeared at 560 nm ($\lambda_{\text{ex}} = 520$ nm). A 1:1 binding stoichiometry was evaluated for binding with Hg^{2+} for both **41** ($\log K = 3.7$) and **42** ($\log K = 3.91$). Lowest detection limits reported for Hg^{2+} for receptors **41** and **42** were 9.4 and 4 ppb, respectively. Further the sensitivity of Hg^{2+} ion recognition by probes **41** and **42** in the presence of excess of plasma protein (BSA) and human blood serum was also investigated.

Among different non-radiative energy transfer processes between two fluorophores, resonance energy transfer (RET) is the most common and important one. RET is a distance dependent physical process by which energy is transferred non-radiatively from an excited molecular fluorophore (the donor) to another fluorophore (the acceptor) by means of intermolecular long-range dipole-dipole coupling. The use of the RET process for the design of a molecular probe is generally preferred, as this help in overcoming the problems posed by phenomena like photo bleaching and aggregated self-quenching.

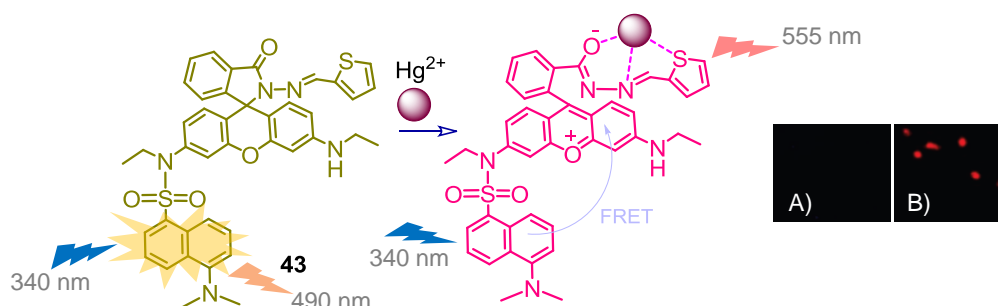


Figure 23. Resonance energy transferring probe during the recognition of Hg^{2+} in Acetonitrile/ Water medium (1:1, v/v) [Inset Use of receptor **43** for the recognition of Hg^{2+} within the *Pseudomonas putida* bacteria viewed under confocal laser microscopy; a) only **43** in the cells, b) **43** in presence of Hg^{2+} within the cells]. Reprinted with permission from ref 40. Copyright 2009 American Chemical Society.

Receptor **43** is a good demonstration of a RET-based reagent, where resonance energy had been transferred from dansyl to xanthene form of the rhodamine moiety on binding to a Hg^{2+} in $\text{CH}_3\text{CN}/\text{water}$ medium (Figure 23).⁴⁰ The RET was confirmed from the rhodamine-based emission observed at 555 nm on excitation at the absorption maxima (λ_{ext} 340 nm) of the dansyl unit. The singlet-singlet energy transfer efficiency (Φ_{ET}) and the rate constant for the energy transfer process between dansyl to ring opened rhodamine acceptor was 83% and $2.84 \times 10^8 \text{ s}^{-1}$, respectively. A moderate association constant of $(5.0 \pm 0.2) \times 10^4 \text{ M}^{-1}$ was evaluated for Hg^{2+} , while this reagent showed a very weak interference from Cu^{2+} . Receptor **43** could detect Hg^{2+} as low as 0.1 ppm level and also could be used as a staining agent for detection of uptake Hg^{2+} in *Pseudomonas putida* bacteria. FRET process was also effectively used by Zeng and co-workers; designing another ratiometric sensor, **44** (Figure 24) for detection of Hg^{2+} ion.⁴¹ FRET process thus achieved was a nice demonstration of self-assembly process that brought the donor and acceptor moieties together.

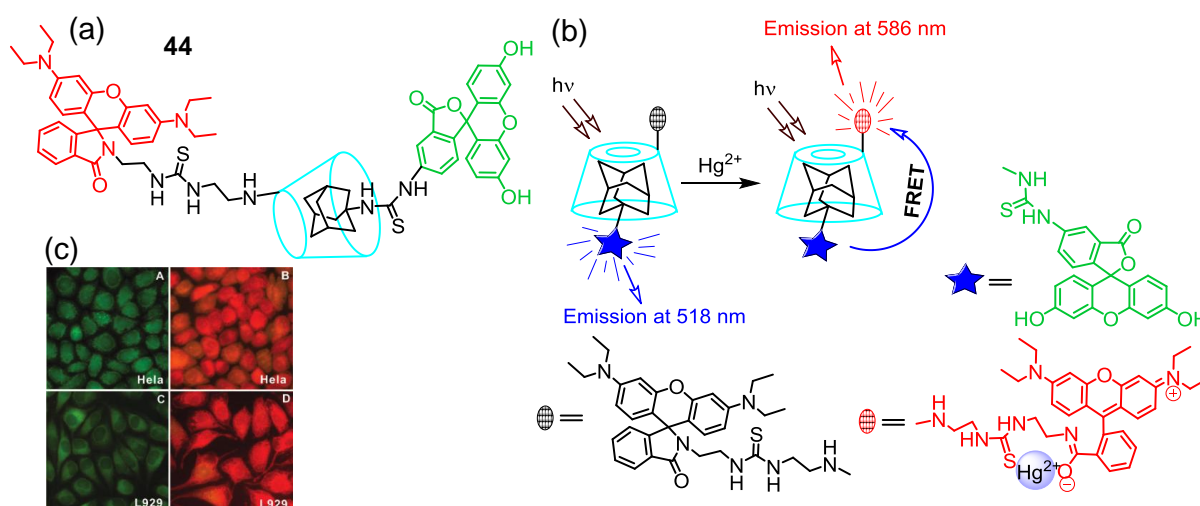


Figure 24. (a) Structure of the chemosensor **44**; (b) Cartoon representation for the FRET-based ratiometric sensing system for Hg^{2+} with $\beta\text{-CD}$ as vehicle; (c) Fluorescence microscope imaging of HeLa and L929 cells stained with CD-based sensor before (A, C) and after (B, D) these were pre-exposed to 1 ppm of Hg^{2+} . Reprinted with permission from ref 41. Copyright 2010 American Chemical Society.

Adamantyl group in aqueous medium is known to form inclusion complex with $\beta\text{-CD}$ and this was used to assemble the donor-acceptor units. On addition of Hg^{2+} , ring-opening process took place and on excitation of the donor at 495 nm (with $\lambda_{\text{Ems}} = 518 \text{ nm}$) FRET process became effective with

acceptor Hg^{2+} -bound rhodamine based emission at 586 nm appeared. The detection limit for Hg^{2+} were determined to be 10 nM; while binding constant of $5.3 \times 10^7 \text{ M}^{-1}$ was evaluated for 1:1 binding stoichiometry. Untreated both HeLa and L929 cells, as well as pre-exposed (and washed) with Hg^{2+} were subsequently stained with **44**; while a fluorescence change from green for untreated to red for cells pre-exposed to Hg^{2+} was observed. This confirmed that the FRET process was operational even in live cells.

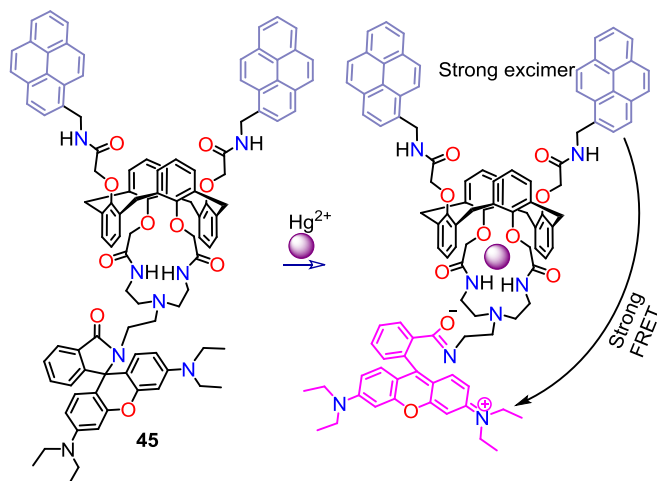


Figure 25. Structure of the chemosensor **45** and Hg^{2+} induced FRET response.

A calix[4]arene derivative-based chemosensor (**45**) was reported by Kim et al. (Figure 25).⁴² A strong spectral overlap between pyrene excimer emission band and rhodamine ring-opened absorption band was observed and initiated a FRET-based response on selective binding to Hg^{2+} ion with an enhancement of emission at 576 nm ($\lambda_{\text{ext}} = 343 \text{ nm}$).

More recently, Das and co-workers developed new rhodamine based chemosensors, **46** and **47** (Figure 26), which were found to show preferences towards Hg^{2+} and Cr^{3+} in presence of large excess of all other competing transition metal ions.⁴³ Specific binding of this reagent either to Hg^{2+} or Cr^{3+} resulted associated changes in their optical and fluorescence spectral behavior, which were significant enough to allow their visual detection. For the reagent **46**, the lower detection limit was even lower than the permissible [Hg^{2+}] or [Cr^{3+}] in safe drinking water as per the standard U.S. EPA norms.

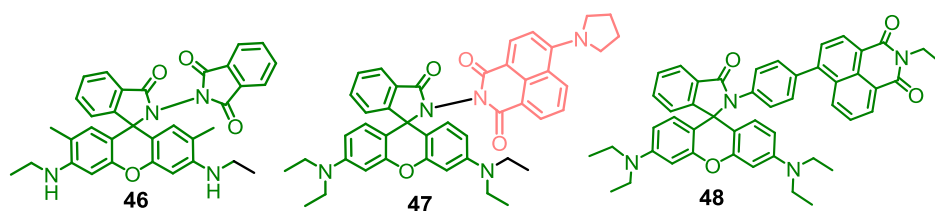


Figure 26. Structure of the chemosensors **46**, **47** and **48**.

While the other receptor **47** could be used as a ratiometric sensor for detection of Hg^{2+} and Cr^{3+} based on the resonance energy transfer (RET) process involving the donor naphthalimide and the acceptor $\text{Hg}^{2+}/\text{Cr}^{3+}$ -bound xanthene fragment. Further, confocal laser microscopic studies confirmed that the reagent **47** could also be used as an imaging probe for detection of uptake of these ions in A431 cells. Reagent **46** was actually synthesized to establish the binding mode while results of reagent **46** and **47** were compared to establish the FRET-based luminescence responses on binding to Hg^{2+} or Cr^{3+} . Authors could also demonstrate that by using an appropriate masking agent (KI), it was further possible to evaluate the concentration of individual metal ions in the solution having a mixture of these two ions. Higher affinity of I^- towards Hg^{2+} lead to the formation of HgI_4^{2-} and allowed the binding of Cr^{3+} to these set of reagents.

Another well-known energy transfer mechanism, through bond energy transfer (TBET), was also utilized for the recognition of Hg^{2+} ions. Unlike RET process, TBET process does not require the spectral overlap between donor emission and acceptor absorption bands and often leads to large pseudo stokes-shifts (~ 200 nm) within rigid system. Most recently, Kumar et al. established a TBET-based chemosensor, **48**, by combining naphthalimide and rhodamine through a conjugated spacer.⁴⁴ Upon addition of Hg^{2+} , to the THF- H_2O (9.5:0.5, v/v) medium of **48** (Figure 26) a new absorption band appeared at 565 nm along with a colour change from colourless to pink, and an emission band characteristic of ring-opened rhodamine also appeared at 578 nm when the chemosensor was excited at 360 nm. Detection limit of 2×10^{-6} M for Hg^{2+} and a 1:1 stoichiometry for the binding mode with a binding constant of $7.1 \times 10^4 \text{ M}^{-1}$ were evaluated. The authors described **48** as a potential fluorescence imaging agent for the detection of Hg^{2+} in live prostate cancer (PC3) cells.

The same group have recently developed a pentaquinone-rhodamine conjugate **49** for the recognition of Hg^{2+} ions in THF-water medium (9.5:0.5, v/v) (Figure 27).⁴⁵ The UV-vis spectrum of **49** exhibits

absorption bands at 275 nm and 322 nm in THF/H₂O due to electronic transitions associated with pentaquinone moiety.

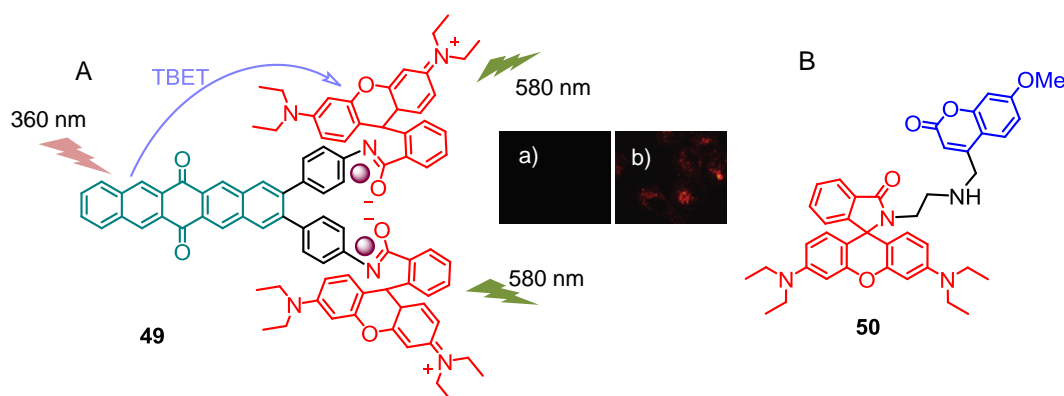


Figure 27. (A) Rhodamine based reversible receptor for the recognition of Hg²⁺ showing TBET mechanism [Inset: PC3 cell lines a) with receptor **49** (1.0 μM), b) in presence of Hg²⁺ (30.0 μM)]. Reprinted with permission from ref 45. Copyright 2012 American Chemical Society. (B) Structure of the chemosensor **50**.

However, upon the addition of Hg²⁺ ions (0-200 mole equivalent), the intensity of these absorption bands was found to increase, however, along with these a new absorption appeared at 554 nm and the solution colour turned pink. Further, on excitation at 360 nm, an intense emission band at 582 nm was observed in presence of Hg²⁺ due to the transfer of resonance energy from pentaquinone to rhodamine via through bond pathway. TBET mechanism was established based on studies with relevant model systems. This reagent could even be used as an imaging reagent for the detection of Hg²⁺ in PC3 cell lines by confocal laser microscopy. Lowest [Hg²⁺] that this reagent could detect was found to be 0.14 ppb, which is lower than the safe limit for [Hg²⁺] for safe drinking water.

Das et al. reported an unique example of interrupted PET coupled TBET phenomena for the selective recognition of Hg²⁺ in MeOH-aq. HEPES buffer (1:1, v/v) (pH 7.2) using a new coumarin-rhodamine conjugate **50** (Figure 27B).⁴⁶ It showed simultaneous enhancement of coumarin based emission at 402 nm and rhodamine based emission at 585 nm ($\lambda_{\text{Ext}} = 320$ nm) upon Hg²⁺ binding. Binding of the Hg²⁺ to the pendant anime moiety (coupled to coumarine fragment) resulted an interruption of PET process and a switched on luminescence response from the coumarine fragment, which in turn initiated a TBET process from Hg²⁺-bound coumarin moiety to the acceptor Hg²⁺-bound rhodamine fragment in Hg²⁺.**50**. The photophysical phenomenon was rationalized based on the luminescence responses of two

appropriate model compounds under identical experimental conditions. Benesi–Hildebrand plot of the emission titration results established a 1:1 stoichiometry with an association constant of $7.3 (\pm 0.6) \times 10^4 \text{ M}^{-1}$ between **50** and Hg^{2+} . Further **50** could be used as an imaging reagent for determining intracellular distribution of Hg^{2+} in MCF7 cells exposed to $[\text{Hg}^{2+}]$ as low as 2 ppb.

Bhalla and Kumar et al. developed two hexaphenylbenzene (HPB) derivatives (**51** and **52**) having rhodamine B moiety for the selective recognition Hg^{2+} in both polar aprotic (CH_3CN and THF) and protic medium (MeOH) (Figure 28).⁴⁷

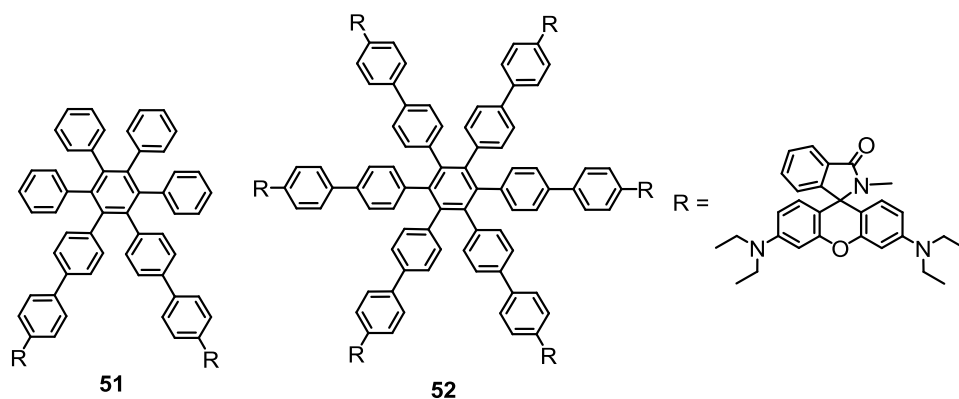


Figure 28. Structures of the chemosensors **51** and **52**.

For both reagents, binding to Hg^{2+} ion resulted opening of the spirolactam ring with a new strong absorption band that had a distinct spectral overlap with the emission band of the HPB moiety ($\lambda_{\text{Ext}} = 290 \text{ nm}$). This accounted for a nonradiative energy transfer from donor HPB moiety to the Hg^{2+} bound rhodamine moiety as the acceptor, which resulted a strong rhodamine based luminescence band with maxima at 585 nm. This resulted a large pseudo-stokes shift of 295 nm. The energy transfer efficiency was better in CH_3CN than THF medium for both **51** and **52**. CH_3CN being a better coordinating solvent, reduced the efficiency of the complexation of Hg^{2+} ion with the rhodamine based receptor. Further these receptors showed through bond energy transfer (TBET) in polar protic solvent MeOH. Receptor **51** displayed higher through bond energy transfer efficiency compared to **52** in the presence of Hg^{2+} ions. Higher conjugation between the donor and acceptor moieties in **52** was accounted for the weaker TBET efficiency in comparison to **51**.

Fluorogenic receptors for Hg^{2+} other than rhodamine

Highly fluorescent 4,4-difluoro-4-bora-3a,4a-diaza-s-indacene (better known as BODIPY, difluoroborondipyrromethene)⁴⁸ derivatives are one of the most popular dye molecules that are being used in biological labelling and electroluminescent devices. It has uses as a fluorescence-based signaling moiety for recognition studies for their rich photo-physical properties. The BODIPY derivatives show relatively high molar absorption coefficient (ϵ), emission quantum yield (Φ) and negligible triplet state formation. These molecules generally have excitation/emission wavelength in visible region fairly stable excited states (τ in the in nano-second time range). Apart from these, synthetic accessibility of various derivatives, good solubility in common solvents, resistance towards self-aggregation in solution has actually made this class of molecule a popular choice for the researchers.

BODIPY fluorophore with the binding site azadioxadithia-15-crown-5-chelator could effectively recognized Hg^{2+} ions. Thus, receptor **53** was designed with two BODIPY units: one as donor and another as an acceptor, while thio-crown ether moiety acted as the receptor fragment for Hg^{2+} ions (Figure 29).⁴⁹ The binding of Hg^{2+} caused blue shifts in the absorption spectrum of the longer wavelength dye. This fact increased the spectral overlap between donor emission and acceptor absorption and thus, the FRET response. As anticipated, a 1:1 complexation with Hg^{2+} with the dissociation constant of $4.5 \times 10^{-7} \text{ M}$ was evaluated in THF medium. Analogous azadioxadithia crown derivative containing receptor **54** in BODIPY system was reported by Zhu et al.⁵⁰ for the recognition of Hg^{2+} (Figure 29). Receptor absorbed at 606 nm while its emission was at 668 nm with very low quantum yield.

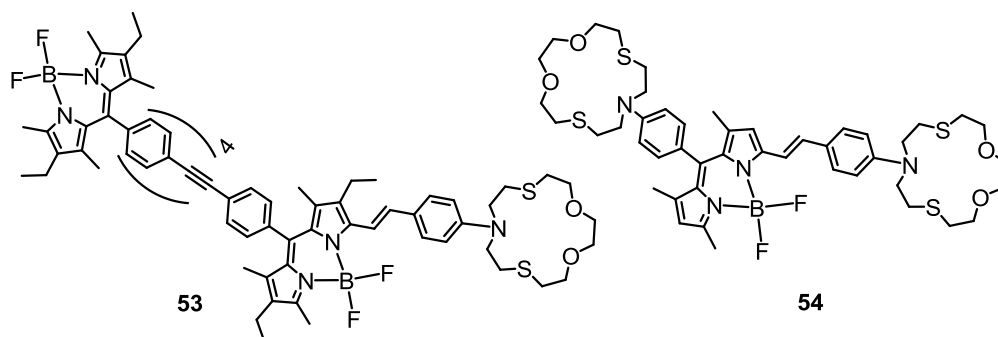


Figure 29. Chemosensors with azadioxadithia-15-crown-5 as a cheater for Hg^{2+} ion recognition.

Addition of Hg^{2+} resulted disappearance of the band at 660 nm with concomitant growth of the band at 564 nm with change in colour from purple to pink-red. On the other hand generation of a new emission band at 578 nm with 7-fold with a hypsochromic shift was observed. These spectral changes were ideally suited for ratiometric fluorescent detection. The coordination of Hg^{2+} to the macro cyclic moiety did not favor the ICT process and this result the observed blue shifts in optical spectra. Another similar BODIPY based receptor, **55**, was developed for the recognition of Hg^{2+} ions in THF medium (Figure 30).⁵¹

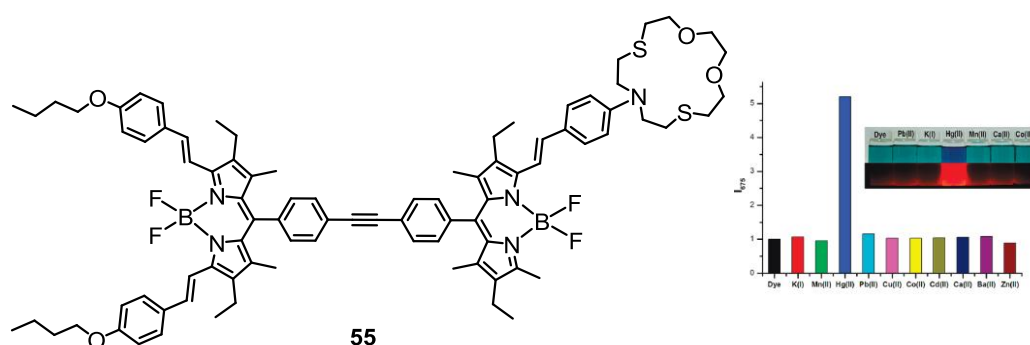


Figure 30. Receptor **55** for the recognition of Hg^{2+} in THF medium [Inset: Change in colouration in presence of Hg^{2+} on excitation with Uv-lamp of wavelength 354 nm and relative intensity changed for Hg^{2+} ions compared to other ions]. Reprinted with permission from ref 51. Copyright 2009 American Chemical Society.

Titration of **55** was performed with Hg^{2+} revealed that the two overlapping absorption spectral bands got resolved as ICT process was interrupted due to coordination of Hg^{2+} to the aza-crown ether moiety. Emission intensity at 675 nm was found to increase gradually on increasing the $[\text{Hg}^{2+}]$. The Benesi-Hildebrand plot revealed the 1:1 binding stoichiometry with the association constant of $7.8 \times 10^5 \text{ M}^{-1}$.

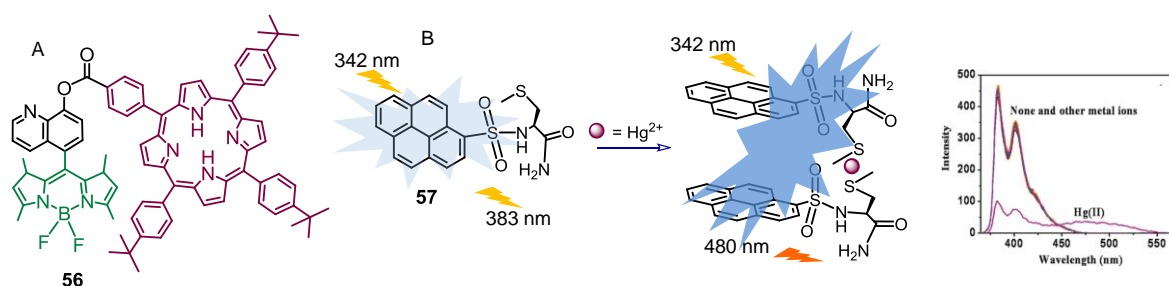


Figure 31. A) BODIPY-porphyrin based versatile fluorescence resonance energy transfer (FRET) ratiometric sensor for Hg^{2+} . B) Pyrene based receptor for Hg^{2+} recognition with excimer formation [emission scanning with different metal ions]. Reprinted with permission from ref 53. Copyright 2011 American Chemical Society.

Receptor **56** was synthesized from BODIPY and Porphyrin, which showed an appreciable spectral overlap between two dyes with larger pseudo-stoke's shifts (Figure 31A).⁵² Also, the FRET process

helped in nullifying the back-scattering problem. 8-hydroxy quinoline benzoate moiety acted as the binding site and also favoured the energy transfer process during the recognition of Hg^{2+} and Fe^{2+} ions. Authors attributed the absorption band at 506 nm to a BODIPY based CT transition, while bands at 420 nm, 550 nm, 591 nm and 648 nm were attributed to porphyrin-based transitions and comparison of the spectra of **56** with those of individual components revealed absence of any ground state interaction. Energy transfer efficiency was found to be 95.4% on binding to Hg^{2+} . Binding stoichiometry of 1:1 and an association constant of $3.5 \times 10^6 \text{ M}^{-1}$ in DMF/MeOH medium (98:2) were reported.

Receptor **57** showed two emission bands at 383 nm and 402 nm corresponds to an individual pyrene emission, while addition of Hg^{2+} lead to the growth of new emission band at 480 nm with lowering the monomer based emissions with an isoemissive point at 443 nm (Figure 31B).⁵³ These emission responses at 383 and 480 nm were found to be ratiometric and could be used for the recognition of Hg^{2+} in 10 mM aq. HEPES buffer-DMF (98:2, v/v) solution of pH 7.4.

Histidine has affinity for Cu^{2+} ions but its selectivity could be changed by introducing the bis-dithiocarbamate moiety and accordingly, receptor **58** was designed (Figure 32).⁵⁴ Receptor **58** showed significant enhancement in emission intensity with 50 nm blue shift (from 590 nm to 540 nm) in the emission maxima in presence of Hg^{2+} in $\text{CH}_3\text{OH-H}_2\text{O}$ (80:20, v/v with 1% Acetonitrile as co-solvent, pH = 7.0) medium with associated change in visually detectable solution fluorescence from red to green on irradiation with 354 nm lamp. The enhancement of Quantum yield (Φ) value was found to increase from 0.022 to 0.402 at 540 nm. Respective binding stoichiometry and association constant was evaluated as 1:1 and $1.25 (\pm 0.4) \times 10^6 \text{ M}^{-1}$. Authors could even prepare a strip, which could be successfully used for the detection of Hg^{2+} in aqueous medium. Also, this could be used as an imaging reagent for detection of the Hg^{2+} uptake in HeLa cells as well as in Zebra fish, exposed to a solution having $[\text{Hg}^{2+}]$ of 10 μM .

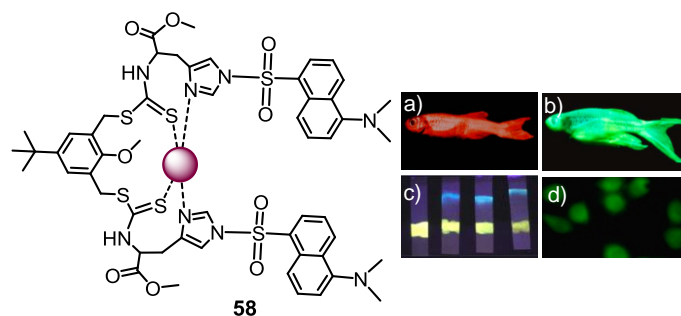


Figure 32. Binding mode of Hg^{2+} in bipodal system [Inset: a) Zebra fish with 10 μM of **58**, b) with 10 μM of **58** and 10 μM of Hg^{2+} ; c) Photographs of the paper strip based sensing with HgNO_3 solutions (left to right): Hg^{2+} 10 μM , 100 μM , and 1 mM Hg^{2+} in aqueous medium buffered at pH 7.0 with HEPES (1 mM) at 25 $^\circ\text{C}$; d) HeLa cells in presence of 10 μM Hg^{2+} viewed under confocal microscopy]. Reprinted with permission from ref 54. Copyright 2012 American Chemical Society.

Quinoline based receptor having azine groups also showed ability to detect Hg^{2+} in THF/ aq-phosphate buffer medium (6:4, v/v; pH = 7.2).⁵⁵ The receptor **59** showed two main absorptions bands at 265 nm and 330 nm, which were attributed to the ^1A to $^1\text{L}_a$ and ^1A to $^1\text{L}_b$ transitions (Figure 33). Electronic spectral studies revealed that on gradual addition of Hg^{2+} , the band at 330 nm was bleached and a new band at 370 nm was developed. Receptor **59** showed only a weak emission at 406 nm.

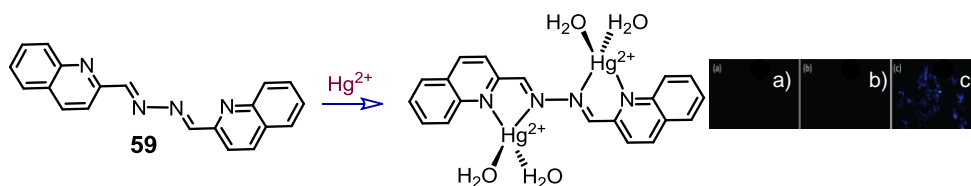


Figure 33. Detection of Hg^{2+} with azine based receptors [Inset: a) KB cells, b) KB cells with **59** (10 μM) and c) 40 μM Hg^{2+} . Reprinted with permission from ref 55. Copyright 2010 American Chemical Society.

The initial weak emission band at 406 nm was enhanced on binding to Hg^{2+} ion. The restricted of C=N isomerization and thereby the restricted conformational flexibility due to coordination to Hg^{2+} was accounted for this fluorescence enhancement and an almost *switch on* responses. The binding stoichiometry of 1:2 was confirmed from job's plot as well as from X-ray crystallography. Receptor **59** could further be used for the recognition of Hg^{2+} in live HeLa cells when viewed under confocal microscopy.

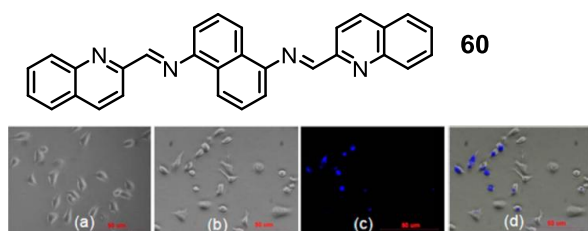


Figure 34. Restricted imine isomerisation showing turn on response in emission in presence of Hg^{2+} of the compound **60** [Inset: Bright field transmission of living HeLa cells incubated with (a) **60** (20 μM) and (b) **60** (20 μM) with Hg^{2+} (10 μM); (c) fluorescence image of HeLa cells incubated with **60** (20 μM) with Hg^{2+} (10 μM); (d) merged image of (b) and (c)]. Reprinted with permission from ref 56. Copyright 2012 American Chemical Society.

Analogous imine-based receptor **60** was also used for specific recognition of Hg^{2+} with ‘turn-on’ fluorescence response (Figure 34).⁵⁶ Receptor **60** showed three bands in absorption spectra at 255 nm, 295 nm and 385 nm of which first two were assigned to the naphthalene and quinolone based inter component charge transfer bands, respectively, and the remaining band at longer wavelength was attributed to a CT transition involving naphthalene donor and quinoline acceptor in THF/ phosphate buffer (6:4, pH 7.4) solution. Solution fluorescence was found to be very weak following excitation at either 255 nm or at 295 nm. PET process involving the lone pair of electrons of nitrogen quenched the quinoline based emission. Coordination to Hg^{2+} led to a ‘turn on’ emission response due to the interrupted PET process and the imine rotation. Reversibility in binding of Hg^{2+} to **60** was established by the follow-up treatment with KI. This reagent also could be used for the detection of Hg^{2+} uptake in HeLa cells exposed to a solution having $[\text{Hg}^{2+}]$ of 20 μM .

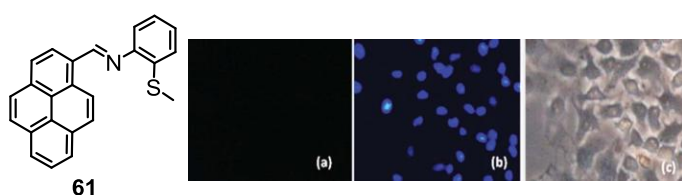


Figure 35. Structure of the chemosensor **61**. Confocal microscopic images of *candida albicans* cells incubated with (a) **61** for 30 min, (b) **61** and 10 mM of Hg^{2+} and (c) a bright field image of probe treated *candida albicans* cells. Reprinted with permission from ref 57. Copyright 2012 Royal Society of Chemistry.

Chellappa and co-workers developed a new pyrene based ‘turn on’ fluorescent chemosensor **61** (Figure 37) which showed significantly enhanced fluorescence intensity on specific binding to Hg^{2+} ions in aq. acetonitrile (30:70, v/v) medium.⁵⁷ Binding of Hg^{2+} to **61** caused an interruption in the PET process involving imino nitrogen as well as from the restriction in C=N isomerism. An intermolecular excimer formation resulted a strong excimer emission at 462 nm ($\lambda_{\text{Ext}} = 365$ nm). Job’s plot and mass

spectral analysis confirmed the 1:1 complex formation with an association constant of $(1.02 \pm 0.102) \times 10^4 \text{ M}^{-1}$. Further **61** could also be used as an imaging reagent for detection of Hg^{2+} present in live *candida albicans* cells.

A unique symmetric fluorescent turn-on and ratiometric chemosensor **62** (Figure 36) was synthesized by Lee and co-workers from cystine dimer, having two dansyl groups, for the selective detection of Hg^{2+} in 100% aqueous medium.⁵⁸ Upon increase in $[\text{Hg}^{2+}]$, a 34 nm blue shift in the emission maxima of **62** in HEPES buffer solution (pH = 7.4) was observed with a 3 fold enhancement in emission intensity. A ratiometric response towards Hg^{2+} with a significant increase of the emission intensity around 507 nm and decrease at 583 nm was observed. A 1:1 stoichiometry was established from Job's plot analysis and a high dissociation constant of $4.12 \times 10^{-8} \text{ M}$ was obtained from non-linear least square fitting of the emission titration results. This reagent was also found to be sensitive and the lower detection limit (10 nM) for Hg^{2+} was much lower than the permissible level as per the EPA norms for safe drinking water.

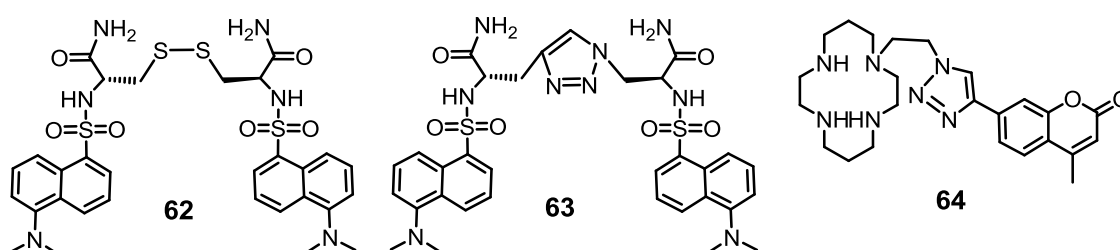


Figure 36. Structures of the chemosensors **62**, **63** and **64**.

Same research group developed another dansylsulphonamide based fluorescent sensor **63** bearing a triazole group was synthesized by solid phase synthesis using click chemistry (Figure 36).⁵⁹ Aqueous solution of **63** showed emission at 530 nm upon excitation at 330 nm which was blue shifted to 530 nm with a decrease in emission intensity in presence of Hg^{2+} ions. Among various ions tested it showed slight decrease in emission intensity only in presence of Cu^{2+} due to the interaction between the triazole unit and Cu^{2+} ion. The 1:1 complexation between the **63** and Hg^{2+} was confirmed by Job's plot and EMI-MS studies. The dissociation constant for Hg^{2+} in aqueous solution was calculated to be 672 nM by the non-linear curve fitting procedure using the emission titration results. ¹HNMR and

UV-Vis spectral analysis revealed that two sulfonamide and triazole groups of **64** played a critical role in the interactions with Hg^{2+} . The sensor showed Hg^{2+} detection limit of 96 nM in aqueous medium. Further **63** could penetrate live cells and able to detect the intracellular Hg^{2+} ions confirmed by confocal fluorescence imaging technique.

Todd and Rutledge et al. reported a cyclam-based fluorescent sensor with a appended triazole moiety having a coumarin unit **64** (Figure 36).⁶⁰ This reagent showed preference towards Hg^{2+} and Cu^{2+} in neutral aqueous solution.⁶⁰ Upon binding of Cu^{2+} and Hg^{2+} ions to the cyclam unit, the coumarin based emission of **64** was quenched, which was accounted for the paramagnetic and the effective spin-orbit coupling, respectively. Fluorescence titrations of **64** with Cu^{2+} and Hg^{2+} confirmed the anticipated 1:1 binding stoichiometry; while association constants of $2.2 \pm (0.3) \times 10^8$ and $7.1 \pm (0.8) \times 10^7 \text{ M}^{-1}$ were estimated for Cu^{2+} and Hg^{2+} , respectively. The addition of specific anions such as I^- and $\text{S}_2\text{O}_3^{2-}$ causes a complete revival of fluorescence only in the case of Hg^{2+} , providing a simple and effective method for distinguishing solutions containing Cu^{2+} , Hg^{2+} or a mixture of both ions, even in doped seawater samples. X-ray crystal structures confirmed that pendant triazole coordination occurred through the central nitrogen atom. Fluorescence, mass spectrometry and ^1H NMR experiments revealed that the mechanism of anion-induced fluorescence revival involved either displacement of pendant coordination or complete removal of the Hg^{2+} from the macrocycle, depending on the anion.

Considering the fact that in-field Hg^{2+} detection are crucial for screening of environmental and industrial samples, Zaccheroni and et al. developed three new coumarin-based fluorescent chemosensors (**65-67**) having mixed thia/aza macrocyclic framework as receptors unit (Figure 37).⁶¹ These probes revealed an fluorescence *ON* response on specific binding to Hg^{2+} in MeCN/ H_2O 4:1 (v/v) medium. This reagent was further used as an *in-vitro* imaging reagent for detection cellular uptake of Hg^{2+} ions in Cos-7(Figure 37). More importantly when included in silica core-polyethylene glycol (PEG) shell nanoparticles or supported on polyvinyl chloride (PVC)-based polymeric membranes, ligands (**65-67**) could also selectively sense Hg^{2+} ions in pure neutral water sample. They have also developed an optical sensing array tacking advantage of the fluorescent properties of ligand **67** based on the computer screen photo assisted technique (CSPT). The obtained results showed that

by using membranes prepared with ligand **67** they could determine the Hg^{2+} content in water samples in concentrations that is well below the maximal presence recommended by WHO and EPA for safe drinking water.

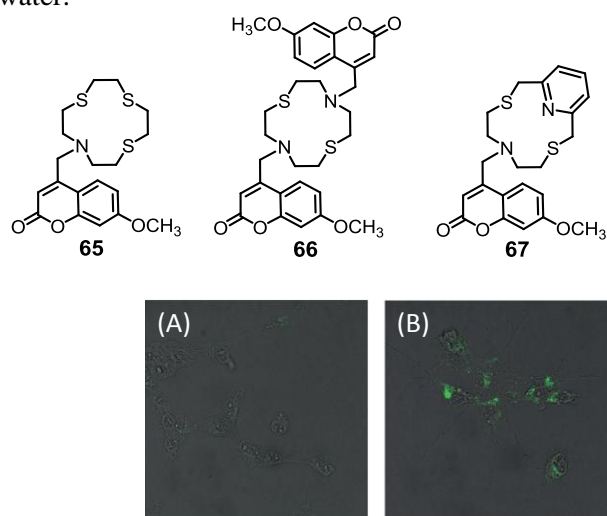


Figure 37. Chemical structure of the fluorescent probes (**65-67**) and (A) Confocal visualization of a Cos-7 cell culture pre-incubated with ligand **67** and b) pre-incubated with Hg^{2+} ions and successively treated with ligand **67**. Reprinted with permission from ref 61. Copyright 2013 Wiley.

In an effort to develop selective fluorometric chemosensor for Hg^{2+} , Bandyopadhyay and co-workers developed a family of A_2B corroles **68**, **69**, **70** and **71** (Figure 38).⁶² In toluene medium they showed a strong emission in the range of 685–705 nm and among them **71** showed the highest emission quantum yield. Upon addition of Hg^{2+} the greenish solution of **71** turned to yellowish-brown along with a blue shift of ~ 27 nm in the UV-Vis spectrum.

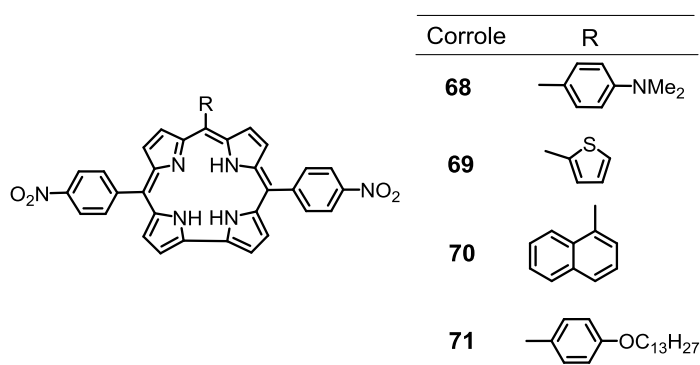


Figure 38. Molecular structures of the chemosensors **68**, **69**, **70** and **71**.

This blue shift was proposed to be due to an interruption in the ICT transitions. However, all these reagents showed fluorescence off response on binding to Hg^{2+} ion and an efficient spin-orbit coupling process for Hg^{2+} was proposed to be the reason for such a response. A 1:1 complex formation with an

association constant in the order of 10^5 M^{-1} between **71** and Hg^{2+} was evaluated from Uv-vis spectral titration. However emission titration provides contradictory result, a 3:1 stoichiometry and an overall association constant of $4.57 \times 10^{15} \text{ M}^{-1}$ between the metal and ligand. To resolve this discrepancy author performed Stern-Volmer plot of the emission quenching studies for varying $[\text{Hg}^{2+}]$ and the plot was linear till one mole equivalent of Hg^{2+} was added. Beyond that $[\text{Hg}^{2+}]$, the plot was exponential, which suggested that a static quenching mechanism for lower $[\text{Hg}^{2+}]$; while for higher $[\text{Hg}^{2+}]$ a dynamic quenching mechanism was operational due to exciplex formation between the excited corrole monomer and mercury ions.

Ng and co-workers developed a NIR emissive distyryl boron dipyrromethene (BODIPY) based chemosensor (**72**) with two bis(1,2,3-triazole)amino substituents and used those for the recognition studies of cations (Figure 39).⁶³ Among various cations it gave selective colour and emission change with only Hg^{2+} and Cu^{2+} in $\text{CH}_3\text{CN}/\text{H}_2\text{O}$ (1:1 v/v) medium. Q band at 686 nm for the absorption band of **72** was significantly blue shifted by 36 or 81 nm on binding to Hg^{2+} or Cu^{2+} ion. Accordingly, the colour of the solution changed from green to pale blue (for Hg^{2+}) or deep blue (for Cu^{2+}).

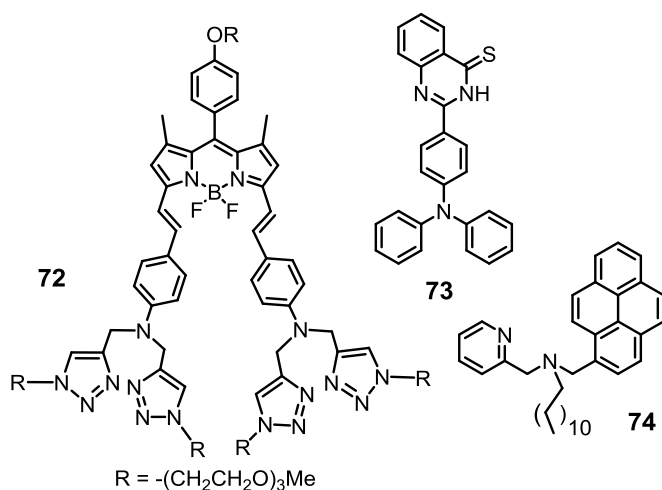


Figure 39. Structures of the chemosensors **72**, **73** and **74**.

Further, the emission maxima of **72** at 726 nm underwent 40 and 82 nm blue shift on binding to Hg^{2+} and Cu^{2+} , respectively. This observed blue shift in both absorption and emission spectra was ascribed to the interruption of ICT upon metal ion coordination with the electron rich donor moiety of **72**. Both Job's plot and emission titration data confirmed the 1:2 binding between the host and guest. The

association constants calculated from the absorption titrations using least square fitting analysis were of $(6.2 \pm 0.6) \times 10^9 \text{ M}^{-2}$ for Cu^{2+} and $(1.1 \pm 0.6) \times 10^9 \text{ M}^{-2}$ for Hg^{2+} .

In an effort to develop a highly selective colorimetric and fluorescent sensor for Hg^{2+} , Tong and co-workers synthesized a 2-substituted quinazoline-4(3H)-thione derivative **73** (Figure 39).⁶⁴ In THF medium **73** showed quinazoline-based π - π^* transition at 366 nm. However, on binding to Hg^{2+} , a new MLCT band appeared at 468 nm with an associated colour change from light yellow to dark yellow. Again quinazoline-based emission at 468 nm ($\lambda_{\text{ext}} = 370 \text{ nm}$) was found to quench gradually with the increase $[\text{Hg}^{2+}]$. Job's plot confirmed 2:1 adduct formation between **73** and Hg^{2+} , while the association constant was evaluated from a nonlinear curve fitting as $4.17 \times 10^8 \text{ M}^{-2}$. Reversibility of the binding to Hg^{2+} was also established. However, usability of this reagent in non-aqueous medium restricted its usability as an imaging reagent.

Ramesh and Das groups reported a pyrene based amphiphilic compound **74** (Figure 39) for the selective recognition of Hg^{2+} in aqueous medium over a broad pH range.⁶⁵ Upon excitation at 340 nm, **74** showed two closely spaced monomer emission bands at around 376 and 394 nm along with a broad structure less band at 516 nm, due to the intermolecular excimer formation. Excitation studies confirmed that the observed excimer formation was static in nature. On formation of a 1:1 complex with Hg^{2+} , the excimer emission was quenched and monomer emission was enhanced due to the decrease in the extent of intermolecular aggregation of ligand **74**. The detection limit of **74** for Hg^{2+} was found to be $8 \times 10^{-9} \text{ M}$ and the binding constant measured from fluorescence titration was found to be $1.12 \times 10^5 \text{ M}^{-1}$. This reagent was used for detection of Hg^{2+} ion uptake in live human cancer cells (HeLa). Again, the hydrophobic part of **74** was efficiently used for the quantitative extraction of Hg^{2+} from an aqueous medium into the organic layer with an efficiency of about 99%.

Bis-heteroleptic Ru(II) complexes could also be useful for the recognition of the toxic metal ions Hg^{2+} in aqueous environment (Figure 40A).⁶⁶ Complex **75** with two benzothiazole amide units of bipyridyl ligand showed 24 fold enhancement by shifting of the emission wavelength from 648 nm to 656 nm with the association constant $\log \beta = 7.8 \pm 0.3$ with a binding stoichiometry of 2:1 for Hg^{2+} :**75** in 0.1M HEPES buffer/ CH_3CN (v/v, 1:1; pH 7.4).⁶⁶ Moreover, this reversible sensor **75** could detect

Hg^{2+} as low as 118 nM level. Interestingly, complex **75** could also recognize Ag^+ ions under the experimental condition but at different emission wavelength, 630 nm. Thus, it could be useful for the dual ions sensors.

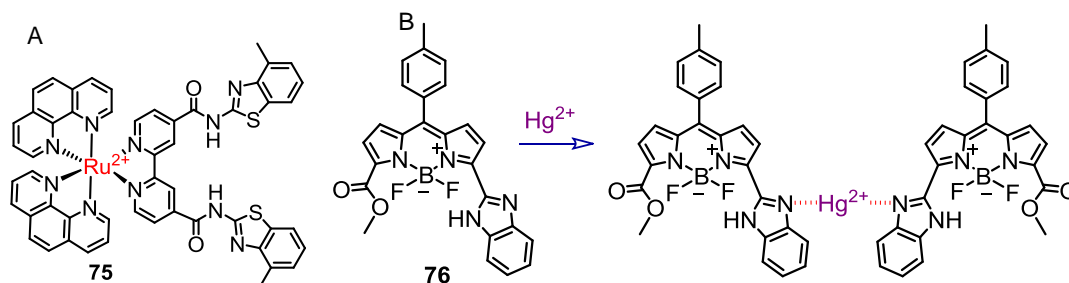


Figure 40. (A) Bis-heteroleptic Ru(II)-complex (**75**) for the recognition of Hg^{2+} ions. (B) Hg^{2+} recognition mechanism of chemosensor **76**.

Ravikanth et. al. recently developed a BODIPY-based receptor (**76**; Figure 40B) with a benzimidazole moiety at the 3-position for the recognition of Hg^{2+} ions in $\text{CH}_3\text{CN}/\text{PBS}$ (7:3; v/v, pH 7.4) solution with the efficiency of the lower detection limit of 0.77 μM .⁶⁷ This system was used as a multi-signaling such as UV-vis, Fluorescence, electrochemical and *in vitro* for the recognition of Hg^{2+} ions with little interference of Cu^{2+} ions. The receptor **76** exhibited blue shifts in absorption spectra from 576 nm to 529 nm with an isosbestic point at 545 nm and allowed a ratiometric recognition of Hg^{2+} . Similar blue shift from 603 nm to 582 nm was also observed in emission spectra with an increase in quantum yield (ϕ) from 0.42 to 0.58 owing to the interruption of photo induced electron transfer (PET) process in presence of Hg^{2+} . The observed association constant calculated from the emission titration was $6.18 \times 10^6 \text{ M}^{-1}$ while binding stoichiometry i.e. receptor to Hg^{2+} was 2:1. The receptor could be useful for the detection of Hg^{2+} in the human breast adenocarcinoma cell line MDA-MB-231 for *in vivo* imaging measurements as well.

Misra and coworkers developed used aggregation induced emission enhancement (AIEE) method for the detection of Hg^{2+} ions.⁶⁸ They have synthesized bathophenanthroline (BA; **77**; Figure 41A) based aggregated microstructures of various morphologies using re-precipitation method and characterized by optical, powder X-ray diffraction and scanning electron microscopy. The aqueous dispersion of **77** microstructures showed AIEE at 384 nm ($\lambda_{\text{ex}} = 270 \text{ nm}$) compared to THF solution of BA. This

luminescent property of aggregated BA hydrosol was used for the detection of metal ions and among various metal ions screened; its AIEE was quenched only in presence of Hg^{2+} ion. The aggregated microstructure can detect even trace amount (10^{-7} M) of Hg^{2+} in aqueous medium. This strong fluorescence quenching of aggregated BA in the presence of Hg^{2+} ions was supposed to be due to the heavy atom induced perturbation by the complexed Hg^{2+} ions on the excited states of the **77**.

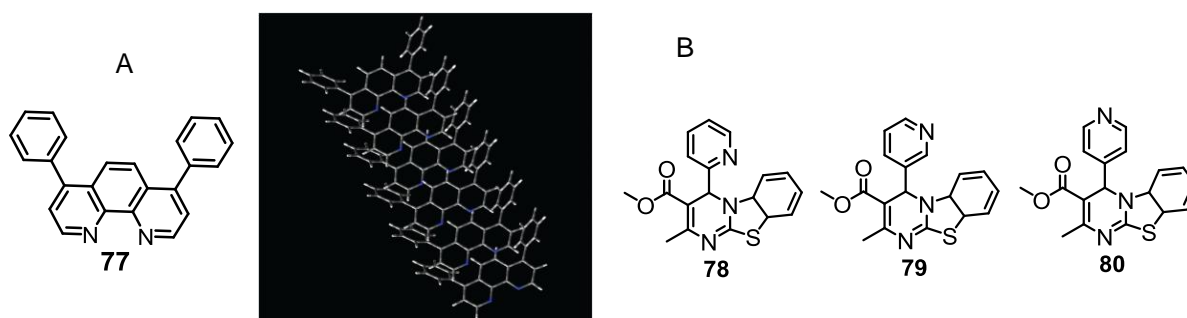


Figure 41. (A) Structure of **77** and analogues aggregated microstructure. Reprinted with permission from ref 68. Copyright 2014 Royal Society of Chemistry. (B) Structures of Biginelli-Based Molecules **78**, **79** and **80**, for the recognition of Hg^{2+} ions.

Singh et. al. recently developed Biginelli-Based Molecules (**78-80**; Figure 41B) with the dimension of nanometre size for the recognition of Hg^{2+} in aqueous Tris buffer medium at pH 7.4 (1 mM).⁶⁹ Only receptor **79** showed selectivity with Hg^{2+} while **80** showed interference for Cu^{2+} but **78** could not show any selectivity for the metal ions under the experimental condition. The organic nanoparticles (ONPs) **79** (size 28 nm), showed ratiometric property with an increase in absorption band at 345 nm and a decrease in band at 386 nm with an isosbestic point 369 nm in presence of Hg^{2+} with the detection limit as low as 1 nM. A continuous decrease in emission spectra with a blue shift from 456 nm to 440 nm was also observed. These changes could be due to the coordination of Hg^{2+} ions with S and N centres (C=N group) leading to the new LMCT band. Addition of Cl^- ions into 79.Hg^{2+} restored original absorption spectra but showed completely different cyclic voltamogram and differential pulse voltammetry. Thus, ONPs was considered as secondary sensors for Cl^- ions rather than the reversible sensor for Hg^{2+} ions.

Kuwar and his group reported easily synthesizable cost effective, noncyclic naphthalene based highly selective fluorescent chemo sensor (**81**; Figure 42).⁷⁰ This receptor showed a selective chromogenic and fluorescent turn-off response towards Hg^{2+} in an ensemble of several other metal ions in DMSO-

H₂O (9:1) system following a binding stoichiometry of 1:1 with a lower detection limit of micromolar level. This composite reagent was found to be cell membrane permeable and could be used as an imaging reagent for detection of the cellular uptake of Hg²⁺ by live HeLa cells as well as the detection of Hg²⁺ present in water in environmental samples. Moreover, the DFT calculations were performed to complement the experimental evidences.

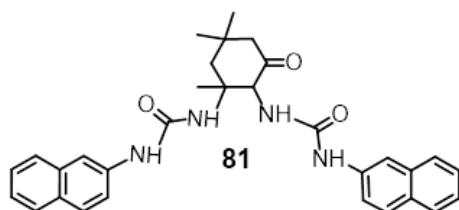


Figure 42: The Chemical structure of the chemosensor **81**.

Recognition of Hg²⁺ using Immobilized of molecular probes

One of the aims of the modern chemists is to develop new materials with the immobilization of the chemosensors on the solid supports as this offer the opportunity of recognition of the target analyte as well as the obvious ease in separating the analyte from solvent or mobile phase. Use of such probes, confined on the surface of a solid material or inside of a porous structure, obviously gets preference over using solution of the same probes as it offers the possibility of *in-field* purification or scavenging along with recognition/detection. In this regards, use of various polymeric backbones, glass particles, gold nanoparticles and different nanostructures with proper design have gained significance. ‘in-field’ use for sensing detection purposes.⁷¹ For real application opportunities, such molecular receptors should ideally be linked to the surface of nanostructured particles (NPs) or to the thin films of membranes or to a porous polymeric substances. Such materials generally have surface-enhanced detection, which allow the sensing of an analyte that is being present at a very low concentration. Significance of such hybrid systems are even more important when binding of the analyte lead to a binding induced changes in output signal that offers the possibility of the real time monitoring of the binding and possible scavenging process. Among various methods that could be monitored for probing the binding process and these include measurable changes in electronic/fluorescence spectral properties, visually detectable colour/ fluorescence changes, redox potentials and electro-generated

chemiluminescence. Appropriate hybrid material and methodology could actually help in avoiding use of expensive and complex analytical instrumentation with long acquisition times and the use of trained personnel. Till date, there are, only a few examples are available in the literature that address such an issue for the detecting and scavenging of Hg^{2+} in aqueous solution. Therefore, development of such a cost-effective alternate hybrid material with simple user friendly operating process is almost essential considering the surge in enhancement in the artificial activities that lead to the increase in possibility of Hg^{2+} pollution in portable water and thus developing simple analysis technique for in field application.⁷²

Solid supported receptors for the detection of Hg^{2+}

Mesoporous silica with immobilised tren-derivative of rhodamine B could be used for the detection of Hg^{2+} (**82**; Figure 43).⁷³ Mesoporous silica surface was functionalized with the spirolactam form of the rhodamine B. Rhodamine B derivatives in their spirolactam form do not show any absorption or emission band beyond 400 nm and thus, such functionalized silica particles are expected to be either colourless or to possess a pale yellow colour. However, binding of Hg^{2+} to such silica-rhodamine hybrid is expected to convert the spirolactam ring to the acyclic xanthene form with simultaneous change in the colour of the modified silica particles. Reversibility in binding to Hg^{2+} could be demonstrated following treatment with $\text{TBA}^+ \text{OH}^-$ solution and thus, these modified silica receptors could be reused for several cycles.

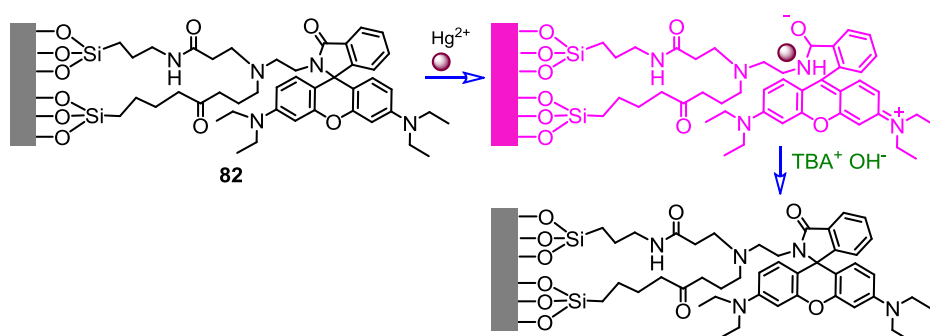


Figure 43. Rhodamine derivative immobilised on mesoporous silica surface, for the reversible recognition of Hg^{2+} .

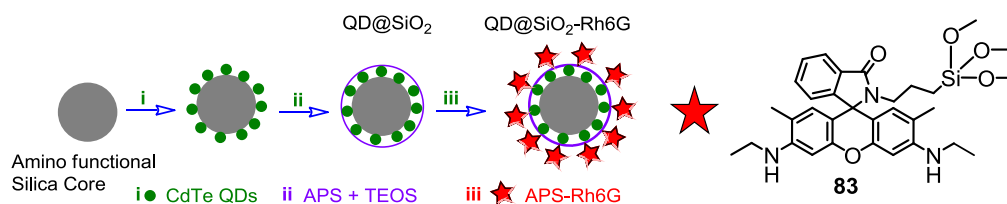


Figure 44. Rhodamine 6G (**83**) grafted on the silica surface in the hybrid receptor for the recognition of Hg^{2+} . Schematic representation for the methodology adopted developing $\text{QDs@SiO}_2\text{-Rh6G}$.

Du, Chen and their co-workers could develop an analogous silica surfaces, where rhodamine 6G was grafted on silica surfaces for use as a solid supported sensor (Figure 44) for Hg^{2+} ion.⁷⁴ For this reagent, the linear concentration range for Hg^{2+} was evaluated as 0.4 to 8.0×10^{-7} M with a lower detection limit ($S/N = 3$) of 2.59×10^{-9} M. In order to achieve the ratiometric fluorescence response following an energy transfer mechanism, CdTe quantum dots (DQs) were used in combination with this modified silica particles. QDs were used to provide the fluorescence background in the ratiometric fluorescence approach and were immobilized in silica nanoparticles to compose $\text{QDs@SiO}_2\text{-Rh6G}$ nanoparticles as shown in Figure 44. These hybrid particles displayed well-resolved dual fluorescence emission, with the Rh6G derivative at 545 nm and the CdTe-QDs at 625 nm and were used successfully in determining Hg^{2+} in water samples having $[\text{Hg}^{2+}]$ of 1.7×10^{-7} M.

A slightly different methodology was adopted for achieving the FRET response on recognition and binding to Hg^{2+} ion in aqueous medium. The close proximity of the donor and acceptor allowed the FRET process to be operational (Figure 45).⁷⁵ Spirolactam form of the rhodamine derivative was covalently linked with the silica surface covering the Cd-Te QDs/silica core. In absence of Hg^{2+} , the nanosurface neither showed any absorbance nor exhibited any fluorescence beyond 400 nm. On binding to Hg^{2+} , FRET process was operational and a strong luminescence, having maxima at 535 nm and a strong pinkish red colouration were obtained as an output signal for probing the Hg^{2+} recognition process. This hybrid sensor was selective towards Hg^{2+} with the lower detection limit of 260 nM and was effective over a wide pH range. It was argued that such strategy could be used to construct QDs-based ratiometric assays for other ions which quench the emission of QDs.

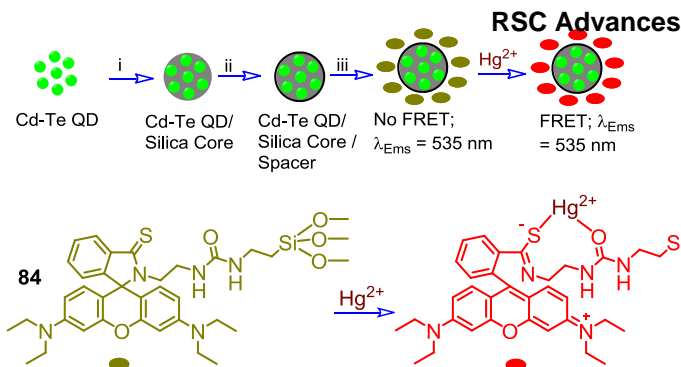


Figure 45. Strategy used for FRET base Hg^{2+} sensor on QDs.

Recently, carbon nanodots (CDs) were functionalised with bis(dithiocarbamato) Cu(II)-complex **85** (Figure 46) was introduced as a fluorescence ‘turn on’ sensors for Hg^{2+} with a lowest concentration detection limit of 4 ppb.⁷⁶ Here, initial Cu^{2+} -complex was non-fluorescence owing to the combined effect of energy transfer and electron transfer mechanism. The higher affinity of the Hg^{2+} ions as compared to Cu^{2+} towards the receptor helped to displace Cu^{2+} ions readily from the surface of CDs led to a more stable sulphur chelated Hg^{2+} -complex with significantly enhanced the emission intensity at $\sim 450 \text{ nm}$. Moreover, it was useful for the detection of Hg^{2+} ions on commercial cellulose acetate inkjet paper under UV-lamp of wavelength 365 nm. However it showed slight interferences with Ag^+ and with AuCl_4^- .

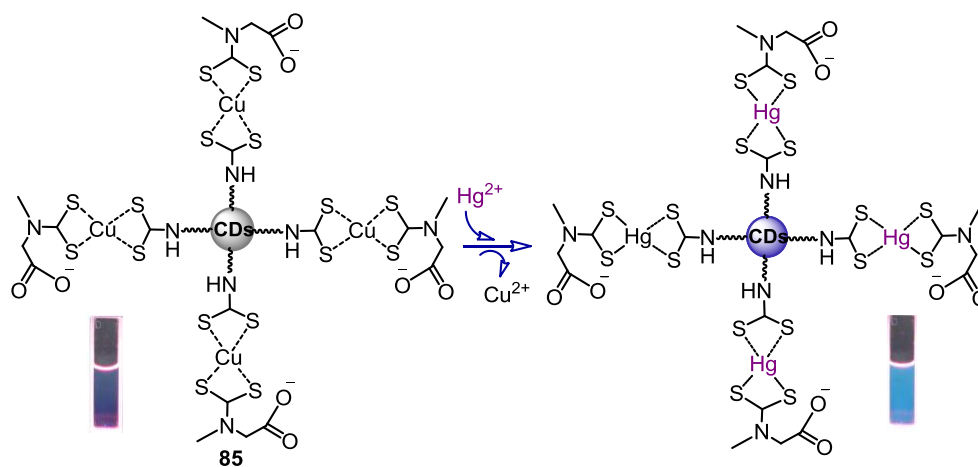


Figure 46. Schematic representation of ‘turn on’ response of Carbon nanodots **85** by displacement of Cu^{2+} ions by Hg^{2+} ions. Reprinted with permission from ref 76. Copyright 2014 American Chemical Society.

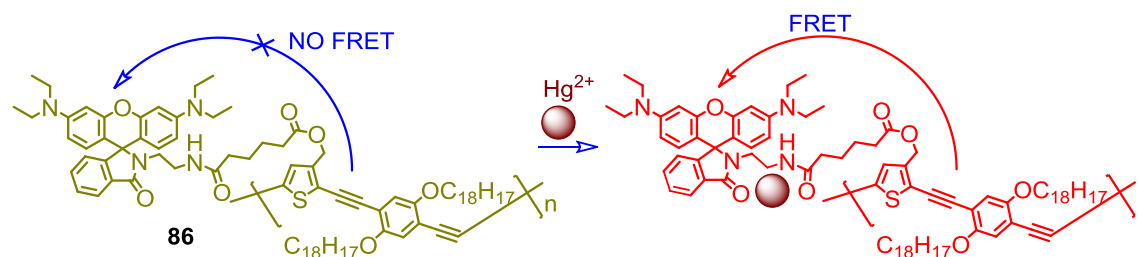


Figure 47. Structure of the polymer back bone in conjugation with rhodamine for the recognition of Hg^{2+} ions. poly[(p-phenyleneethynylene)-alt-(thienyleneethynylene)] conjugated polymer back bone (**86**) showed absorption at 441 nm and emission at 487 nm, which had a substantial spectral overlap with the absorption spectral band of the Hg^{2+} -bound xanthene form. This initiated an effective FRET between the polymer as the donor and the Hg^{2+} -bound rhodamine fragment as the acceptor unit (Figure 47) and a new emission band appeared at 575 nm along with an isosbastic point at 552 nm.⁷⁷ However, use of THF as the solvent has actually restricted the application potential of this receptor.

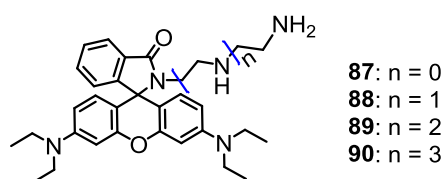


Figure 48. Structure of the receptors (**87–90**) doped onto polymer sheets.

Kaewtong and his co-workers have developed a series of new amino ethyl rhodamine B derivatives with varying spacer between two amine functionalities, which showed specificity in binding to Hg^{2+} with a binding constant of $83,000 \text{ M}^{-1}$ for a 1:1 binding stoichiometry in acetonitrile medium (Figure 48).⁷⁸ This also showed a weak affinity towards Cu^{2+} , however, affinities for Hg^{2+} were at least 300 times higher than Cu^{2+} for receptors **87–90**. A polymeric thin film can be obtained by doping poly(methyl methacrylate) or PMMA with chemosensor **89**. This non-fluorescent thin polymer film showed emission on spraying Hg^{2+} on top of it. The reversibility in binding process was demonstrated by treatment with NaOH solution, which restored the original colour and intensity of the doped polymer film. However, the limitation of using acetonitrile as the only solvent has limited its use for most practical applications.

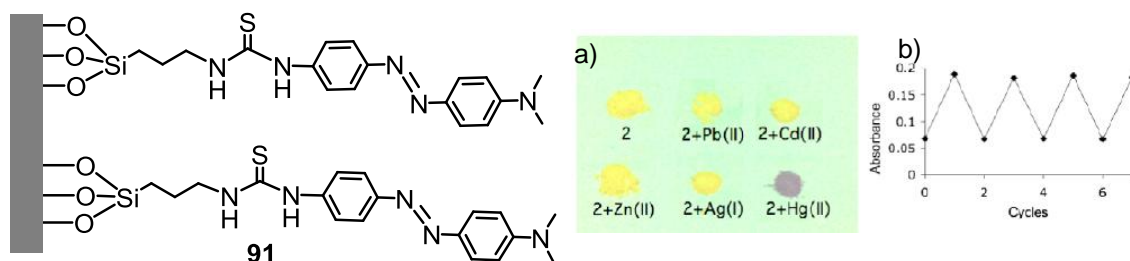


Figure 49. Modified mesoporous silica for chromogenic recognition of Hg^{2+} . [Inset: a) change in colour of **91** in presence of different metal ions, b) Cycles of Hg^{2+} absorption after washing with water]. Reprinted with permission from ref 79. Copyright 2013 Royal Society of Chemistry.

Another silica supported solid sensor **91** was prepared in the reactions of aminopropyltriethoxysilane monolayer coated mesoporous silica nano particle (MCM-41 SiNPs) and 4-(4-isothiocyanatophenylazo)-N,N-dimethyl aniline (Figure 49).⁷⁹ In the absorption titration with Hg^{2+} , in the suspension of **91** showed purple colouration and decrease of the band at 416 nm while appearance of new band at 540 nm with consequent ratiometric behaviour. The minimum detection limit obtained was as low as 2 ppm with for the 1:1 binding stoichiometry and the association constant of $20,0038 \text{ M}^{-1}$ in THF medium. The functionalised nano particles **91** could be regenerated by addition of polar protic solvents like water and could be used for several cycles. However, use of this supported receptor was also restricted as it could only be used in THF medium.

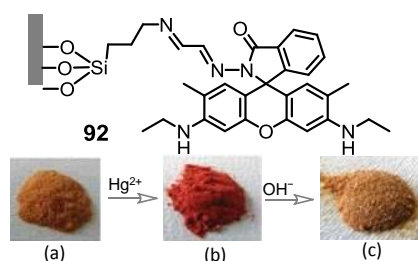


Figure 50. Rhodamine based solid support for the recognition of Hg^{2+} [Inset (a) Colour changes for **92** solid without, (b) with metal binding after isolation from the aqueous suspension; and (c) upon successive immersion in 1 M TBA^+OH^- aqueous solution]. Reprinted with permission from ref 80. Copyright 2012 Royal Society of Chemistry.

Analogous receptor **92** with rhodamine moiety immobilized on silica surface was used to make a dual probe for the recognition of Hg^{2+} from the aqueous medium (Figure 50).⁸⁰ The absorption and emission experiments were performed in the water suspension where the pale yellow colour of the modified silica particles turned red in colour in presence of Hg^{2+} with concomitant enhancement of the emission signal at $\sim 550 \text{ nm}$. The red solid obtained after detection of Hg^{2+} could be regenerated into its original form (Figure 50) by the treatment of TBAOH and it could be recycled for at least three times. The adsorption ability of **92** for Hg^{2+} in neutral water was also estimated by atomic absorption spectroscopy, which revealed an efficiency of about 72%. However, it showed a weak interference from Cu^{2+} ions.

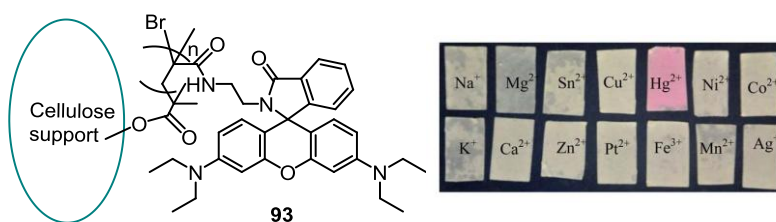


Figure 51. Rhodamine derivative on modified cellulose filter paper [Inset: Optical photograph of cellulose paper in presence of different metal ions]. Reprinted with permission from ref 81. Copyright 2013 Royal Society of Chemistry.

Fu et. al. have recently developed a rhodamine based sensor **93**, supported on cellulose surface for the recognition of Hg²⁺ in aqueous medium. Abundance, bio-degradability and cost-effectiveness (Figure 51) are the key advantages of using cellulose as the support material in an attempt to develop an efficient metal ion scavenger.⁸¹ Rhodamine derivative was covalently linked to cellulose surfaces through appropriate functionalization in order to avoid leaching of the sensors in aqueous environment. After proper characterisation, the colourless cellulose paper was immersed into the Tris-HNO₃ buffer (pH 7.24) solution containing Hg²⁺, while it turned red and a new characteristic absorption band centered at 553 nm was observed. This was found to enhance with increasing [Hg²⁺] within 2 min. Studies in emission spectroscopy revealed a new stitch on emission band at 574 nm with a lower detection limit for Hg²⁺ was 5.0 x 10⁻⁵ M. More importantly, it showed reversibility in binding to Hg²⁺ on treatment with 1.0 x 10⁻³ M solution of Na₂S with 85 % recovery of its original emission pattern.

Zhu et. al. have used salen for its well-known ability to bind to certain metal ions and thus to achieve chelation enhancement fluorescence on binding to those transition metals (Figure 52).⁸² For the receptor **94**, highly emissive perylene was covalently attached to salen building block in order to develop a fluorescent as well as a colorimetric sensor for the recognition of Hg²⁺. This reagent showed selectivity towards Hg²⁺ over Na⁺, K⁺, Ca²⁺, Ag⁺, Ni²⁺, Cd²⁺, Pb²⁺, Cr³⁺, Al³⁺, Fe³⁺, Co²⁺ and Zn²⁺.

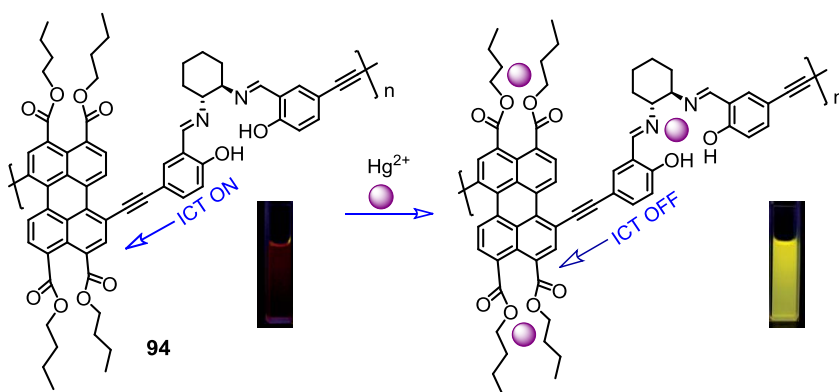


Figure 52. Polymer based system for the recognition of Hg^{2+} through coordination induced ICT 'ON-OFF' process. Reprinted with permission from ref 82. Copyright 2012 Royal Society of Chemistry.

The parent polymer used in **94** showed weak ICT-based emission at 635 nm (λ_{ext} of 440nm) involving salen moiety as donor and perylene as an acceptor moiety. On binding to Hg^{2+} , a 26-fold enhancement in the emission signals with 85 nm blue shift in emission maxima was observed and this allowed a lower detection limit of 7.28×10^{-7} M for Hg^{2+} .

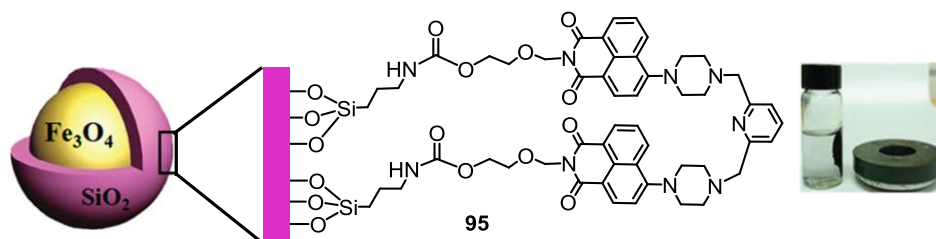


Figure 53. Structure of the functionalised nano particle for the detection of Hg^{2+} [Inset: Photograph of a magnet attracting **95** in water]. Reprinted with permission from ref 83. Copyright 2010 Royal Society of Chemistry.

Lee, Jung and their co-workers have demonstrated that an aminonaphthalimide functionalised Fe_3O_4 nano particles, within the core of SiO_2 , could detect and able to separate Hg^{2+} from drinking water (Figure 53).⁸³ The naphthalimide based emission became quenched upon addition of Hg^{2+} while the original emission of the reagent was restored on addition of EDTA (0.01N). The job's plot confirmed a 1:1 binding stoichiometry, while the binding affinity was reported to be $1.05 \times 10^5 \text{ M}^{-1}$. Moreover, **95** could detect Hg^{2+} as low as 1.02 ppb. However, the emission of **95** was quenched below pH 4 due to protonation on the nitrogen atoms and thus, this reagent could be useful for detection of Hg^{2+} within the pH range 6-11.

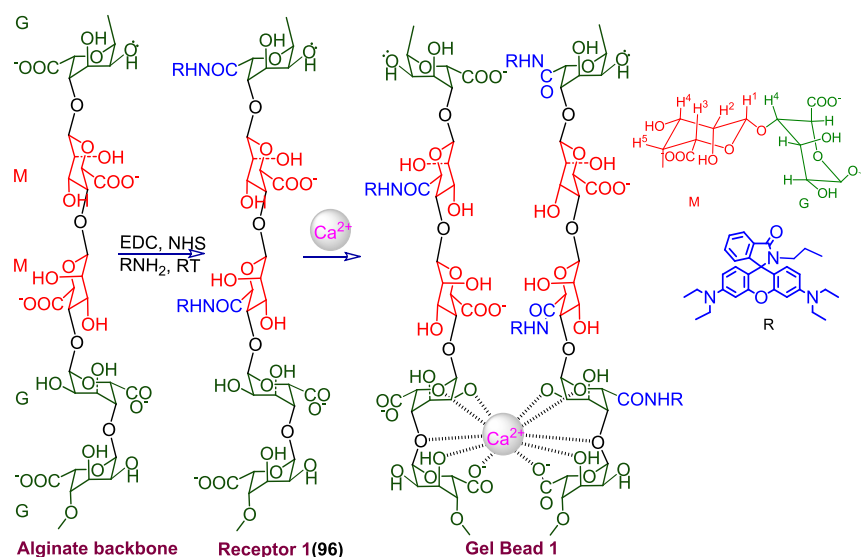


Figure 54. Bio-polymeric gel bead of rhodamine-alginate conjugate was used for the detection and for the removal of Hg^{2+} from its aqueous solution.⁸⁴

Das et al. have reported a self indicating scavenger for Hg^{2+} ion from its aqueous solution using Ca-salt of rhodamine-alginate bio-polymeric gel bead (**96**, Figure 54).⁸⁴ This reagent also showed some affinity towards Cr(III). However, judicious use of appropriate masking agent like I^- , it was possible to detect Cr(III) quantitatively even in presence of Hg^{2+} . Thus, this reagent could be used for detection of total amount of $\text{Hg}^{2+} + \text{Cr}^{3+}$ present in an ensemble of several other metal ions, as well as the individual concentration of Cr^{3+} and Hg^{2+} in aqueous solution. Alginate is a natural polymer and easily accessible. Such hybrid beads turned pink-red on binding to Hg^{2+} and/or Cr^{3+} , and thus, could be used for self indicating $\text{Hg}^{2+}/\text{Cr}^{3+}$ -sponge. Further studies reveal that such beads could be reused and useful for use as a stationary phase in a column for removal of these two ions. The unique technique demonstrated that such hybrid material derived from rhodamine-alginate gel could be used as a stationary phase for reducing the $[\text{Hg}^{2+}]$ below the toxic level (2 ppb).

Huang et al. developed a novel reversible cellulose based colorimetric Hg^{2+} sensor by immobilizing monolayer of a ruthenium dye **97** onto TiO_2 ultrathin gel film pre-coated cellulose nanofibres (Figure 57).⁸⁵ The resultant sensor material exhibited extraordinary selectivity and sensitivity with associated colour change from purple to orange in the presence of Hg^{2+} in aqueous solution. The reported detection limit was ~ 10 ppb for naked eye. Reversibility of the binding process was established in presence of KI solution. This was efficient for trapping Hg^{2+} ions in aqueous media.

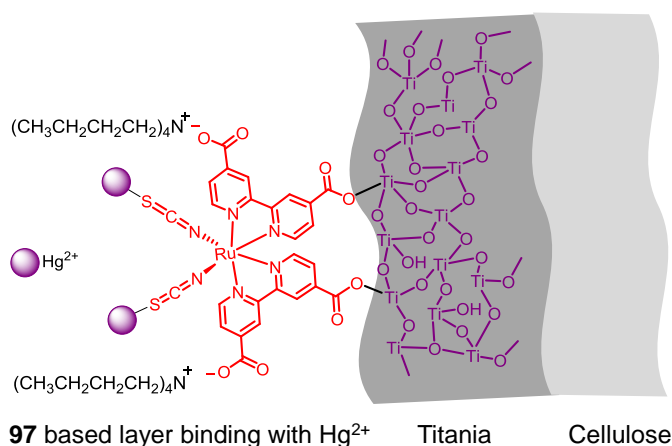


Figure 57. Hg^{2+} ion recognition using TiO_2 -**97** multilayer modified natural cellulose substance.⁸⁵

Cheng and co-workers utilized click reaction to develop a highly selective and sensitive polymer based fluorescence sensor **98** having triazole unit (Figure 58A) for Hg^{2+} detection.⁸⁶ In MeOH/ H_2O (1:1, v/v) medium, **98** showed emission at 425 nm with a shoulder at ~ 450 nm on excitation at 381 nm. This emission was appreciably (86%) quenched in presence of Hg^{2+} . This could have happened due to either of two or a combination of two influences; namely, binding to Hg^{2+} had an adverse influence on the ICT process and the efficient spin-orbit coupling process involving the Hg^{2+} ion. Visually detectable fluorescence of the polymer disappeared on binding to Hg^{2+} . The lowest limit for Hg^{2+} detection of **98** was $4.69 \times 10^{-7} \text{ molL}^{-1}$. An interference of Ag^+ was also reported for this reagent.

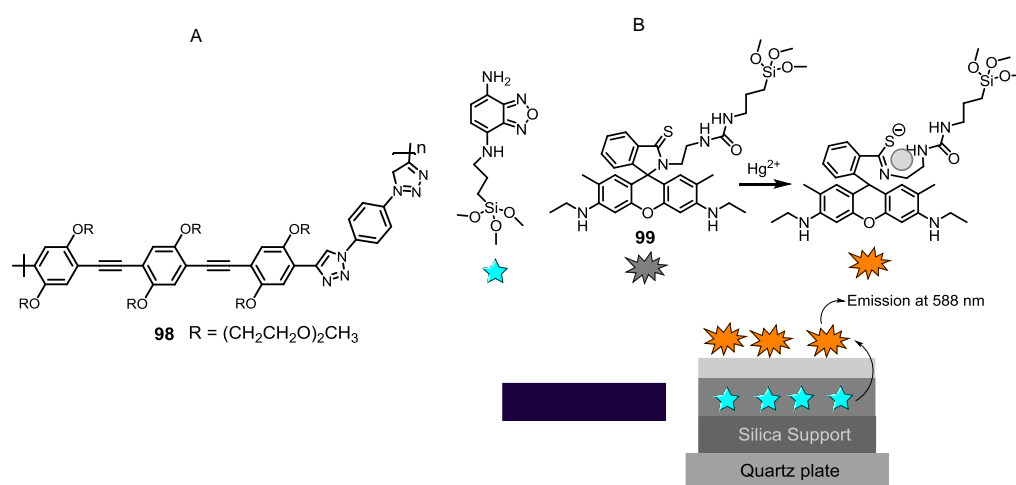


Figure 58. (A) Molecular structure of the reagent **98** and (B) Hg^{2+} detection mechanism of silica FRET based sensor **99**.

Zeng and Wu et al. developed a multilayered silica film (**99**; Figure 58B) on a quartz plate for the FRET based ratiometric detection of Hg^{2+} in aqueous medium.⁸⁷ They consecutively deposited silica functionalized donor (a nitrobenzoxadiazolyl derivative, NBD) layer, spacer layer and finally the acceptor (rhodamine) layer at the outside for the binding of metal ions. In aqueous medium only in presence of Hg^{2+} among various metal ions it shows absorption at 560 nm and emission at 580 nm due to the opening of the spirocyclic ring of the rhodamine moiety. However upon excitation at 430 nm FRET from the NBD unit to the ring opened rhodamine moiety happened and the system showed ratiometric behaviors. Further this device could able to detect even $1 \mu\text{M}$ conc. of Hg^{2+} ions in aqueous medium.

Ding and coworkers developed a novel polyaniline (PANI) based sensor (**100**; Figure 59) for the colorimetric detection of Hg^{2+} ions in aqueous medium.⁸⁸ This hierarchical structured nanofibrous sensing membranes were composed of electrospun nanofibers and ultrafine nanowires demonstrate enhanced homogeneity, interconnectivity and porosity, which greatly boost the colorimetric sensing properties. The sensor shows decrease in reflectance intensity at 440 and 645 nm with change in colour from white to yellow/green, green and blue upon exposure to aqueous solution of Hg^{2+} . The leucoemeraldine based PANI probe has specific interaction with Hg^{2+} ions and caused the change in colour. This could detect Hg^{2+} ion in aqueous medium as low as 5 nM with visually detectable colour change. The sensor showed a good reversibility which was exerted in several cycles. Further the author developed a concentration gradient for the detection of Hg^{2+} using the sensor.

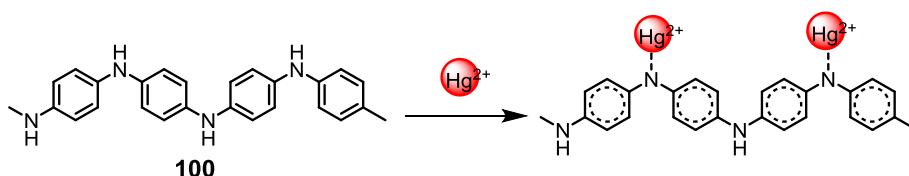


Figure 59. Structure of the chemosensor **100** and its Hg^{2+} binding mechanism.

Heng and his Co-workers reported an fluorescence based silole-infiltrated photonic crystal hexaphenylsilole (HPS) infiltrated photonic crystal (PC) film (**101**; Figure 60) for effective and reversible detection of Fe^{3+} and Hg^{2+} ions.⁸⁹ PCs show amplified fluorescence due to the slow photon effect of PC and electron transfer of HPS molecules and metal ions. The original fluorescence was amplified by the slow photon effect of PC and was quenched significantly due to electron transfer between HPS and Fe^{3+} , Hg^{2+} and Ag^+ ions having higher electrode potential (ions have higher standard electrode potentials (Fe^{3+} , 0.77 V; Hg^{2+} , 0.85 V; Ag^+ , 0.8 V). However, the quenching efficiency was maximum for Hg^{2+} and Fe^{3+} (70%-65%) and that for Ag^+ was ~ 5.6%. smaller diameter. This attributed to the larger ionic diameter for the Ag^+ . The amplified fluorescence could help in enhancing the sensitivity with a detection limit of 5 nM for both these ions.

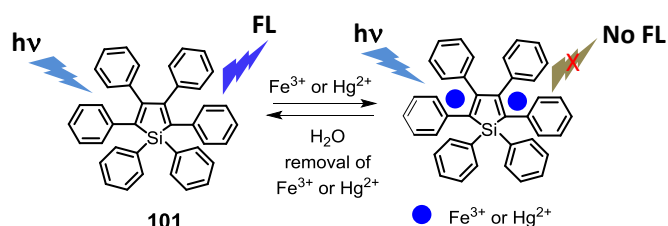


Figure 60. Proposed sensing mechanism for the detection of metal ions ($\text{Hg}^{2+}/\text{Fe}^{3+}$) by HPS-PC film sensor (**101**).

Since the luminescence of probe may also be quenched by other metal ions and emission quenchers in a complicated background, those ‘*on-off*’ sensors suffer from limited sensitivity towards specific analyte.⁹⁰ Additionally these probes usually need the photoexcitation in UV and blue region, where some other chromophores may also be excited, leading to the defect of background light interference. It seems that the combination of ‘*off-on*’ sensor and excitation source based on near-infrared to visible upconversion material can meet the above requirement.⁹¹ As for the excitation source, the upconversion material can transfer infrared radiation to visible photo excitation, so that probes can be efficiently excited, with the chromophores unexcited. For this purpose NaYF_4 lattice has been widely recognized as a promising host for upconversion materials.⁹²

In this regards Wang and his co-workers developed a turn-On Hg (II) sensor system (**102**; Figure 61) excited by near infrared to visible up conversion nanorods.⁹³ For this purpose they had successfully assembled a Hg (II)-sensing system (**102**), with the upconversion nanorods of $\beta\text{-NaYF}_4:\text{Yb}^{3+}/\text{Er}^{3+}$ as the excitation source and a rhodamine derivative as the signaling probe. The morphological aspect and photophysical property of this composite material have been well characterized by electron microscopy, XRD analysis, IR spectra, TGA/DTG analysis and the energy transfer process between the excitation source and the probe was also investigated by excitation/emission spectra and excited state lifetime analysis. It is found that $\beta\text{-NaYF}_4:\text{Yb}^{3+}/\text{Er}^{3+}@Rb$ (**102**) owns a rod-shaped morphology with silica shell as slim as $\sim 10\text{nm}$. The rhodamine-based probe is covalently grafted onto the surface of $\beta\text{-NaYF}_4:\text{Yb}^{3+}/\text{Er}^{3+}$ nanorods and the doping content is 9.6%. The upconversion emission from $\beta\text{-NaYF}_4:\text{Yb}^{3+}/\text{Er}^{3+}$ nanorods can effectively excite the probe. Then the sensing behavior towards Hg(II) was evaluated by emission spectra and the Stern–Volmer plot. A good linear response in the range of

0–12 μM is obtained. Additionally, $\beta\text{-NaYF}_4\text{:Yb}^{3+}/\text{Er}^{3+}\text{@Rb}$ (**102**) shows a good selectivity towards Hg(II) , which makes itself a promising sensing system.

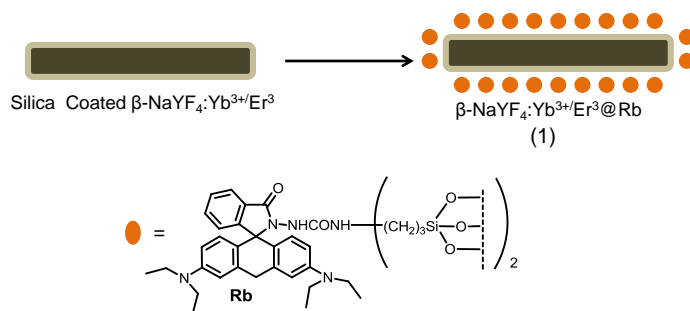


Figure 61. The pictorial representation of the Hg(II) sensing nanocomposite material (**102**) constructed with silica coated $\beta\text{-NaYF}_4\text{:Yb}^{3+}/\text{Er}^{3+}$ nanorods and rohadimine derivative.

Xu and coworkers have successfully constructed a nanocomposite (**103**; Figure 62) for specific recognition of Hg^{2+} .⁹⁴ The nanocomposite with rod-shaped morphology and diameter of ~ 160 nm was appropriately characterized using electron microscopy, XRD, IR/UV–Vis/emission spectroscopy and thermogravimetry. This nanocomposite was covered with a uniform silica shell (thickness ~ 15 nm) to improve the dispersibility in aqueous solutions. Rhodamine-based receptor was then grafted onto the silica shell with doping content of 4.01% through silylation reaction. The Forster radius calculation and excited state lifetime analysis suggested an efficient energy transfer between the excitation core and the probe. This constructed sensing system owned a linear response towards increasing $[\text{Hg(II)}]$ with a “turn-on” response. This composite showed high specificity towards Hg(II) as well as high photostability. However, possible use of such nanocomposite as an imaging reagent was not described.

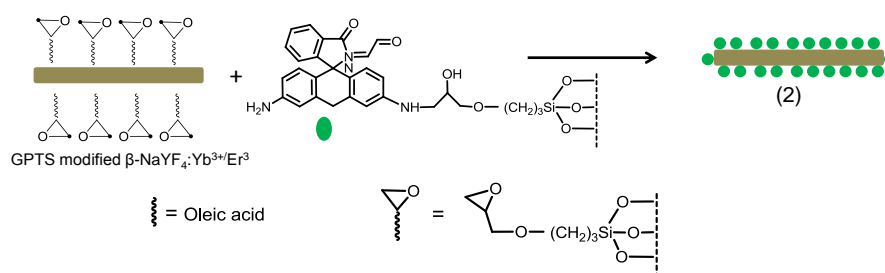


Figure 62. The pictorial representation of the Hg(II) sensing nanocomposite system (**103**) constructed with $\beta\text{-GPTS}$ modified $\text{NaYF}_4\text{:Yb}^{3+}/\text{Er}^{3+}$ nanorods and rohadimine derivative.

Cui et. al. reported a turn on sensor for the detection of Hg^{2+} using the above mentioned energy transfer mechanism involving similar type of $\beta\text{-NaYF}_4\text{:Yb}^{3+}/\text{Er}^{3+}$ -rhodamine composite nanorods as a

sensing probe for Hg^{2+} .⁹⁵ Based on the results of the upconversion as well as the time resolved emission studies, FRET based energy transfer from the Hg^{2+} -bound rhodamine moiety to the phosphor material was established and this emission response was utilized for Hg^{2+} ion recognition. However, interference from other metal ions like Fe^{2+} , Cu^{2+} , Cd^{2+} , Pb^{2+} and Ag^{+} was also reported.

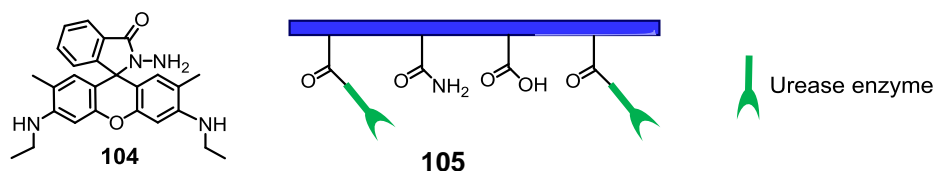


Figure 63. (A) The Chemical structure of the Rhodamine derivative **104**. (B) Polymer based photonic crystal hydrogel sensor **105**.

Arunbabu and coworkers developed a novel polymer based photonic crystal hydrogel sensor (UPCCA) for the selective detection of toxic Hg^{2+} ions in aqueous medium (**105**; Figure 63B).⁹⁶ This colloidal polymeric photonic crystal could diffract visible light at 764 nm in aqueous medium and the diffraction wavelength shifted owing to the volume phase transitions experienced by the polymer hydrogel upon exposure to the different mercury ion concentrations. UPCCA consisted of urease enzyme which could hydrolyze the urea substrates and produces the HCO_3^- and NH_4^+ ions inside the hydrogel. These ions decreased the electrostatic repulsion between carboxylates and the polyacrylamide backbone and led to the shrinkage of hydrogel. Hg^{2+} ion inhibited the urease-urea hydrolysis reaction and thus suppressed the ion production and did not allow the hydrogel to shrink as it was the case in absence of Hg^{2+} and simultaneously affect the diffraction wavelength of the incident light on these colloidal particles.

Detection of toxic Hg^{2+} ions by highly photo-active chemodosimeters

To avoid the problem of high solvation energy of Hg^{2+} in aqueous medium and thus to achieve the detection process in polar solvent like water as well as in physiological condition, chemodosimetric approach as a detection methodology and diagnostic tool has gained importance more recently. In this approach, probe molecule reacts with the desired analyte and undergoes chemical transformation with associated change(s) in output signal that allows the quantitative estimation of the target analyte. These chemodosimeters are generally categorised into two types in terms of the changes in their

optical output signals: firstly, optical chemodosimeters that allows detection/quantification of the analyte either through ‘on-off’ or through ‘off-on’ changes in their optical (fluorescence or/and absorbance) output signals owing to the specific chemical reaction on the course of analyte recognition and secondly, ratiometric chemodosimeter that show ratiometric changes in absorption or/and emission spectra with a certain isosbestic or isoemissive point on reaction with the desired analyte.⁹⁷ Again, in some cases analytes react directly with the probes while in some cases analytes catalysed the chemical transformation with consequent change in the optical properties.^{3b} These approaches often get preference over normal probes in terms of selectivity and sensitivity, more specifically in aqueous medium.

Chemodosimeters for the detection of Hg²⁺ ions.

According to hard-soft acid base theory, Hg²⁺ is soft acid; consequently it has very high affinity towards the soft base sulphur. This high thiophilic character of Hg²⁺ has been utilized for its recognition. Chemodosimeter is one class of chemosensor which recognize analyte following an irreversible mechanism.

Tae et al. developed a rhodamine-6G derivative **106**, which works as a highly selective and sensitive chemodosimeter for Hg²⁺ in aqueous solution (Figure 64A).⁹⁸ Hg²⁺-promoted an irreversible oxadiazole-forming reaction for **83** with visually detectable changes in fluorescence and colour. Thus, monitoring either of these spectral changes one could probe the Hg²⁺ ion recognition process at room temperature in a 1:1 stoichiometric manner to the amount of Hg²⁺ present. Shin et al. could further utilize this system for demonstrating a real-time method for monitoring the concentration of mercury ions in living cells, particularly vertebrate organisms (Figure 64B).⁹⁹

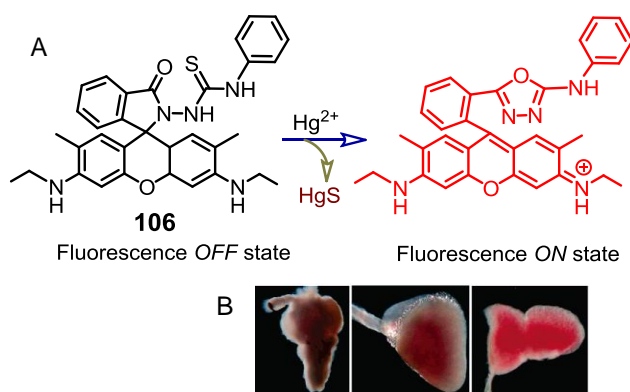


Figure 64. (A) Schematic representation of Hg^{2+} -promoted oxadiazole-forming reaction of the reagent **106** and (B) images of zebrafish organs treated with 5 nM HgCl_2 and 10 μM **106**. Reprinted with permission from ref 99. Copyright 2006 American Chemical Society.

Bharadwaj, and Kim and their coworkers developed a cryptand-rhodamine conjugate (**107**), for the detection of Hg^{2+} .¹⁰⁰ The geometric arrangement of aliphatic N-atoms in the cryptand core in **107** offered the appropriate binding sites for Hg^{2+} (Figure 65). Selective binding of Hg^{2+} to **107** followed a 1:3 stoichiometry in EtOH- H_2O medium (2:5, v/v). Composite association constant of $\sim 7.0 \times 10^{11} \text{ M}^{-3}$ was reported. Control experiment with HEK 293 cells incubated only with **107** displayed a very weak fluorescence image, however strong cellular fluorescence was observed when similar cells pre-exposed to Hg^{2+} cells were incubated with **107**.

Yoon and co-workers have introduced a rhodamine 6G thiolactone derivative **108** (Figure 65) as a selective and colorimetric sensor for Hg^{2+} at pH 7.4.¹⁰¹ An 'off-on' type fluorescence and colorimetric responses were observed in the presence of Hg^{2+} in CH_3CN -HEPES buffer (1:99, v/v, pH 7.4) medium. X-Ray structure of $\text{Hg}^{2+} \cdot [\mathbf{108}]_2$ confirmed the 1:2 binding stoichiometry. Importantly, reagent **108** could detect Hg^{2+} in the nanomolar range of concentration and could be used for *in vivo* imaging of *C. elegans* for detection of Hg^{2+} ion uptake. Further, Yoon and Shin's group together designed a unique selenolactone based probe **109** (Figure 65) for the detection of inorganic mercury and methylmercury species through anticipated fluorescence and UV-vis spectral change.¹⁰² Spectral studies also confirmed the 1:1 stoichiometry between **109** and Hg^{2+} -species. This reagent was further used for the detection of inorganic mercury as well as the potent neurotoxin, methylmercury in cells and Zebrafish.

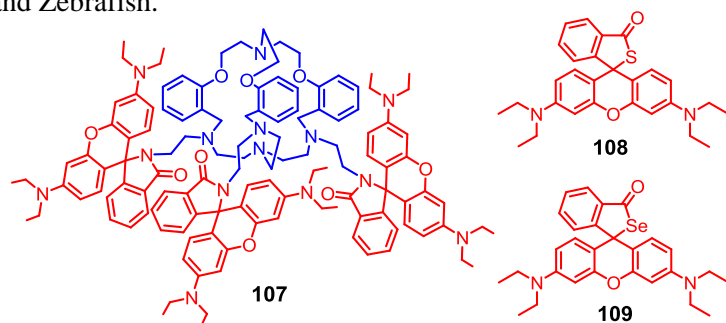


Figure 65. Molecular structures of reagents **107**, **108** and **109**.

The reactivity of the disulphide linkage towards Hg^{2+} was also utilized for Hg^{2+} ion recognition. A new rhodamine based chemodosimeter (**110**) was utilised for this purpose (Figure 66).¹⁰³ The receptor

110 exhibited selectivity only for Hg^{2+} with generation of the absorption band at 560 nm and emission band at 580 nm in ethanol/water medium (80:20, v/v) due to the generation of the acyclic xanthene form. Other alkali, alkaline earth metals and transition metals remained inactive toward the ring opening under the experimental condition.

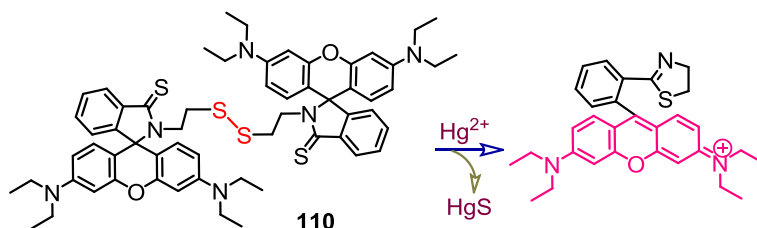


Figure 66. Reaction of disulphide linkage with Hg^{2+} ions led to the formation of acyclic xanthenes form.

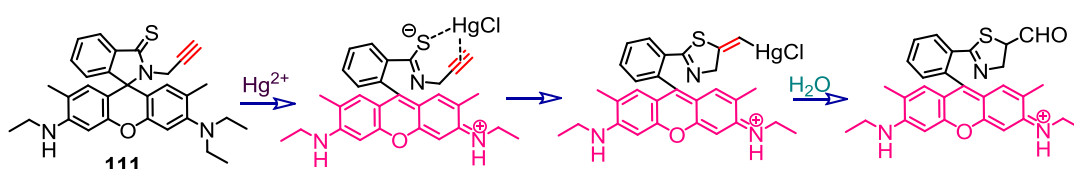


Figure 67. Reaction pathway for the formation of formyl thiazole with lactam ring opening.

Electron rich alkynes are known to react with Hg^{2+} to undergo a further hydrolysis reaction to yield the aldehyde functionality. Reaction of Hg^{2+} with sulphur and alkyne functionality led to the formation of thiazole ring with a mercurated exocyclic double bond (Figure 67).¹⁰⁴ However, the exocyclic alkene bond underwent a facile hydrolysis reactions to yield the corresponding formyl derivative with large red emission in the visible region (~ 560 nm). The mechanism of co-operative interaction was explained on the basis of control experiments. The alkyne derivative without S-atom and *vice versa* could not produce any change in emission, which further corroborated the proposed mechanism for the recognition process as well as the fluorescence on response.

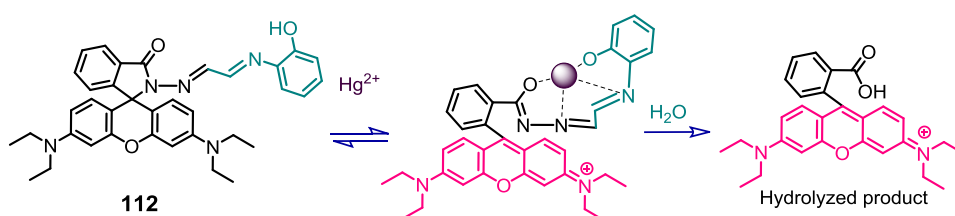


Figure 68. Hydrolysis protocol of the chemodosimeter **112** in presence of Hg^{2+} led to the formation of rhodamine B.

Schiff's bases are also known to be prone towards hydrolysis and this reaction becomes more effective in presence of Hg^{2+} . This property was utilized for designing the chemodosimeter **112** for specific

recognition and quantitative estimation of Hg^{2+} , which basically act as a catalyst in inducing this hydrolysis reaction (Figure 68).¹⁰⁵ The reported lower detection limit for Hg^{2+} ions was as low as ppb level in natural water. Coordination of Hg^{2+} centre to **112** lead to the opening of the lactam ring and the generation of the highly emissive and strongly absorbing xanthene form, which underwent further hydrolysis to generate the carboxy derivative as the final product with 379 fold enhancements in emission intensity at ~ 580 nm. Moreover, this methodology nullified any interference of sulphide containing bio-analytes such as cysteine/homocysteine and glutathione, especially for live cells imaging. Reaction of Hg^{2+} with alkynes first leads to the mercuriation reaction, which on hydrolysis i.e. on demercuration produces the corresponding ketone (Figure 69A).¹⁰⁶ This methodology has been introduced for the development of a chemodosimeter **113** for Hg^{2+} with 'turn on' response showing 219 fold enhancement in emission intensity with maxima at 523 nm.¹⁰⁶ More importantly, probe **113** was used for the detection of Hg^{2+} ions in Solomon fish-tissue after dissolving in Me_4NOH in presence of strong oxidant NCS (N-succinimide), at the pH 7.0. The strong fluorescence signal, suggested that **113** could be used to monitor mercury concentrations in fish and in other tissues as 95% of mercury species exist as MeHg^+ in fish. The receptor **113** could detect Hg^{2+} as low as 8 ppb level ($\text{S/N} = 3$). Vinylic ether also has affinity for Hg^{2+} ions and eventually leads to the formation of acetaldehyde and the corresponding phenolate (Figure 69). Thus, non-fluorescent receptor moiety **114** showed fluorescence in presence of Hg^{2+} with 'turn on' signal at 525 nm and the observed detection limit was lower than 1 ppb (Figure 69B).¹⁰⁷ Importantly, chemodosimetric reagent **114** could detect of Hg^{2+} in river water and from dental samples.

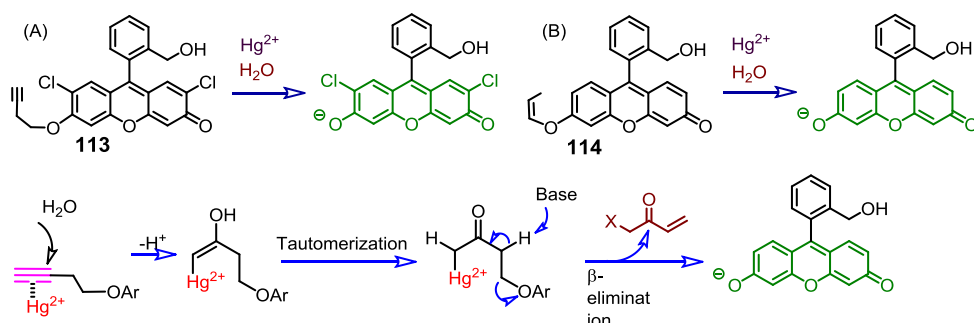


Figure 69. Detection of Hg^{2+} based on the of oxymercuration and demercuration reaction of electron rich π -bonds and the proposed mechanistic pathway for the elimination reaction.

Basak et. al. have synthesized a 3-amino derivative (**115**; Figure 70A). This took part in an irreversible ring opening reaction while specifically interacting with Hg^{2+} .¹⁰⁸ This led to an *in situ* formation of 1,3,5-oxazole ring with ‘turn on’ enhancement of fluorescence in the water-ACN (60/40 v/v) medium.⁶ Chemodosimeter **115** showed 26-fold enhancement upon addition of one equivalent Hg^{2+} with shift in emission maxima from 579 nm to 583 nm within 3 minutes under the experimental condition. The spirolactam ring structure for this chemodosimeter **115** was found to be maintained within the pH range 4-10. Confocal microscopic studies revealed that this reagent was effective for recognition of Hg^{2+} in live HeLa, HEK293T, MN9D, and RN46A cells and also the *in vivo* studies in Zebra.

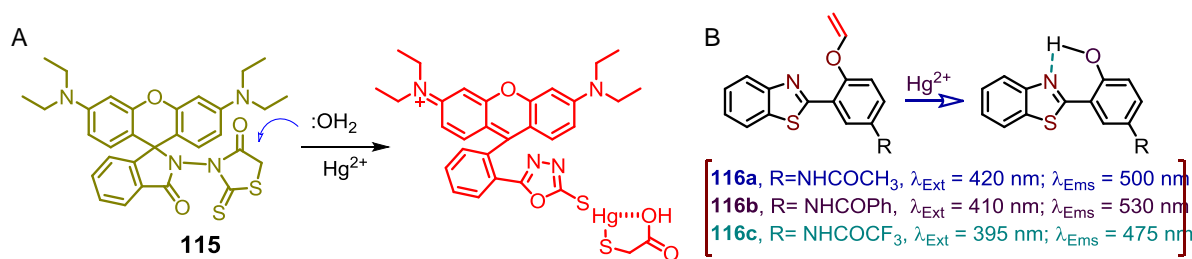


Figure 70. (A) Hg^{2+} mediated oxazole formation. (B) Hg^{2+} ions promoted hydrolysis of vinylic ethers and excited state intramolecular proton transfer leading to change in emission signals.

A set of new oxymercuration derivatives (**116a-116c**) were reported by Ahn and his coworkers (Figure 70B).¹⁰⁹ These derivatives showed large shifts in emission maxima with ratiometric response. The absorption maximum of **116a** was shifted from 295 nm to 330 nm with an isosbestic point at 318 nm in presence of HgCl_2 and the consequent colour was changed from blue to cyano. The corresponding emission signal was found to shift from 420 nm to 500 nm in PBS buffer medium (1% CH_3CN , pH 7.4). More interestingly, it was observed that 2-(benzthiazol) phenol and their derivatives in their keto form showed emission at longer wavelength compared to the corresponding phenol derivatives due to an excited state intramolecular proton transfer mechanism. It was also observed that the hydrolysis reaction with HgCl_2 was faster in presence of electron withdrawing group at the *para*-position with respect to the vinyl ether bond. However, the lowest detection limit that could be achieved was 20 ppb, which is little higher than that is required to qualify as an efficient reagent for detection of Hg^{2+} for safe drinking water.

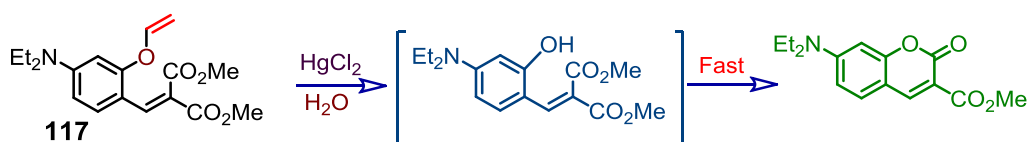


Figure 71. HgCl_2 induced hydrolysis of vinyl ether and cyclization reaction.

Mercury ion promoted hydrolysis of vinyl ether **117** (Figure 71) generated the corresponding hydroxyl derivative, which was followed by an intramolecular nucleophilic addition reaction for generating of the highly fluorescent coumarin moiety with as associated ‘turn on’ emission response. This ideology was exploited for designing the receptor **117** for sensing of Hg^{2+} in PBS buffer solution in DMSO- H_2O (5:95, v/v; pH 7.4).¹¹⁰ An increase in emission intensity at 475 nm on reaction of HgCl_2 with **117** was observed and formation of the coumarin derivative as the eventual product was even isolated and characterized.

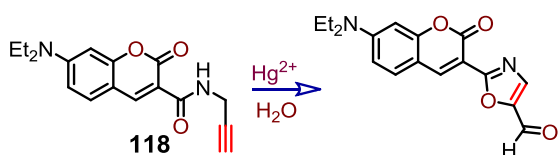


Figure 72. Hg^{2+} mediated oxazole ring formation leading to change in photophysical property.

Propargyl amide containing chemodosimeter **118**, was also found to be converted into corresponding oxazole derivative on reaction Hg^{2+} (Figure 72).¹¹¹ The oxazole formation was associated with large bathochromic shifts in absorption band from 428 to 475 nm with an isosbestic point at 438 nm. Systematic increase in $[\text{Hg}^{2+}]$ showed gradual bleach in intensity at 428 nm and an enhancement of the emission intensity at 475 nm. This allowed a ratiometric detection of Hg^{2+} . This transformation was complete within 40 min and the rate constant for this reaction was $3.9 \times 10^{-2} \text{ M}^{-1} \text{ s}^{-1}$. Emission spectra for **118** was recorded in absence and presence of Hg^{2+} , which clearly revealed a ratiometric response with a shift in the emission band maxima from 469 to 492 nm ($\lambda_{\text{Ext}} = 428 \text{ nm}$). An increase in the quantum yield value from 0.05 to 0.15 and the lower detection limit of 2.7 μM were reported. Cyclodextrines is biologically benign and has the ability to penetrate easily through the phospholipid and cholesterol containing cell membranes.

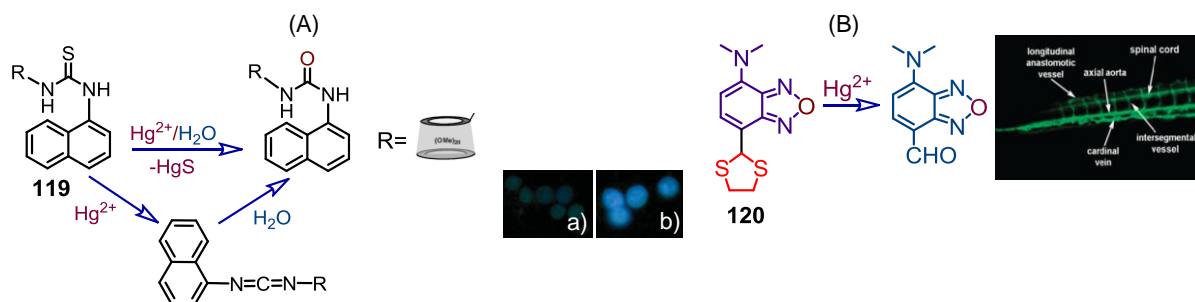


Figure 73. (A) Proposed mechanism of Hg^{2+} detection using receptor **119**. [Inset: a) dark field image of **119**, b) dark field image of **119** in presence of Hg^{2+} under fluorescence microscopy]; Reprinted with permission from ref 112. Copyright 2011 Royal Society of Chemistry. (B) Hg^{2+} mediated deprotection of aldehyde led to bright change in emission [Inset: confocal microscopic image of the tail of a 5-day-old zebrafish larva incubated with $10\ \mu\text{M}$ of **120** for 20 min followed by incubation with $1\ \mu\text{M}$ Hg^{2+} (20 min)]. Reprinted with permission from ref 113. Copyright 2012 Royal Society of Chemistry.

A new probe **119** was designed from naphthylthiourea, covalently linked to β -Cyclodextrine for the recognition of Hg^{2+} in aqueous medium and its detection in live cells (Figure 73A).¹¹² The chemodosimetric reagent **119** showed weak fluorescence at 380 nm due to PET process that was operational between sulphur as donor and naphthalene as acceptor units; while addition of Hg^{2+} led to significant emission enhancement without any interference of other metal ions. Detailed studies confirmed the desulphurisation mechanism and the minimum detection limit for Hg^{2+} for this method was 3.7×10^{-7} M. Chemodosimeter **119** could also be used for the detection of Hg^{2+} ions in yeast cells. Another, new fluorescent ‘turn-on’ probe **120** was successfully demonstrated for the detection of Hg^{2+} , where dithian protection of benzoxadiazole was removed upon addition of Hg^{2+} . The internal charge transfer from N,N-dimethyl amino group to dithian was very low due to low electron withdrawing capacity, thus, it showed low fluorescence (Figure 73B).¹¹³ However, on addition of Hg^{2+} in the solution of **120** in aq.-HEPES buffer:CH₃CN (4:1, v/v; pH 7.40) media a substantial increase (230 fold) in emission intensity at 585 nm (λ_{ext} of 455nm) was observed along with the increase in relative quantum yield by $\sim 35\%$ due to a favored ICT process. The absorption spectra of was shifted from 448 nm to 458 nm with generation of new π - π^* -based transition band at 316 nm upon reaction with Hg^{2+} . An associated colour changing from pale yellow to bright yellow was observed. The virtual ‘turn-on’ emission response of **120** in presence of Hg^{2+} was utilised as an imaging reagent for the detection of Hg^{2+} in 5-days old Zebra fish larvae using laser confocal microscopy.

Analogous strategy that was adopted for reagent **120**, was also adopted for **121** for the selective recognition of Hg^{2+} in aq. PBS buffer (pH 7.4) (Figure 75A).¹¹⁴ Strong thiophilicity of Hg^{2+} selectively induced the deprotection of the thioketal group of **121** and generated the acyl group, which initiated an intramolecular charge transfer (ICT) process between the electron-donor methylamino group and the electron-acceptor acyl group. This resulted an increase in the emission intensity for **121** at 503 nm ($\lambda_{\text{Ext}} = 380$ nm) with increase in $[\text{Hg}^{2+}]$. The absorption maxima of **121** also shifted from ~ 295 to 355 nm in presence of Hg^{2+} ions due to the generation of pull–push ICT process. Fluorescence studies also allowed detection of the acute neurotoxin CH_3Hg^+ . Compound **121** was pH-insensitive and thus could be adopted for Hg^{2+} sensing in biotic environments. It could detect trace of Hg^{2+} present in live HeLa cells through two photon microscopy.

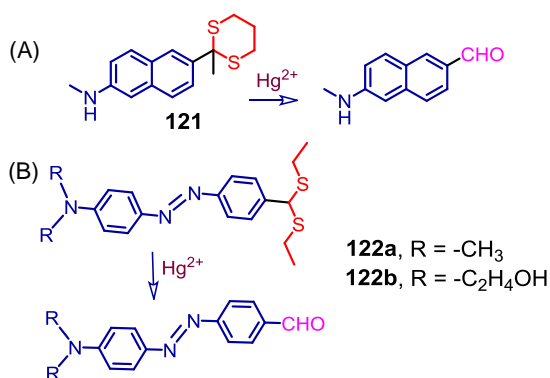


Figure 75. Hg^{2+} mediated hydrolysis of the dithian moiety leading to change in photophysical property.

Li and co-workers synthesized colorimetric chemodosimeter **122a** and **122b** using similar dithioacetal binding moiety for the selective recognition of Hg^{2+} ions (Figure 75B).¹¹⁵ On addition of Hg^{2+} the colour of the acetonitrile solution of **122a** changed from yellow to red due to the formation of aldehyde compound on hydrolysis of dithioacetal moiety due to a favored ICT process. As a result the absorption spectra shifted from 420 nm to 455 nm at low $[\text{Hg}^{2+}]$, this spectra further shifted from 455 to 515 nm at even higher $[\text{Hg}^{2+}]$. Compound **122b** showed similar colour change and spectral shifts in CH_3CN medium. However, compound **122b** showed better sensitivity towards Hg^{2+} . Compound **122b** could recognize as low as $20 \mu\text{M}$ of Hg^{2+} through visually detectable colour change. Having two extra hydroxyl groups, compound **122b** had better solubility and could detect Hg^{2+} colorimetrically in $\text{CH}_3\text{CN}/\text{H}_2\text{O}$ (9/1 (v/v), 20 mM HEPES, pH 7.0) medium. Test strips were prepared by immersing

filter paper into a CH_3CN solution of **122b** ($1 \times 10^{-3} \text{ mol L}^{-1}$) and drying in air. These were used for detection of Hg^{2+} in aqueous medium using ‘dipstick’ method.

Cheng and co-workers developed a new series of ICT based chemodosimeters (**123**, **124** and **125**; Figure 76) by attaching various electron-donating thiophenes groups to a triphenylamine backbone with a dithioacetal moiety as a binding site for the metal ions.¹¹⁶ Upon addition of Hg^{2+} to the THF solution of **125**, the emission intensity at 440 nm was found to decrease and a new emission appeared at 525 nm due to the favoured ICT process after Hg^{2+} induced the hydrolysis of the dithioacetal unit and led to the generation of the more electronegative aldehyde moiety. Thus compound **125** showed the ratiometric behaviour on reaction with Hg^{2+} . Further the absorption maxima of **125** at 385 nm gradually disappeared, while a new absorption band centered at 422 nm was observed. This was accounted for the change in solution colour from colorless to yellow. Similar to **125**, dithioacetals **126** and **127** were also used for the detection of Hg^{2+} ions. Compared to **125** and **126**, the higher conjugation in **127** results a better ICT effect after reaction with Hg^{2+} ion led to the formation of the aldehyde moiety. This was further confirmed by molecular simulation studies. They had further synthesized a polymeric chemodosimeter **P125** by introducing compound **125** to the backbone of conjugated polymers (P) and used for the recognition of Hg^{2+} . In THF medium, an increase in $[\text{Hg}^{2+}]$ caused a steady decrease in the emission band intensity for **P125** at 462 nm and a concomitant increase in band intensity of a new emission band at 564 nm was observed. Thus, this reagent (**P125**) could be used for ratiometric detection of $0.1 \mu\text{M}$ of Hg^{2+} . However, reagent **125** could be used successfully as an imaging reagent for the detection of Hg^{2+} in HeLa cells.

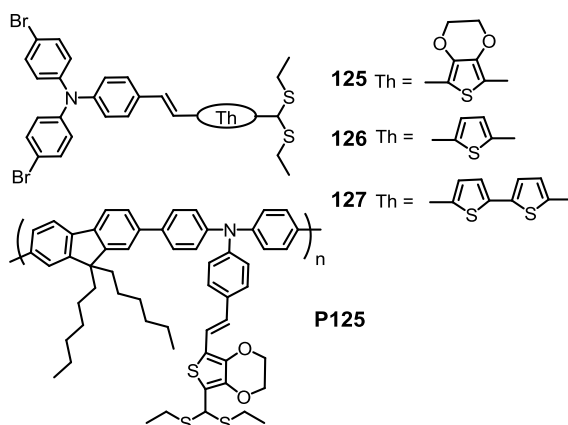


Figure 76. Structure of the chemodosimeters **125**, **126**, **127** and **P125**.

Das and coworkers developed a dithiane derivative of BODIPY (**128**; Figure 77) for the selective detection of Hg^{2+} in physiological condition.¹¹⁷ This dithiane reagent reacts specifically with Hg^{2+} to regenerate the parent BODIPY-aldehyde with consequential change in visually detectable optical responses and this provides the possibility of using this reagent as a colorimetric probe or as a fluorescent biomarker/imaging reagent. Further, non-covalent interactions could be utilized for formation of an inclusion complex with biologically benign β -cyclodextrin for enhancing its solubility in aqueous environment and this included adduct could be used as a fluorescent marker and imaging reagent for Hg^{2+} . Uptake of Hg^{2+} ions in live HeLa cells, exposed to a solution having Hg^{2+} ion concentration as low as 2 ppb, could also be detected by confocal laser microscopic studies.

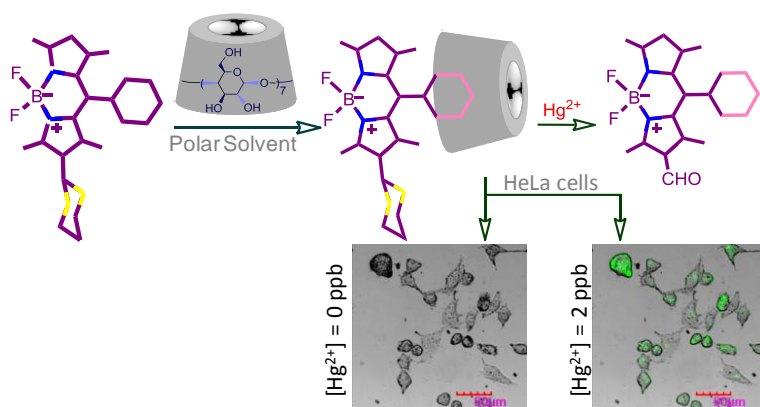


Figure 77. (A) Chemodosimetric recognition and detection of Hg^{2+} by the reagent **128** with possible inclusion complex formation with β -CD with confocal images of live HeLa cells, supplemented with 2 ppb of $\text{Hg}(\text{ClO}_4)_2$ in the growth media for 15 min at 37 °C and was followed by staining with 5.0 μM **128** for 1.0 h at 37 °C (λ_{exc} of 488 nm, λ_{mon} filter range of 494–502 nm). Reprinted with permission from ref 117. Copyright 2013 Royal Society of Chemistry.

Like Sulphur, high stability of HgSe complex could also be utilised for the detection of Hg^{2+} following the chemodosimetric approach with consequent change in the photophysical properties. The new reagent **129** having the λ_{max} of 319 nm was found to shift to 326 nm on reaction with Hg^{2+} due to the formation of HgSe (Figure 78A).¹¹⁸ However, the chemical reaction was probed by monitoring the ~100-fold enhancement in emission intensity with consequent increase in quantum yield from 0.002 to 0.2. This chemodosimetric reagent **129** could even detect Hg^{2+} as low as 0.18 ppb.

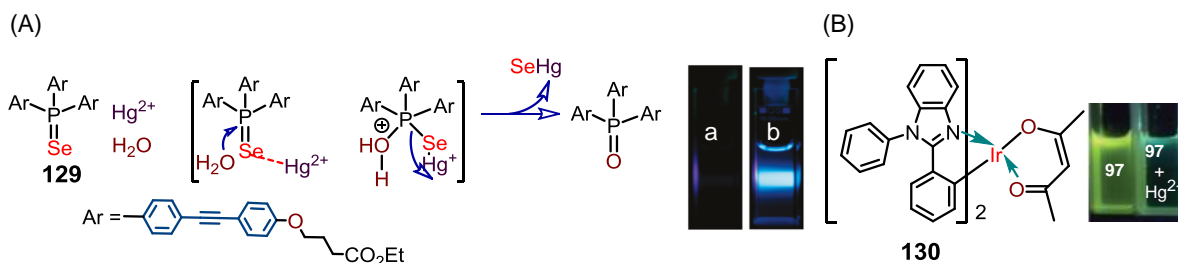


Figure 78. (A) Mechanism showing removal of selenide atom on the action of Hg^{2+} led to change in photophysical properties [Inset: change observed under Uv-light a) only **129**, b) **129** in presence of Hg^{2+}]. (B) Iridium based chemodosimeter for the recognition of Hg^{2+} ions [Inset: Change in colour of **130** upon addition of Hg^{2+} under Uv-radiation]. Reprinted with permission from ref 119. Copyright 2012 Royal Society of Chemistry.

A cyclometallated Ir(III) complex, derived from benzimidazole moiety (**130**) could also detect Hg^{2+} with high specificity and sensitivity utilizing the change in optical and electrochemical properties (Figure 78B).¹¹⁹ This Ir(III)-complex (**130**) exhibited two distinct absorption bands; band at 300-400 nm was assigned as a ligand based spin allowed $^1(\pi-\pi^*)$ transition, while the other band at 400-525 nm was assigned to a MLCT and spin-orbit coupling enhanced $^3(\pi-\pi^*)$ transition. Addition of Hg^{2+} ions into the solution of **130** caused a lowering of the intensity of MLCT band while gradual but subsequent increase in the intensity for the $\pi-\pi^*$ transition band was observed. This resulted a change in solution colour from yellowish green to colourless and the ratiometric spectral responses allowed probing the $[\text{Hg}^{2+}]$ in solution. A decomposition of the Ir(III)-chelate with the rapture of the relatively weak Ir-O bond was induced by Hg^{2+} ion without the compulsory involvement of a pre-coordination step between the lone-pair electrons on the ligand and Hg^{2+} . This was further confirmed from NMR and ESI-MS spectroscopy. Electrochemical studies revealed that the Ir^{III/IV}-based redox potential of 0.44 V for **130** was found to shift to 1.02 V on reaction with one equivalent of Hg^{2+} , which also supported the decomplexation phenomena.

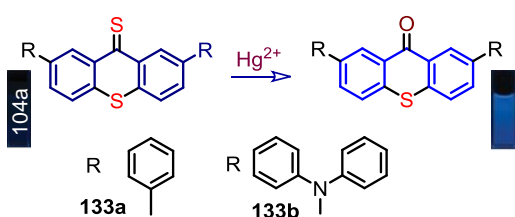


Figure 79. Fluorescence changes in the presence of Hg^{2+} and proposed sensing mechanism: desulfurization of **133a** and **133b**, promoted by Hg^{2+} ions. Reprinted with permission from ref 120. Copyright 2012 Royal Society of Chemistry.

Hg^{2+} could also induce the desulphurization of thioxanthene-9-thione derivatives (**133a** and **133b**) (Figure 79) with associated changes in visually detectable change in solution colour from orange to

colourless.¹²⁰ The absorption band for **133a** was shifted from 487 to 397 nm in CH₃CN-H₂O medium (1:1, v/v), while significant luminescence changes were also observed for the transformation of thioxanthen-9-thione to thioxanthen-9-one. Detectable lowest concentration for Hg²⁺ was reported as 21 nM for the reagent **133a**.

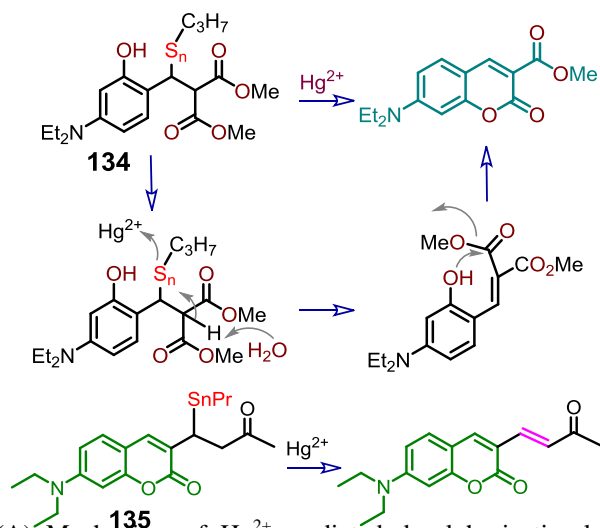


Figure 80. (A) Mechanism of Hg²⁺ mediated desulphurization-lactonization of **134**. (B) Hg²⁺ recognition mechanism of **135**.

Chemodosimeter **134** revealed a ‘turn on’ response in presence of Hg²⁺ in pure aqueous medium due to facile desulphurization-lactonization cascade transformation for the generation of highly fluorescent product from the non-fluorescent one (Figure 80A).¹²¹ This resulted a ‘turn-on’ luminescence response with 50-fold enhancement of the band intensity at ~ 480 nm only in presence of Hg²⁺ ($\lambda_{\text{Ext}} = 430$ nm) within 30s. Reaction stoichiometry evaluated for this process was 1:2. The lower detection limit for Hg²⁺ was reported as $1 \times 10^{-8} \text{ M}^{-1}$ considering the signal to noise ratio of 3.

Liu and Wang et al. developed a new ratiometric and chemodosimeter (**135**, Figure 80B) for Hg²⁺ using chemoselective Hg²⁺ promoted desulfurization of a thioether to form an extended conjugated fluorescent system as a design strategy.¹²² In the absence of Hg²⁺, **135** displayed the coumarin based emission at 488 nm on excitation at 435 nm in 0.1 M phosphate buffer (containing 0.5% acetonitrile) at pH 7.4. In presence of 2.0 equiv. of Hg²⁺, the emission at 488 nm disappeared and a new emission peak appeared at 560 nm and the absorbance maxima was switched from 400 nm to 460 nm. These red shift in the absorbance and emission spectra and the ratiometric emission responses were due to the Hg²⁺ assisted desulfurisation of **135**, which resulted in a α,β -unsaturated system i.e. the extended

conjugation in the fluorophore. The probe could even produce a pronounced fluorescent signal change when Hg^{2+} was as low as 2×10^{-8} M. Moreover **135** could be used as intracellular fluorescent imaging reagent for the detection of Hg^{2+} in living cells.

Kim and co-workers synthesized two squarylium dye based receptors **136** and **137** (Figure 81).¹²³ Interestingly, these sensors could detect Hg^{2+} in DMSO medium following two different mechanisms. Coordination of Hg^{2+} to **136** caused desulphurisation with blue shift in absorption spectra from 659 nm to 625 nm; while for **137** the absorption spectra at 683 nm gradually disappeared with development of a new spectral band at 562 nm. Isosbestic point at 615 nm confirmed that Hg^{2+} ·**137** was present in the equilibrium. A stable 1:2 complex formation was proposed (Figure 81). Thus, **136** is a chemodosimeter while **137** is a chemosensor.

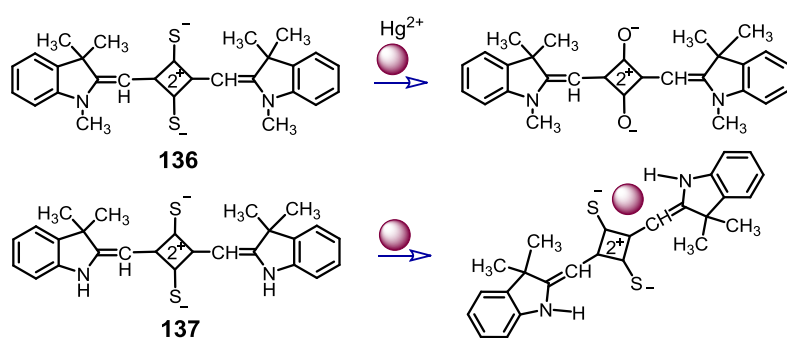


Figure 81. Representation of the proposed reaction of Hg^{2+} with reagents **136** and **137**.

In most cases, Hg^{2+} leads to desulphurization and this leads to the perturbation of the energies of the frontier orbitals (HOMO and LUMO) with consequential changes in absorption and emission spectral pattern. This basic principal was utilized receptor by Xiao, Qian and their co-workers for designing a new chemodosimeter (**138**) for Hg^{2+} ion (Figure 82).¹²⁴ Reaction of the Hg^{2+} with the thiourea fragment led to the formation of oxadiazole derivative with associated opening of spirolactam ring of the rhodamine moiety and this eventually led to the generation of new absorption band 560 nm along with BODIPY-based absorption at 501 nm in ethanol-water medium (4:1, (v/v); pH 7.0). This helped in using this reagent as colorimetric reagent for Hg^{2+} detection aqueous sample.

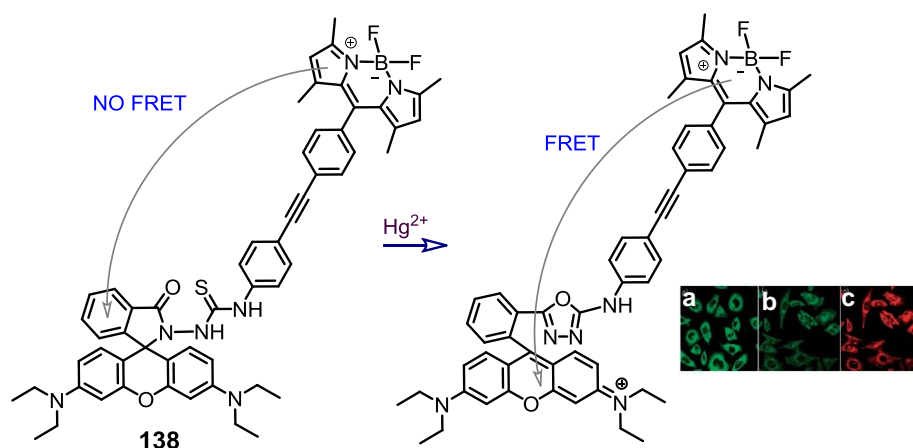


Figure 82. Hg^{2+} induced oxadiazole formation leading to the FRET process from BODIPY to rhodamine [Inset: Confocal images; a) MCF7 cells incubated with **138** ($5\ \mu\text{m}$) for 30 min at room temperature, emission measured at (514 ± 15) nm; b) and c) MCF7 cells incubated with **138** ($5\ \mu\text{m}$) and then further incubated with Hg^{2+} ions ($5\ \mu\text{m}$), emission measured at (514 ± 15) , (b) nm and (589 ± 15) , (c) nm]. Reprinted with permission from ref 124. Copyright 2008 Wiley.

Using a similar strategy, Xiao and Qian and their co-workers had synthesized other FRET-based sensors, **139** and **140**, incorporating BODIPY as donor fragment and tetramethylrhodamine (TMR) unit as acceptor (Figure 83) for the detection of Hg^{2+} .¹²⁵ BODIPY-rhodamine platform (BRP) showed reversible switching of a rhodamine dye between a zwitterion and a lactone as a function of the media polarity and proticity.

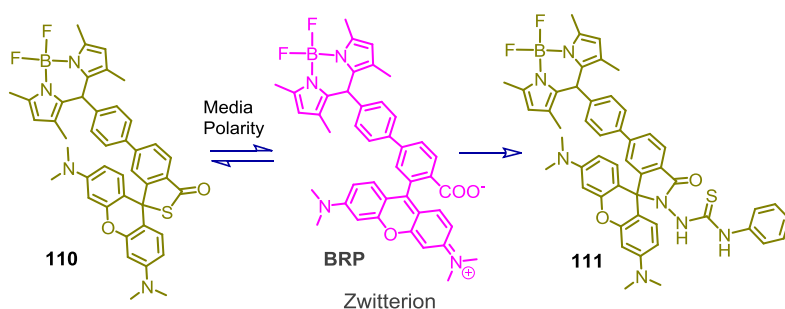


Figure 83. Molecular structures of the reagents **139** and **140**.

In aprotic solvent, such as acetonitrile, BRP emitted a strong green fluorescence; with λ_{max} of 510 nm typical for BODIPY unit. In protic solvent (methanol), BRP showed an orange fluorescence with λ_{max} of 568 nm, characteristic for rhodamine fragment even upon excitation of BODIPY unit at 488 nm. This clearly demonstrated that an effective FRET was switched on in methanol. The rhodamine unit existed in the form of a ring-opened zwitterion in protic solvent like methanol that had a characteristic absorption peak at 540 nm, which was suited for inducing the FRET process. Emission spectral studies

reveal that the BODIPY based emission at 514 nm was found to bleach gradually with simultaneous growth in emission intensity of new xanthene form of rhodamine based band at 589 nm upon reaction with increasing amount of Hg^{2+} following a FRET process (with λ_{ext} 488). The FRET efficiency calculated for **140** was 99% where the distance between donor-acceptor was 58.9 Å. The fluorescence images of the MCF-7 cells were observed under confocal microscopy with the double channel fluorescence images at (514±15) nm and (589±15) nm in presence and absence of HgCl_2 . Observed change in emission signal from green to red further confirmed that the FRET process was operational. A chromofluorogenic dual functionalised hybrid material (**141**) was made of mesoporous material with homogeneously distributed pores having ~ 2-3 nm in size with specific surface area of 1000 m^2g^{-1} for the detection of Hg^{2+} in aqueous environment. The nano sized silica particles were covalently linked to the thiol functionality as the binding site by silylation reaction and thiols groups are also covalently linked to the signaling unit, squaraine dye.¹²⁶

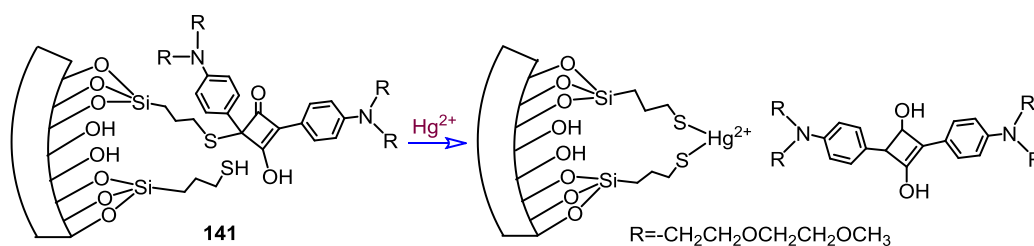


Figure 84. Protocol used for the detection and removal of Hg^{2+} from aqueous environment.

The actual strategy was designed in such way that Hg^{2+} would react readily with thiol functionality with releasing the highly colored and emissive squaraine dye as shown in Figure 84. This probe could allow detection of Hg^{2+} as low as ppb, while the solid material could absorb Hg^{2+} for the concentration range of 0.7–1.7 mmolg^{-1} (depending on the degree of the functionalization) in acetonitrile/water medium (1:1, v/v, pH 3). Thus, this material could be used as Hg^{2+} ion sponge with fluorescence responses.

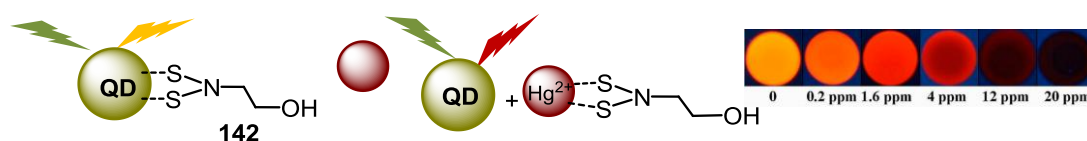


Figure 85. Quantum dot based Hg^{2+} sensors [Inset: colour change observed on cellulose acetate paper on dropping solution of Hg^{2+}]. Reprinted with permission from ref 127. Copyright 2012 American Chemical Society.

Water soluble CdSe-Zns based DQs was functionalized with 2-hydroxyethyl dithiocarbamate and this modified QDs shown ability to detect Hg^{2+} from its aqueous solution (Figure 85).¹²⁷ Preferential binding of the thiol functionality to Hg^{2+} , led to the leaching of the 2-hydroxyethyl dithiocarbamate moiety from the CdSe-Zns based DQ surfaces with associated change in solution colour from orange to red with the detection limit of 1 ppb. The corresponding shift in emission maxima was from 596 nm to 603 nm. The quantum dot based sensors was also utilised on cellulose acetate paper. A visually distinguishable fluorescence (from orange to red) could be clearly observed depending on the concentration of Hg^{2+} to which this modified cellulose papers were exposed. The lowest detection limit obtained in this method was 0.2 ppb.

Triboelectric nanogenerator for the Hg^{2+} recognition:

Apart from these conventional colorimetric, fluorometric sensors, a new kind of recognition phenomena observed by Wang and his coworkers.^{128,129} They demonstrated an innovative and unique approach toward self powered detection of Hg^{2+} .

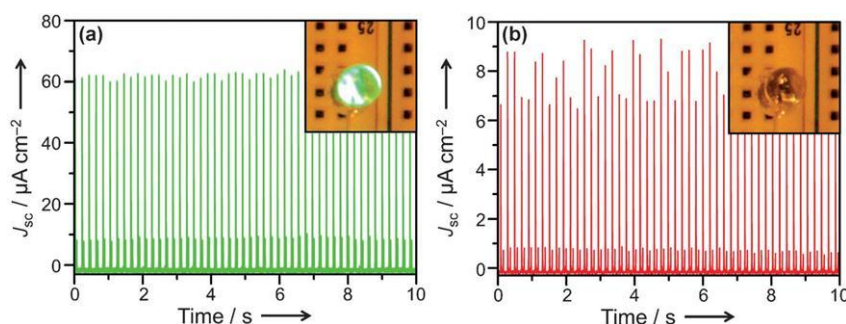


Figure 86: Rectified J_{sc} of the as-developed TENG before (a) and after (b) the interaction with $5 \mu\text{M}$ Hg^{2+} ions. Insets: photograph of the indicated LED lamp before (a) and after (b) interaction with $5 \mu\text{M}$ Hg^{2+} ions, as an indication of detected concentration. Reprinted with permission from ref 129. Copyright 2013 Wiley.

They developed the first triboelectric nanogenerator (TENG) effect based highly sensitive and selective sensor for the detection of Hg^{2+} ions by using 3-MPA (mercapto propionic acid) modified AuNPs as electrical performance enhancer and recognition element. Based on the high power density (6.9 mWcm^{-2}) of this as-developed TENG, a commercial LED lamp can be used as an indicator

instead of expensive electrometers. This novel TENG based sensor system is quite sensitive (detection limit of 30 nM and linear range of 100 nM–5 μ M) and selective for the detection of Hg^{2+} ions. With its high sensitivity, selectivity and simplicity, the TENG holds great potential for the determination of Hg^{2+} ions in environmental samples.

Conclusion:

For Hg(II), the “heavy atom” effect favours an enhanced spin-orbit coupling constant (ζ) and generally induces a strong luminescence quenching of the bound luminophore. This together with the high hydration enthalpy (1824 kcal mol⁻¹) for Hg^{2+} ion pose a challenge to the researchers for achieving the seemingly simple but the tricky issue of the Hg^{2+} recognition with *luminescence on* or *enhancement* response either in aqueous environment or in physiological conditions. Luminescence enhancement/on response is crucial for designing reagent for imaging application for detection of the cellular uptake of this ion. This is significant in developing efficient reagent for diagnostic application and environmental sample analysis—apart from addressing the other crucial issue of sensitivity. Further, specific detection of Hg^{2+} in presence of other soft transition metal ions like Cu^{2+} , Cd^{2+} , Pb^{2+} and Ag^+ remains a challenge for the researchers. In this report we have summarized a brief but extensive account of all such reports along with the reports on colorimetric reagent that are conducive for in-filed sample analysis with yes-no type binary response. Attempts to develop self-indicating solid surfaces for Hg^{2+} detection and scavenging are also summarized in this article.

Acknowledgements:

A.D. thanks DST (India) and CSIR (India) for financial support. H.A. acknowledges CSIR for his research fellowship.

References

- 1) E. M. Nolan and S. J. Lippard, *Chem. Rev.*, 2008, **108**, 3443.
- 2) E. L. Que, D. W. Domaille and C. J. Chang, *Chem. Rev.*, 2008, **108**, 1517.
- 3) (a) G. Aragay, J. Pons and A. Merkoçi, *Chem. Rev.*, 2011, **111**, 3433; (b) D. T. Quang and J. S. Kim, *Chem. Rev.*, 2010, **110**, 6280; (c) X. Chen, T. Pradhan, F. Wang, J. S. Kim and J. Yoon, *Chem. Rev.*, 2012, **112**, 1910; (d) H. N. Kim, W. X. Ren, J. S. Kim and J. Yoon *Chem. Soc. Rev.*, 2012, **41**, 3210.
- 4) Z.-X. Han, X.-B. Zhang, Z. Li, Y.-J. Gong, X.-Y. Wu, Z. Jin, C.-M. He, L.-X. Jian, J. Zhang, G.-L. Shen and R.-Q. Yu, *Anal. Chem.*, 2010, **82**, 3108.
- 5) A. P. de Silva and S. A. de Silva, *J. Chem. Soc. Chem. Commun.*, 1986, 1709.
- 6) B. Valeur and I. Leray, *Coord. Chem. Rev.*, 2000, **205**, 3.
- 7) J. R. Lakowicz, *Principles of Fluorescence Spectroscopy*, Third Edition, Springer, New York, USA, 2006.
- 8) R. Bandichhor, A. D. Petrescu, A. Vespa, A. B. Kier, F. Schroeder and K. Burgess, *J. Am. Chem. Soc.*, 2006, **128**, 10688.
- 9) X. Chen, X. Tian,; I. Shin and J. Yoon, *Chem. Soc. Rev.*, 2011, **40**, 4783.
- 10) B. Valeur, *Molecular Fluorescence*, 2nd ed.; Wiley-VCH: New York, 2005.
- 11) (a) A. Misra and M. J. Shahid, *Phys. Chem. C*, 2010, **114**, 16726. (b) *Threshold Limit Values for Chemical Substances and Physical Agents and Biological Exposure Indices*. American Conference of Governmental Industrial Hygienists. ISBN 1-882417-49-6. Cincinnati (OH); (c) *Toxicological profile for Mercury, 1999*. U.S. Department of Health and Human Services, Centers for Disease Control and Prevention, Agency for Toxic Substances and Disease Registry. Atlanta (GA).
- 12) M. Zhu, M. Yuan, X. Liu, J. Xu, J. Lv, C. Huang, H. Liu, Y. Li, S. Wang and D. Zhu, *Org. Lett.*, 2008, **10**, 1481.
- 13) H. Lee and S. Lee, *Org. Lett.*, 2009, **11**, 1394.
- 14) S. Tatay, P. Gaviña, E. Coronado and E. Palomares, *Org. Lett.*, 2006, **8**, 3857.
- 15) A. Kumar, V. Kumar and K. K. Upadhyay, *Tetrahedron Lett.*, 2011, **52**, 6809.
- 16) R. Shunmugam, G. J. Gabriel, C. E. Smith, A. K. Aamer and G. N. Tew, *Chem. Eur. J.*, 2008, **14**, 3904.
- 17) S.-K. Chung, Y.-R. Tseng, C.-Y. Chen and S.-S. Sun, *Inorg. Chem.*, 2011, **50**, 2711.
- 18) G.-L. Wang, X.-Y. Zhu, H.-J. Jiao, Y.-M. Dong and Z.-J. Li, *Biosens. Bioelectron.*, 2012, **31**, 337.
- 19) P. Mahato, A. Ghosh, S. Saha, S. Mishra, S. K. Mishra and A. Das, *Inorg. Chem.*, 2010, **49**, 11485.

- 20) P. Das, A. Ghosh, H. Bhatt and A. Das, *RSC Adv.*, 2012, **2**, 3714.
- 21) H. N. Kim, M. H. Lee, H. J. Kim, J. S. Kim and J. Yoon, *Chem. Soc. Rev.*, 2008, **37**, 1465.
- 22) K. N. Kim, M. G. Choi, J. H. Noh, S. Ahn and S.-K. Chang, *Bull. Korean Chem. Soc.*, 2008, **29**, 571.
- 23) H. Yang, Z. Zhou, K. Huang, M. Yu, F. Li, T. Yi and C. Huang, *Org. Lett.*, 2007, **9**, 4729.
- 24) J. Huang, Y. Xu and X. Qian, *J. Org. Chem.*, 2009, **74**, 2167.
- 25) H. Zheng, Z.-H. Qian, L. Xu, F.-F. Yuan, L.-D. Lan and J.-G. Xu, *Org. Lett.*, 2006, **8**, 859.
- 26) Y. Wang, Y. Huang, B. Li, L. Zhang, H. Song, H. Jiang and J. Gao, *RSC Adv.*, 2011, **1**, 1294.
- 27) W. Huang, X. Zhu, D. Wua, C. He, X. Hu and C. Duan, *Dalton Trans.*, 2009, 10457.
- 28) H. Wang, Y. Li, S. Xu, Y. Li, C. Zhou, X. Fei, L. Sun, C. Zhang, Y. Li, Q. Yang and X. Xu, *Org. Biomol. Chem.*, 2011, **9**, 2850.
- 29) M. Suresh, A. Shrivastav, S. Mishra, E. Suresh and A. Das, *Org. Lett.*, 2008, **10**, 3013.
- 30) W. Huang, P. Zhou, W. Yan, C. He, L. Xiong, F. Li and C. Duan, *J. Environ. Monit.*, 2009, **11**, 330.
- 31) L. Tang, F. Li, M. Liu and R. Nandhakumar, *Spectrochim. Acta, Part A*, 2011, **78**, 1168.
- 32) D. Wu, W. Huang, Z. Lin, C. Duan, C. He, S. Wu and D. Wang, *Inorg. Chem.*, 2008, **47**, 7190.
- 33) Y. Shiraishi, S. Sumiya, Y. Kohno and T. Hirai, *J. Org. Chem.*, 2008, **73**, 8571.
- 34) K. Ghosh, T. Sarkar A. Samadder, and A. R. Khuda-Bukhsh, *New J. Chem.*, 2012, **36**, 2121.
- 35) S. K. Kim, K. M. K. Swamy, S. -Y. Chung, H. N. Kim, M. J. Kim, Y. Jeong and J. Yoon, *Tet. Lett.*, 2010, **51**, 3286.
- 36) S. Saha, P. Mahato, G. U. Reddy, E. Suresh, A. Chakrabarty, M. Baidya, S. K. Ghosh and A. Das, *Inorg. Chem.*, 2012, **51**, 336.
- 37) K. Ghosh, T. Sarkar and A. Samadder, *Org. Biomol. Chem.*, 2012, **10**, 3236.
- 38) Z. Yang, L. Hao, B. Yin, M. She, M. Obst, A. Kappler and J. Li, *Org. Lett.*, 2013, **15**, 4334.
- 39) N. Kumari, N. Dey and S. Bhattacharya, *RSC Adv.*, 2014, **4**, 4230.
- 40) M. Suresh, S. Mishra, S. K. Mishra, E. Suresh, A. K. Mandal, A. Shrivastav and A. Das, *Org. Lett.*, 2009, **11**, 2740.

- 41) G. Fang, M. Xu, F. Zeng and S. Wu, *Langmuir*, 2010, **26**, 17764.
- 42) Y. H. Lee, M. H. Lee, J. F. Zhang and J. S. Kim *J. Org. Chem.* 2010, **75**, 7159.
- 43) P. Mahato, S. Saha, E. Suresh, R. Di Liddo, P. P. Parnigotto, M. T. Conconi, M. K. Kesharwani, B. Ganguly and A. Das, *Inorg. Chem.*, 2012, **51**, 1769.
- 44) M. Kumar, N. Kumar, V. Bhalla, H. Singh, P. R. Sharma and T. Kaur, *Org. Lett.*, 2011, **13**, 1422.
- 45) V. Bhalla, Roopa, M. Kumar, P. R. Sharma and T. Kaur, *Inorg. Chem.*, 2012, **51**, 2150.
- 46) S. Saha, P. Mahato, M. Baidya, S.K. Ghosh and A. Das, *Chem. Commun.*, 2012, **48**, 9293.
- 47) V. Bhalla, V. Vij, R. Tejpal, G. Singh and M. Kumar, *Dalton Trans.*, 2013, **42**, 4456.
- 48) A. Loudet and K. Burgess, *Chem. Rev.*, 2007, **107**, 4891.
- 49) A. Coskun and E. U. Akkaya, *J. Am Chem Soc.*, 2006, **128**, 14474.
- 50) M. Yuan, Y. Li, J. Li, C. Li, X. Liu, J. Lv, J. Xu, H. Liu, S. Wang and D. Zhu, *Org. Lett.*, 2007, **9**, 2313.
- 51) R. Guliyev, A. Coskun and E. U. Akkaya, *J. Am. Chem. Soc.*, 2009, **131**, 9007.
- 52) Y. Chen, L. Wan, X. Yu, W. Li, Y. Bian and J. Jiang, *Org. Lett.*, 2011, **13**, 5774.
- 53) M.-H. Yang, P. Thirupathi and K.-H. Lee, *Org. Lett.*, 2011, **13**, 5028.
- 54) J. Hatai, S. Pal, G. P. Jose and S. Bandyopadhyay, *Inorg. Chem.*, 2012, **51**, 10129.
- 55) M. Suresh, A. K. Mandal, S. Saha, E. Suresh, A. Mandoli, R. D. Liddo, P. P. Parnigotto and A. Das, *Org. Lett.*, 2010, **12**, 5406.
- 56) A. K. Mandal, M. Suresh, P. Das, E. Suresh, M. Baidya, S. K. Ghosh and A. Das, *Org. Lett.*, 2012, **14**, 2980.
- 57) G. Sivaraman, T. Anand and D. Chellappa, *RSC Adv.*, 2012, **2**, 10605.
- 58) B. P. Joshi, C. R. Lohani and K.-H. Lee, *Org. Biomol. Chem.*, 2010, **8**, 3220.
- 59) L. N. Neupane, J. M. Kim, C. R. Lohani and K.-H. Lee *J. Mater. Chem.*, 2012, **22**, 4003.
- 60) Y. H. Lau, J. R. Price, M. H. Todd and P. J. Rutledge, *Chem. Eur. J.*, 2011, **17**, 2850.
- 61) C. Bazzicalupi, C. Caltagirone, Z. Cao, Q. Chen, C. D. Natale, A. Garau, V. Lippolis, L. Lvova, H. Liu, I. Lundstrom, M. C. Mostallino, M. Nieddu, R. Paolesse, L. Prodi, M. Sgarzi and N. Zaccheroni. *Chem. Eur. J.*, 2013, **19**, 14639.
- 62) J. Hatai, S. Pal, G. P. Jose, T. Sengupta and S. Bandyopadhyay, *RSC Adv.*, 2012, **2**, 7033.
- 63) W.-J. Shi, J.-Y. Liu and K. P. Ng, *Chem. Asian J.*, 2012, **7**, 196.

- 64) Q. Mei, L. Wang, B. Tian, F. Yan, B. Zhang, W. Huang and B. Tong, *New J. Chem.*, 2012, **36**, 1879.
- 65) C. Kar, M. Deb, Adhikari, A. Ramesh and G. Das, *RSC Adv.*, 2012, **2**, 9201.
- 66) S. Khatua, M. Schmittel, *Org. Lett.*, 2013, **15**, 4422.
- 67) S. Madhu, D. K. Sharma, S. K. Basu, S. Jadhav, A. Chowdhury, M. Ravikanth, *Inorg. Chem.* 2013, **52**, 11136.
- 68) P. Mazumdar, D. Das, G. P. Sahoo, G. Salgado-Mora'n and A. Misra *Phys. Chem. Chem. Phys.*, 2014, **16**, 6283.
- 69) A. Singh, T. Raj, R. Aree, N. Singh., *Inorg. Chem.* 2013, **52**, 13830.
- 70) K. Tayde, B. Bondhopadhyay, A. Basu, G. K. Chaitanya, S. K. Sahoo, N. Singh, S. Attarde and A. Kuwar, *Talanta*, 2014, **122**, 16.
- 71) G. Aragay, J. Pons and A. Merkoçi, *Chem. Rev.*, 2011, **111**, 3433.
- 72) J. H. Jung, J. H. Lee and S. Shinkai, *Chem. Soc. Rev.*, 2011, **40**, 4464.
- 73) M. H. Lee, S. J. Lee, J. H. Jung, H. Lima and J. S. Kim, *Tetrahedron*, 2007, **63**, 12087.
- 74) Liu, H.; Yu, P.; Du, D.; He, C.; Qiu, B.; Chen, X.; Chen, G. *Talanta*, **2010**, **81**, 433.
- 75) B. Liu, F. Zeng, G. Wu and S. Wu, *Analyst*, 2012, **137**, 3717.
- 76) C. Yuan, B. Liu, F. Liu, M.-Y. Han, Z. Zhang, *Anal. Chem.*, 2014, **86**, 1123.
- 77) M. Zhu, C. Zhou, Y. Zhao, Y. Li, H. Liu and Y. Li, *Macromol. Rapid Commun.*, 2009, **30**, 1339.
- 78) C. Kaewtong, B. Wannoo, Y. Uppa, N. Morakot, B. Pulpoka and T. Tuntulani, *Dalton Trans.*, 2011, **40**, 12578.
- 79) G. Sánchez, D. Curiel, I. Ratera, A. Tárraga, J. Veciana and P. Molina, *Dalton Trans.*, 2013, **42**, 6318.
- 80) W. Huang, D. Wu, G. Wua and Z. Wang, *Dalton Trans.*, 2012, **41**, 2620.
- 81) L. Q. Xu, K. -G. Neoh, E. -T. Kang and G. D. Fu, *J. Mater. Chem. A*, 2013, **1**, 2526.
- 82) J. Li, Y. Wu, F. Song, G. Wei, Y. Cheng and C. Zhu, *J. Mater. Chem.*, 2012, **22**, 478.
- 83) M. Park, S. Seo, I. S. Lee and J. H. Jung, *Chem. Commun.*, 2010, **46**, 4478.
- 84) S. Saha, M. U. Chhatbar, P. Mahato, L. Praveen, A. K. Siddhanta and A. Das, *Chem. Commun.*, 2012, **48**, 1659.
- 85) X. Zhang and J. Huang, *Chem. Commun.*, 2010, **46**, 6042.
- 86) Y. Wu, Y. Dong, J. Li, X. Huang, Y. Cheng and C. Zhu, *Chem. Asian J.*, 2011, **6**, 2725.
- 87) B. Liu, F. Zeng, Y. Liu and S. Wu *Analyst*, 2012, **137**, 1698.

- 88) Y. Si, X. Wang, Y. Li, K. Chen, J. Wang, J. Yu, H. Wang and B. Ding *J. Mater. Chem. A*, 2014, **2**, 645.
- 89) Y. Zhang, X. Li, L. Gao, J. Qiu, L. Heng, B. Z. Tang and L. Jiang, *ChemPhysChem*, 2014, **15**, 507.
- 90) (a) V. Bhalla, V. Vij, R. Tejpal, G. Singh and M. Kumar, *Dalton. Trans.*, 2013, **42**, 4456; (b) V. Bhalla, Roopa, M. Kumar, P.R. Sharma and T. Kaur, *Inorg. Chem.*, 2012, **51**, 2150.
- 91) (a) Y. Wang, B. Li, L. Zhang, P. Li, L. Wang and J. Zhang, *Langmuir*, 2012, **28**, 1657; (b) Y. Wang, B. Li, L. Zhang, L. Liu, Q. Zuo and P. Li, *New J. Chem.*, 2010, **34**, 1946.
- 92) Z.Q. Li and Y. Zhang, *Angew. Chem. Int. Ed.*, 2006, **45**, 7732.
- 93) M. Wang, X. An and J. Gao, *Journal of Luminescence*, 2013, **144**, 91.
- 94) G. Xu, *Sensors and Actuators B*, 2014, **195**, 230.
- 95) X. Cui, H. M. Zhang, *Journal of Luminescence*, 2014, **145**, 364.
- 96) D. Arunbabu, A. Sannigrahi and T. Jana *Soft Matter*, 2011, **7**, 2592.
- 97) Y. Yang, Q. Zhao, W. Feng and F. Li, *Chem. Rev.*, 2013, **113**, 192.
- 98) Y.-K. Yang, K.-J. Yook and J. Tae, *J. Am. Chem. Soc.*, 2005, **127**, 16760.
- 99) S.-K. Ko, Y.-K. Yang, J. Tae and I. Shin, *J. Am. Chem. Soc.*, 2006, **128**, 14150.
- 100) A. Jana, J. S. Kim, H. S. Jung and P. K. Bharadwaj, *Chem. Commun.*, 2009, 4417.
- 101) X. Chen, S.-W. Nam, M. J. Jou, Y. Kim, S.-J. Kim, S. Park and J. Yoon, *Org. Lett.*, 2008, **10**, 5235.
- 102) X. Chen, K.-H. Baek, Y. Kim, S.-J. Kim, I. Shin and J. Yoon, *Tetrahedron*, 2010, **66**, 4016.
- 103) W. Liu, L. Xu, H. Zhang, J. You, X. Zhang, R. Sheng, H. Li, S. Wu and P. Wang, *Org. Biomol. Chem.*, 2009, **7**, 660.
- 104) W. Lin, X. Cao, Y. Ding, L. Yuan and L. Long, *Chem. Commun.*, 2010, **46**, 3529.
- 105) J. Du, J. Fan, X. Peng, P. Sun, J. Wang, H. Li and S. Sun, *Org. Lett.*, 2010, **12**, 476.
- 106) F. Song, S. Watanabe, P. E. Floreancig and K. Koide, *J. Am. Chem. Soc.*, 2008, **130**, 16460.
- 107) S. Ando and K. Koide, *J. Am. Chem. Soc.*, 2011, **133**, 2556.
- 108) K. Bera, A. K. Das, M. Nag and S. Basak, *Anal. Chem.* 2014, **86**, 2740.
- 109) M. Santra, B. Roy and K. H. Ahn, *Org. Lett.*, 2011, **13**, 3422.
- 110) Y. -S. Cho and K. H. Ahn, *Tet. Lett.*, 2010, **51**, 3852.

- 111) H. Lee and H.-J. Kim, *Tet. Lett.*, 2011, **52**, 4775.
- 112) Y. Chen, Z.-H. Sun, B.-E. Song and Y. Liu, *Org. Biomol. Chem.*, 2011, **9**, 5530.
- 113) Y. Chen, C. Zhu, Z. Yang, J. Li, Y. Jiao, W. He, J. Chen and Z. Guo, *Chem. Commun.*, 2012, **48**, 5094.
- 114) R. Huang, X. Zheng, C. Wang, R. Wu, S. Yan, J. Yuan, X. Weng, and X. Zhou *Chem. Asian J.*, 2012, **7**, 915 – 918.
- 115) X. Cheng, Q. Li, C. Li, J. Qin, and Z. Li *Chem. Eur. J.*, 2011, **17**, 7276.
- 116) X. Cheng, S. Li, H. Jia, A. Zhong, C. Zhong, J. Feng, J. Qin, and Z. Li, *Chem. Eur. J.*, 2012, **18**, 1691.
- 117) S. Saha, H. Agarwalla, H. Gupta, M. Baidya, E. Suresh, S. K. Ghosh and A. Das *Dalton Trans.*, 2013, **42**, 15097.
- 118) I. Samb, J. Bell, P. Y. Toullec, V. Michelet and I. Leray, *Org. Lett.*, 2011, **113**, 192.
- 119) H. Zeng, F. Yu, J. Dai, H. Sun, Z. Lu, M. Li, Q. Jianga and Y. Huang, *Dalton Trans.*, 2012, **41**, 4878.
- 120) L. Ding, Q. Zou, Y. Qu and J. Su, *RSC Adv.*, 2012, **2**, 4754.
- 121) W. Jiang and W. Wang, *Chem. Commun.*, 2009, 3913.
- 122) W. Xuan, C. Chen, Y. Cao, W. He, W. Jiang, K. Liu and W. Wang, *Chem. Commun.*, 2012, **48**, 7292.
- 123) Y. Wang, S.-Y. Gwon and S.-H. Kim, *Fiber Polym.*, 2011, **12**, 836.
- 124) X. Zhang, Y. Xiao and X. Qian, *Angew. Chem. Int. Ed.*, 2008, **47**, 8025.
- 125) H. Yu, Y. Xiao, H. Guo and X. Qian, *Chem. Eur. J.*, 2011, **17**, 3179.
- 126) J.V. Ros-Lis, R. Casasús, M. Comes, C. Coll, M. D. Marcos, R. Martínez-Mañez, F. Sanceón, J. Soto, P. Amorós, J. E. Haskouri, N. Garró and K. Rurack, *Chem. Eur. J.*, 2008, **14**, 8267.
- 127) C. Yuan, K. Zhang, Z. Zhang and S. Wang, *Anal. Chem.*, 2012, **84**, 9792.
- 128) (a) M. Lee, J. Bae, J. Lee, C.-S. Lee, S. Hong and Z. L. Wang, *Energy Environ. Sci.* 2011, **4**, 3359; (b) I. F. Akyildiz and J. M. Jornet, *Nano Commun Networks.*, 2010, **1**, 3.
- 129) Z-H, Lin, G. Zhu, Y. S. Zhou, Y. Yang, P. Bai, J. Chen and Z. L. Wang, *Angew. Chem.*, 2013, **125**, 5169.